DISS. ETH NO. 24753

Molecularly-imprinted polymers for compound-specific isotope analysis of polar organic micropollutants in aquatic environments

A thesis submitted to attain the degree of
DOCTOR OF SCIENCES of ETH ZURICH
(Dr. sc. ETH Zurich)

presented by

Rani Bakkour

MSc Water Sc, Duisburg-Essen University
born on September 19, 1982
citizen of Syria

accepted on the recommendation of
PD Dr. Thomas B. Hofstetter, examiner
Prof. Dr. Kristopher McNeill, co-examiner
Prof. Dr. Daniel Hunkeler co-examiner

2018

Acknowledgment

I would like to express a sincere gratitude to my PhD advisor Thomas Hofstetter whose exceptional enthusiasm offered me a source of motivation throughout this journey. I am grateful to all what you have offered and shared during these four years in a number of ways from regular meetings, to encouragement, and detailed feedback on the dissertation that enriched this work. Your organized and systematic style at work will always stay one of many inspiring skills I will remember you for.

I owe special thanks to Kris McNeil and Daniel Hunkeler for being on the committee. I appreciate the time and efforts you dedicated to review the dissertation and to be at the first row at the defense day. In particular, thanks to Daniel who had to travel early on Monday morning to make it to the defense at Eawag. To Kris goes additional thanks for all the time and advises he offered before and during submitting the thesis.

I would further like to acknowledge all our collaborators and project partners. In particular, Clara Torrentó for providing me with the gigantic bottles that accompanied me in sampling campaigns, Aileen Melsbach for showing me how to purify samples at her preparative chromatography system at Helmholtz center in Munich, and Martin Elsner for all the invaluable discussions at project meetings. To Börje Sellergren, I owe many thanks for providing his expert advises on molecular imprinting that were helpful in overcoming obstacles I couldn't otherwise surpass on my own.

I share the credits of my work with many people who have helped, supported, or facilitated different parts of this work. To Stefanie Jucker goes immense gratitude for her meticulous work during the master thesis which was not only excellent but have also created fun in the lab. Thanks to all the talented technicians at Eawag, in particular, Jakov Bolotin for keeping the GC/IRMS instruments alive and reliable despite all the damage my notorious samples often brought to his flawless GC systems. Thanks to Philip Longrée, Birgit Beck, and Andreas Maccagnan for the continuous support on the very important daily technical details at the environmental chemistry department. I am

grateful to Elisabeth Salhi for the extraordinary support on the IC. For endless support from Ausbilduing and Analytik department at Eawag, I thank all the department members, especially: Samuel Derrer, Natalie Gsteiger, Denise Freudemann, Madeleine Langmeier, and all their talented and smart apprentices with whom I was happy to meet and work: Marius Wiesmann, Alessandra Sodero, and Adriana Tell. I am indebted as well to Silvio Canonica who gave me a generous access to his photoreactor without which I couldn't synthesize the MIPs in this work.

It's a pleasure to thank fellow officemates and labmates for the nice and friendly company through different parts of the journey: Sarah Pati, Stephanie Spahr, Iris Schilling, Bridget Ulrich, Ashley Brown, Simon Mangold, and Michele Heeb. Special thanks go to Andrea Rösch and Jonas Mechelke for translating the dissertation summary to German, and for Jennifer Schollée for proofreading the language of different parts. Additionally, I am indebted to Bernadette Vogler for her lab support on glyphosate analysis. To Heinz Singer, I am heartily thankful for invaluable discussions and generous financial support in the last stage of this dissertation. To the magnificent department of environmental chemistry at eawag, I want to express my sincere gratitude for the love and care they have shown throughout the years.

Lastly, I appreciate the generous support and patience of many friends and family members. I owe an immense gratitude to Eugen and Uschi for endless talks in- and outside science. To Reem, thank you for your generous understanding for my unavailability during the time of thesis writing. To Hassan, Hanna, Rami, and Nour, who were often in my thoughts on this journey - you are all missed.

Table of contents

Summary

The widespread occurrence of polar organic micropollutants in the environment such as pesticides and pharmaceuticals raises major concerns about their fate. Demonstrating their degradation under field conditions is difficult because changes in compound concentration can be subscribed to concurrent processes . In contrast, changes of the isotope ratios, which is monitored by compound-specific isotope analysis (CSIA), offers conclusive evidence of (bio)degradation of the contaminant. Unfortunately, due to the high detection limits for analysis by gas- or liquid chromatography / isotope-ratio mass spectrometry (GC/IRMS or LC/IRMS) and the low occurrence of these contaminants in environmental waters, ng L^{-1} to µg L^{-1}, large volumes of water need to be processed to obtain the required analyte masses for analysis. While enrichment of the required analyte masses is often possible using conventional solid-phase extraction (SPE) methods, the lack of selectivity towards the target analytes leads to inevitable co-enrichment of organic matrices, which compromises the acquired isotopic signatures. Synthetic polymers with selective binding sites can be obtained by molecular-imprinting techniques that are engineered to specifically enrich certain target analytes, but their application to stable-isotope analysis has not been studied. Therefore, it was the goal of this dissertation to investigate the effectiveness of increasing the overall selectivity of sample preparation workflows for GC/IRMS and LC/IRMS using molecularly-imprinted polymers (MIP).

Carbon- and nitrogen isotope analysis of 1*H*-benzotriazole, a typical corrosion inhibitor in dishwashing detergents, was investigated in different environmental samples as an example of a ubiquitous polar organic micropollutant. Procedures for the treatment of $>$ 10 L water samples were developed in this work. The synthesis of MIP enabled the selective cleanup of the analyte in organic solvent, which was obtained by previous enrichment by conventional SPE. Through an assessment of imprinting factors, interaction enthalpies, and ^{15}N isotope effects, it was determined hydrogen bonding between the traziole ring of 1*H*-benzotriazole and the produced MIP were responsible for the

selective interactions. The procedure was applied successfully without inducing isotope fractionation of the analyte to river water samples, as well as influent and effluent samples of a wastewater treatment plant containing 4 µg L^{-1} 1*H*-benzotriazole and dissolved organic carbon (DOC) loads of up to 28 mg C L^{-1}.

Interferences caused by organic matter from surface waters on the GC/IRMS measurements were investigated for varying loads of DOC compared to constant amount of atrazine. A DOC:micropollutant ratio of 10 in the extracted sample was the maximum limit of GC/IRMS for accurate and precise δ^{13}C, which corresponds to river water containing 7 µg L^{-1} atrazine and 0.3 mg C L^{-1} DOC. A cleanup procedure of the river water extracts using MIP allowed accurate and precise δ^{13}C in samples with an initial DOC:micropollutant ratio up to 100. Presence of traces of protic solvents in the environmental extract prior to the cleanup with MIP caused complete loss of atrazine, desethyl-atrazine, and desisopropyl-atrazine. The DOC:micropollutant ratio was found to be a useful apriori indicator for assessing effectiveness of GC/IRMS measurements of contaminants in environmental waters.

Direct extraction of the herbicide glyphosate and its transformation product AMPA was performed without chemical derivatization from different environmental waters using a MIP based on ionic interactions. A method for quantification of the analytes was successfully developed and optimized using ion chromatography-electrospray ionization-tandem mass spectrometry. Method quantification limits ranged from 17 to 82 ng L^{-1} for glyphosate and from 37 to 54 ng L^{-1} for AMPA with recoveries from 26 to 97% and from 63 to 105%, respectively. Complexation of glyphosate with leaching organic carbon from the MIP was initially responsible for loss of 80% of the analyte, for which sodium hydroxide was used to break the complex and recover the analyte. Natural organic matter in water that bound to the investigated MIP was efficiently removed by percolation of the MIP extract over reversed-phase cartridge with no loss of the analytes. δ^{13}C measurements of the analytes on LC/IRMS at different steps of the sample preparation showed no isotope fractionation.

The results from this work demonstrate that molecular-imprinting techniques prior to CSIA are an effective tool for the selective extraction/cleanup of polar organic micropollutants from different environmental waters. Two approaches for the implementation of MIP in sample preparation are possible: (i) Organic extracts of aquatic samples after reversed-phase SPE can be used for a further selective cleanup step with MIP, whereas, (ii) water-compatible MIP can be used for the direct extraction of ionized organic con-

taminants from water samples. The coupling of MIP with either of these two approaches to GC/IRMS and LC/IRMS broadens the reach of CSIA by enabling the measurement of environmental samples. For future work on CSIA, the developed approaches can be used and expanded to many other polar organic micropollutants to investigate their sources and fate in the field- and catchment-scale studies, offering thereby new perspectives to CSIA.

Zusammenfassung

Das verbreitete Vorkommen von polaren organischen Mikroverunreinigungen in der Umwelt, wie zum Beispiel von Pestiziden und Arzneimitteln, liefert Anlass zur Sorge über ihren Verbleib. Es ist schwierig ihren Abbau unter Feldbedingungen aufzuzeigen, da Änderungen der Schadstoffkonzentrationen auf verschiedene gleichzeitig ablaufende Prozesse zurückzuführen sind. Im Gegensatz dazu liefern Änderungen der Isotopenzusammensetzung von Schadstoffen, die mittels substanzspezifischer Isotopenanalyse (engl. compound-specific isotope analysis, CSIA) gemessen werden, eindeutige Nachweise über den (biologischen) Abbau eines Schadstoffs. Da die Analyse via Gas- oder Flüssigkeitschromatographie gekoppelt mit Isotopenverhältnis-Massenspektrometern - (GC/IRMS oder LC/IRMS) hohe Nachweisgrenzen aufweist, während viele Schadstoffe nur in geringen Konzentrationen im ng/L bis µg/L Bereich in natürlichen Gewässern vorkommen, müssen grosse Wasservolumina aufgearbeitet werden, um ausreichend Analyt für die chemische Analyse bereitzustellen. Während die Anreicherung der benötigten Analytmasse häufig mittels herkömmlicher Festphasenextraktion (engl. solid-phase extraction, SPE) möglich ist, kommt es aufgrund unzureichender Selektivität, neben der Anreicherung der gewünschten Analyten, zu der unvermeidbaren Anreicherung organischer Matrix und somit zur Beeinträchtigung der Isotopenverhältnisanalyse. Durch 'molekulares Prägen' (engl. molecular-imprinting) können Polymere mit selektiven Bindungsstellen synthetisiert werden, die es erlauben, ausgewählte Analyten gezielt anzureichern. Die Verwendung dieser Polymere in Kombination mit der stabilen Isotopenanalyse wurde bislang noch nicht untersucht. Ziel dieser Dissertation war es deshalb, die Selektivität der Probenaufarbeitung für die GC/IRMS und LC/IRMS mittels molekular geprägten Polymeren (engl. molecularly-imprinted polymers, MIP) zu erhöhen und ihre Wirksamkeit zu untersuchen.

Die Isotopenzusammensetzung von Kohlenstoff und Stickstoff wurde für 1H-Benzotriazol, einer häufig vorkommenden polaren organischen Mikroverunreinigung, enthalten

als Korrosionsschutzmittel in Maschinengeschirrspülmitteln, in verschiedenen Umweltproben untersucht. Ein Verfahren für die Aufarbeitung von Wasserproben mit Volumina > 10 L wurde in dieser Arbeit entwickelt. Ein eigens gefertigtes MIP ermöglichte die selektive Aufreinigung von 1*H*-Benzotriazol ausgehend von einem organischen Lösungsmittelextrakt, das durch vorherige Anreicherung mit herkömmlicher SPE erhalten wurde. Durch das Bestimmen von Prögefaktoren, Interaktionsenthalpien und ^{15}N-Isotopeneffekten wurde herausgefunden, dass Wasserstoffbrckenbindungen zwischen dem Triazolring von 1*H*-Benzotriazol und dem hergestellten MIP für die selektiven Wechselwirkungen verantwortlich waren. Das Verfahren wurde erfolgreich angewandt ohne eine Isotopenfraktionierung des Analyten in Flusswasserproben sowie in Proben von Zu- und Ablauf einer Kläranlage herbeizuführen. Die Klärwasserproben enthielten 4 µg/L 1*H*-Benzotriazol und gelöste organische Kohlenstoffgehalte (engl. dissolved organic matter, DOC) von bis zu 28 mg C/L.

Störungen der GC/IRMS-Messung, hervorgerufen durch in Oberflächengewässern enthaltene organische Matrix, wurden für verschiedene DOC-Gehalte untersucht und mit einem konstanten Atrazingehalt verglichen. Ein Verhältnis DOC:Mikroverunreinigung von 10 in den extrahierten Proben war die Obergrenze für die GC/IRMS-Analyse und somit für die Bestimmung genauer und präziser δ^{13}C Werte. Durch die Aufreinigung der Flusswasserextrakte mittels MIP konnten genaue und präzise δ^{13}C Werte in Wasserproben mit einem Verhältnis DOC:Mikroverunreinigung von bis zu 100 erzielt werden. Die Anwesenheit von Spuren eines protischen Lösungsmittels in den Probenextrakten vor der Aufreinigung mit MIP verursachte einen kompletten Verlust von Atrazin, Desethylatrazin und Desisopropylatrazin. Es zeigte sich, dass das Verhältnis DOC:Mikroverunreinigung ein nützlicher erster Indikator ist, um die Wirksamkeit von GC/IRMS-Messungen fr Schadstoffe in Gewässern einzuschätzen.

Eine direkte Extraktion des Herbizids Glyphosat und seines Transformationsprodukts AMPA aus verschiedenen Oberflächengewässern wurde ohne chemische Derivatisierung mithilfe eines MIP basierend auf ionischen Wechselwirkungen durchgeführt. Eine Methode zur Quantifizierung dieser Analyten mittels Ionenchromatographie-Elektrosprayionisation-Tandem-Massenspektrometrie wurde erfolgreich entwickelt und im Anschluss optimiert. Die Bestimmungsgrenzen bewegten sich zwischen 17 und 82 ng/L für Glyphosat und zwischen 37 und 54 ng/L für AMPA. Die Wiederfindung lag bei 26% bis 97% für Glyphosat und bei 63% bis 105% für AMPA. Die Komplexierung von Glyphosat mit organischem Kohlenstoff, der aus dem MIP ausgewaschen wurde, war anfangs für einen Verlust von 80% des Analyten verantwortlich. Die Zugabe von Natriumhy-

droxid erlaubte es, die Komplexierung aufzuheben und den Analyten zurückzugewinnen. Natürliches organisches Material in Wasser, das an das verwendete MIP band, konnte wirksam und ohne Verlust des Analyten durch die Elution der MIP-Kartusche über einer Umkehrphasenkartusche entfernt werden. δ^{13}C-Messungen der Analyten mittels LC/IRMS in Proben, genommen während verschiedener Schritte in der Probenaufarbeitung, zeigten keine Isotopenfraktionierung.

Die Ergebnisse dieser Arbeit zeigen, dass Methoden molekularen Prägens vor der CSIA ein wirksames Werkzeug für die selektive Extraktion/Aufreinigung von polaren organischen Mikroverunreinigungen sind. Zwei Ansätze fr die Anwendung von MIP während der Probenaufarbeitung sind möglich: (i) organische Extrakte wässriger Proben gewonnen durch Umkehrphasen-SPE können für eine weitere selektive Aufreinigung mit MIP verwendet werden, wohingegen (ii) wasserverträgliches MIP für die direkte Extraktion ionisierter organischer Schadstoffe aus Wasserproben verwendet werden kann. Die Kopplung der beschriebenen MIP-Methoden mit GC/IRMS und LC/IRMS erweitert die Anwendbarkeit der CSIA auf Umweltproben. In zukünftigen Studien mit CSIA können die entwickelten Ansätze angewandt und um viele weitere polare organische Schadstoffe erweitert werden. Somit ist es möglich, Ursprung und Verbleib dieser Schadstoffe in Feldstudien und Studien, welche ein gesamtes Einzugsgebiet umfassen, zu untersuchen. Damit eröffnet sich der CSIA ein bisher unzugängliches Anwendungsgebiet und folglich neue Perspektiven.

Chapter 1

Introduction

Organic chemicals are among the most common contaminants of natural waters impacting human health and the environment.[1,2] Increasing focus has been put in the recent years on polar organic micropollutants such as pesticides, consumer chemicals, and pharmaceuticals due to their frequent detection in natural water systems.[3–8] Despite their typical low occurrences at ng L^{-1} to µg L^{-1} range, ecotoxicological data raises concerns about the potential toxic effects on aquatic organisms.[9] Furthermore, persistence of many of these highly mobile contaminants may last for decades which increase their transport and consequently the impacted areas. For example, pesticides that have been long phased out of use are still detected in groundwater till today affecting the water quality and threatening the dependent users.[10]

The occurrence of such toxic or persistent organic micropollutant highlights the need for assessment of its degradation in the impacted environment. Unfortunately, demonstration of degradation under field conditions remains elusive.[11] Studies that use simulated systems, such as microcosms or lysimeters, are often challenging to extrapolate to the relevant impacted environments. On the other hand, significant changes in concentrations are not necessarily indicators of degradation since other concurrent processes in the impacted environment can affect concentration dynamics. In contrast, significant changes of isotope-ratios within the organic micropollutant is a conclusive indicator of the molecule breakdown.[12–15] Notably, the information provided by the isotopes is independent of mass balances or detection of transformation products.

1.1 Assessment of contaminants fate using compound specific isotope analysis

In recent years, the analysis of variations in stable-isotope composition at natural abundance has increasingly become a useful tool for source identification and in-situ (bio)degradation of contaminants.[12–18] Using gas- and liquid-chromatography coupled to isotope-ratio mass spectrometry, isotope ratios of many elements (e.g. H, C, N, O) can be measured in individual organic compounds.[19–23] The approach is referred to as compound-specific isotope analysis (CSIA). Stable-isotope ratio (R) of heavy isotope (^hE) to light isotope (^lE) for element E is usually measured relative to an international reference material ($R_{ref} = {}^h E/{}^l E_{ref}$) and expressed in the so-called delta notation ($\delta^h E$),

as shown in Equation 1.1:

$$\delta^h E = \frac{R}{R_{ref}} - 1 = \frac{{}^hE/{}^lE}{{}^hE/{}^lE_{ref}} - 1 \tag{1.1}$$

The concept of CSIA relies on the fact that only the formation or cleavage of a chemical bond in rate-determining step results in a significant change in the isotopic signature, $\delta^h E$, of a molecule.[12,13,15,24] Discrimination of isotopic signatures may happen during production of chemicals due to different precursor materials or manufacturing processes. In this way, constant isotopic signatures of the contaminant in the impacted environment can be used as fingerprints to allocate its source.[25–30] On the other hand, different reaction mechanisms may lead to observing a continuous isotopic fractionation over time that can be used as footprints to elucidate a possible pathway and its extent.[31–38] Despite the considerable advantages for CSIA, critical analytical challenges renders its application to environmental samples under field conditions difficult for polar organic micropollutant. The following section discusses in details these challenges and proposed strategies to overcome them.

1.1.1 Lack of selectivity in sample preparation

Isotope-ratio mass spectrometers (IRMS) are dedicated mass spectrometers for measurements of isotope ratios at natural abundance levels within required precisions of 10^{-4} to 10^{-6}.[39] Such high precisions with IRMS are possible only after conversion of the target analytes to small measurement gases, such as CO_2 and N_2, where a minimum mass of 10 ng C and 42 ng N is typically required.[40] Given the required mass for IRMS and the typical occurrences of polar organic micropollutants in aquatic environments at 0.1-1 µg L^{-1}, enrichment is inevitably required from large volumes of water exceeding 10 L. This corresponds to enrichment factors in the range from 10^5 to 10^8 as shown in Table 1.1.

Enrichment techniques using conventional sorbents such as reversed-phase solid-phase extraction (SPE) may have low breakthrough volumes for very polar organic compounds[41] but they are easy to scale up to obtain the required retention capacity. However, they lack selectivity to exclusively retain the analytes,[41,42] which leads to inevitable co-enrichment of organic matter from the natural water matrices. On the other hand, good chromatography is an essential key prior to CSIA where separation of the target analytes from other components in the sample is a prerequisite for measurements

of inherent isotopic signature of the individual analytes.[19,40,43,44] Unfortunately, the substantial amount of interfering organic carbon in the environmental extract is often not resolvable by the chromatography, which impedes acquisition of accurate and precise isotopic measurements for the target analytes[16] (see Figure 1.1).

Table 1.1: The enrichment factors required for extraction of polar organic micropollutants from environmental waters illustrated for benzotriazole, diclofenac, and metformin as examples for measurement on GC/IRMS.

	contaminant			
	benzotriazole	diclofenac	metformin	unit
structure	6	14	4	C
	3	1	5	N
	119	296	129	g/mol
environmental		100-1000		ng/L
occurrence	5.0-50	4.7-47	3.1-31	ng C L^{-1}
	2.5-25	0.3-3.4	3.9-39	ng N L^{-1}
IRMS		10×10^6		ng C L^{-1}
requirement[a]		42×10^6		ng N L^{-1}
minimum enrichment	**(2-20)$\times10^5$**	(2-21)$\times10^5$	(3-32)$\times10^5$	for δ^{13}C
factor	(2-17)$\times10^6$	**(1-12)$\times10^7$**	(1-11)$\times10^6$	for δ^{15}N

[a] calculated based on 10 ng C, 42 ng N[40] using splitless or on-column injection of 1 µL of the extract on GC/IRMS.

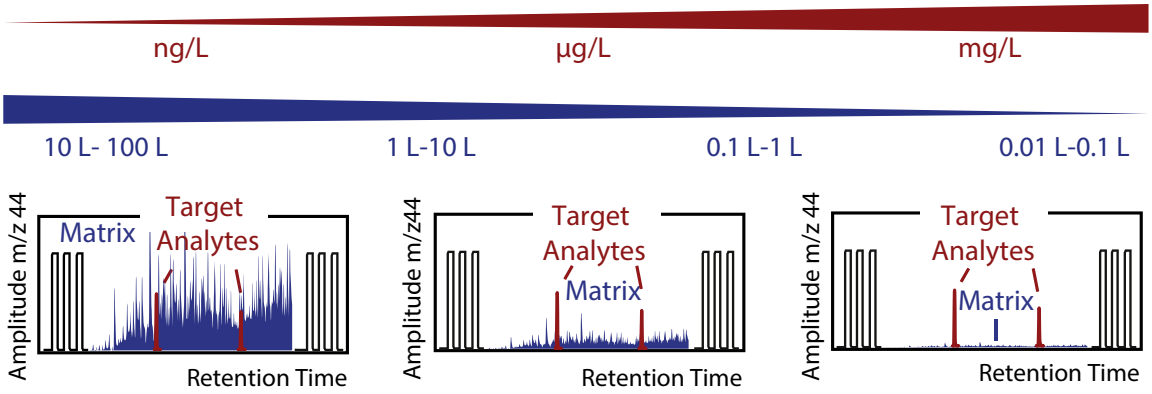

Figure 1.1: Correlation of pollutant's occurrence in natural waters (red scale) with the required sample volume for enrichment (blue scale) and its impact on carbon-isotope measurements (rectangular boxes). Adapted from Elsner and Imfeld[16].

The lack of selectivity in sample preparation is a major bottleneck for analysis of polar organic micropollutants in environmental waters.[41] Thus, increasing the selectivity for sample preparation procedures may offer a strategy for attenuation of the co-extracted matrix components . In the last two decades, the technology of molecular imprinting has offered stable synthetic polymers that possess specific recognition properties towards certain molecules.[45–50] The concept of molecular imprinting relies on complex formation between a functional monomer and the molecule of interest (called template) through covalent- or non-covalent bonds. Polymerization of the template-monomer complex with cross-linkers produces rigid polymers embedding the template in a conformational cavity. Once the template is removed, the free cavity in the produced polymer can act as a specific interaction site towards the imprinted molecule and closely-related structures. Stable-isotope analysis can benefit from the selectivity of imprinting techniques for sample preparation of environmental waters resulting in extracts that are clean enough to meet the stringent needs of GC/IRMS and LC/IRMS.

1.2 Molecular imprinting in environmental analytical chemistry

Different research domains have applied molecularly-imprinted polymers (MIP).[45] Environmental applications, for example, using triazine-imprinted polymers found in the database of molecular imprinting society[51] amounted to 136 papers as shown in Figure 1.2. Such studies included 50 on analytical chemistry for trace- and ultra-trace analysis,[52–54] 40 on sensing and rapid detection in the environment,[55–57] 35 on novel imprinting techniques,[58–60] 6 on water treatment for selective removal of pollutants,[61] and 4 on other domains such as catalytic degradation.[62] The prepared extracts using MIPs can be measured on different analytical instruments coupling various separation techniques with different detectors for quantification purposes. Separation techniques such as liquid chromatography (LC)[63,64], gas chromatography (GC)[53], and capillary electrophoresis (CE)[65] can be used. The most common applied detectors is ultra violet (UV)[52,63,65,66] and mass spectrometry (MS).[54,67] The imprinted-polymers are most frequently applied in SPE format,[66,68] whereas other formats such as solid-phase microextraction (SPME),[64] stir-bar sorptive extraction (SBSE),[69] and membrane extraction (ME)[70] are also found. For most analytical applications, non-covalent interactions are employed since reversible interactions between the target analyte and the imprinted

polymer are necessary in order to recover the sorbed analyte for measurement.[71] Non-covalent interactions such as hydrogen-bonding, ionic interactions, and $\pi - \pi$ stacking are therefore the most-widely employed forces in analytical chemistry, which means it is not likely to benefit from the more selective covalent interactions.[71]

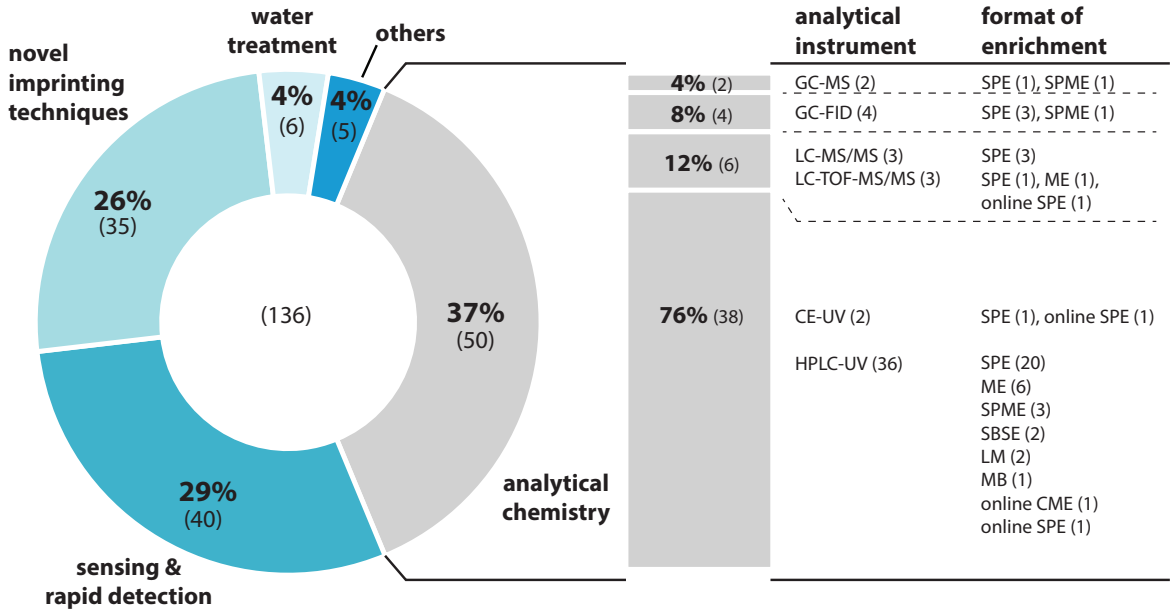

Figure 1.2: One-hundred thirty-six scientific publications on triazine-imprinted polymers listed by the database of society for molecular imprinting by 11 September 2017 (www.MIPdatabase.com). The pie chart represents the publication categories in bold text, the share of the corresponding category in bold percentage, and number of publications in parenthesis. The column in grey shows publication statistics for analytical chemistry applications along with the analytical instrument and format of enrichment.

1.2.1 Strategies for application to CSIA

To date, no studies have been seen that show the use of imprinted-polymers for any stable-isotope technique, including CSIA. The numerous studies published on the use of MIP in analytical chemistry are exclusively applied to the field of trace- and ultra trace analysis (i.e. quantification in the range ng L^{-1}-µg L^{-1}). While the chromatographic systems are similar for ultra trace analysis and CSIA, the detectors are very different, as well as the samples for end-measurements. Therefore, the pitfalls that may render the application of MIP to CSIA ineffective are highlighted in the next paragraphs along with proposed strategies to overcome the expected challenges.

Non-covalent imprinting using hydrogen-bonding is one of the most frequently ap-

plied approaches for imprinted polymers in analytical chemistry and it requires the use of aprotic porogens during synthesis to favor the template-monomer interactions. The formed imprint often shows the best recognition towards the target analyte when the sample is loaded from an aprotic solvent restoring thereby the prevailed conditions during imprinting. Thus, the large water volumes necessary for CSIA cannot be directly extracted on hydrogen-bonding-based-MIP since the analyte-imprint interaction can easily be disrupted by the abundant water molecules. (i) A two-steps enrichment approach can overcome this shortcoming whereby the first step uses conventional SPE to extract the target analyte and remove the disruptive water, whereas, the second step uses MIP after exchange to the compatible organic solvent for a selective cleanup of analyte-containing extract. (ii) On the other hand, direct enrichment of large volumes of water can be achieved for ionized organic molecules by employing ionic interactions where water molecules do not compete with the target analyte for the imprint.

Furthermore, forces employed for MIP such as hydrogen-bonding and ionic interactions exhibit enthalpies ranging from 8-60 kJ/mol compared to 0.1-1 kJ/mol for van der Waals and dipole-dipole interactions[72] which are typically exploited in reversed-phase SPE. Due to the stronger interactions employed for MIP, it is expected that MIP might be more prone to isotopic biases caused by incomplete recoveries of the target analytes. Quantification of the expected isotope effects might be necessary in case of incomplete recoveries. Full recoveries of the analytes from the MIP, on the other hand, can be paid additional attention in order to avoid such effects.

Extraction procedures for trace analysis use relatively small amounts of MIP sorbent (15-200 mg) which is sufficient for extracting enough analyte mass for UV and MS detectors. The absolute amount of target analytes required for CSIA is typically much higher and would therefore require larger amounts of sorbent. For example, Ferrer et al.[73] used 50 mg of MIP to enrich 100 mL groundwater spiked with 1 µg L^{-1} atrazine. To analyze the same water for $\delta^{13}C$ of atrazine on GC/IRMS, approximately 10 L are needed for extraction which means scaling up Ferrer et al. method by 100 would require 5 g MIP. The available enrichment protocols in literature can not, therefore, be used as is for CSIA purposes and development of enrichment protocols that meet CSIA requirements are necessary.

1.3 Objectives and approach

The overall goal of this work was to investigate effectiveness of molecularly-imprinted polymers (MIP) as a key step within sample preparation workflow for CSIA of polar organic micropollutants in natural waters. To this end, sample preparation methods using SPE and MIP were developed for 1*H*-benzotriazoles, glyphosate, AMPA, and triazines at µg L^{-1} range and in variant aquatic matrices such as river-, ground-, wastewater, and treated wastewater. Implementation of the MIP followed two approaches (i) after SPE using aprotic solvent which was applied to 1*H*-benzotriazole and triazines, and (ii) directly to water which was applied to glyphosate and AMPA. Along the variant steps of sample preparation, quantification of the investigated analytes was performed, as well as carbon- and nitrogen-isotope ratios measurements. The specific objectives of this work were the following:

1. To investigate the effectiveness of generic imprinting techniques on carbon- and nitrogen-isotope analysis of a polar organic micropollutant using the non-covalent approach.

2. To study the direct enrichment of ionized organic micropollutants from natural waters using water-compatible MIP and to investigate the associated matrix effects.

3. To study the effects of organic carbon in natural matrices on accuracy and precision of GC-IRMS measurements for aquatic samples prepared with and without selective cleanup with MIP.

In chapter 2, synthesis of benzotriazole-imprinted polymer was performed using methacrylic acid as a monomer and ethylene glycol dimethacrylate as crosslinker. The resulting polymer was investigated for selectivity, isotope fractionation, carbon- and nitrogen-isotope analysis of 1*H*-benzotriazole in river- and wastewater. Chapter 2 addressed objective 1.

Chapter 3 investigated the effects of dissolved organic carbon extracted from river water on carbon-isotope ratio measurements using GC-IRMS. It represents also a developed cleanup method and its impact on GC-IRMS measurements. Objective 1 and 3 are addressed in chapter 3.

Chapter 4 provides a systematic study of matrix effects associated with direct enrichment of glyphosate and AMPA on MIP from surface- and ground-water. The chapter represents analytical implications for concentration analysis using ion chromatography-electrospray ionization-tandem mass spectrometry (IC-ESI-MS/MS) and stable-isotope analysis using LC-IRMS. Objective 2 is addressed in chapter 4.

Chapter 5 presents the most important conclusions of the current work and highlights remaining open questions for future research.

Chapter 2

Synthesis, assessment, and application of molecularly-imprinted polymers for δ^{13}C and δ^{15}N measurements of $1H$-benzotriazole in aquatic environments

2.1 Introduction

The analysis of stable-isotope ratios in organic soil and water contaminants has become a widely used approach to identify sources of pollution and (bio)degradation pathways.[12–14,16,40,74,75] Whereas constant ratios of $^{13}C/^{12}C$, $^{2}H/^{1}H$, $^{15}N/^{14}N$, and of other elements in a compound enable one to infer precursor materials, synthesis routes, and formation pathways of pollutants,[25–30] changes of isotope ratios lead to stable-isotope fractionation patterns that reveal the (bio)chemical reaction by which a pollutant is degraded.[31–35,37] However, due to the high limits of detection of gas and liquid chromatography used in combination with isotope-ratio mass spectrometry,[19,23,76] the applications of compound-specific isotope analysis (CSIA) have largely focused on so-called legacy contaminants such as halogenated solvents and pesticides, nitroaromatic explosives, and fuel constituents .[77,78] Those compounds are often found in the high µg L^{-1} to mg L^{-1} concentration range and can be extracted from the environmental matrices in straightforward procedures, for example, through transfer of the analytes into the gas phase and enrichment onto solid sorbents .[36,79–82] Unfortunately, such procedures are not necessarily applicable for CSIA of polar organic micropollutants of current interest[2] such as pesticides, pharmaceuticals, and consumer chemicals. Their low µg L^{-1} concentrations in natural and treated waters require large sample volumes greater than 10 L by solid-phase extractions (SPE, e.g.,[83]) to obtain the necessary analyte mass for isotope ratio mass spectrometry. Moreover, the inherently poor selectivity of SPE-based procedures will inevitably lead to a co-enrichment of organic matter of unknown isotopic composition and thus compromise accurate isotope ratio measurements.

One promising option to increase the selectivity of sample preparation procedures is the use of molecularly-imprinted polymers (MIPs). MIPs are synthetic, typically custom-made materials capable of molecular recognition of a target analyte through specific intermolecular interactions.[84–88] Synthesis is carried out in presence of the target analyte and involves the polymerization of functional monomers that are selected based on their ability to interact with functional groups of the target molecule. Therefore, the final materials exhibit a three-dimensional structure with high specificity .[48] Even though the concept of solid-phase extraction with molecularly-imprinted solid-phase extraction (MISPE) has been used successfully for years,[84,89] it has never been applied in combination with isotopic analyses. In fact, MISPE based on non-covalent interaction between analyte and sorbent seems ideally suited for the treatment of SPE-extracts, in which polar organic micropollutants are normally enriched from large volumes of water

samples.[8] Only µL volumes of organic solvents can be injected onto gas chromatographs coupled to isotope-ratio mass spectrometers. The substantial analyte enrichment to the mg L^{-1} level causes concomitant enrichment of organic matrix and, therefore, requires further cleanup of the extract. Because those extracts typically consist of organic solvents, polar organic micropollutants can be cleaned up based on H-bonding with the MIP without interferences of water.

The goal of this work was to explore sample treatment strategy based on generic imprinting technique, using the non-covalent approach, for stable-isotope analysis of polar organic micropollutants in aquatic environments. The work focused on the analysis of δ^{13}C and δ^{15}N of 1*H*-benzotriazole (1H-BT) as a model compound for polar organic micropollutants that is frequently used as corrosion inhibitor in different consumer chemicals. Like many polar organic micropollutants, 1H-BT is too persistent to be degraded in waste water treatment plants (WWTP) and therefore found in µg L^{-1} concentrations in rivers as well as in influents and effluents of WWTPs.[90–92] The specific objectives of this work were to (a) synthesize benzotriazole-imprinted polymer and assess its specificity towards 1H-BT in comparison with closely-related structures, (b) develop sample treatment procedures including MISPE in multi-steps approach for stable-isotope analysis of 1H-BT, and (c) illustrate the applicability of MISPE-based procedures for CSIA in different matrices through analysis of δ^{13}C and δ^{15}N of 1H-BT in riverwater, influent and effluent of a WWTP, as well as in dishwasher detergent taps.

2.2 Experimental section

A list of all chemicals including suppliers and purities is provided in the supporting information S2.1. Suppliers of the investigated dishwasher detergents, as well as their formats and contents of 1*H*-benzotriazole are provided in S2.2.

2.2.1 Safety considerations

Milling and sieving the synthesized polymers can generate dust. The processing of materials should therefore be carried out under the fumehood. Additionally, gloves, goggles and respiration mask are advised to be worn. The radical generator, azobisisobutyronitrile, decompose at temperatures $\geq$ 45 °C and may explode if large amounts are exposed to high temperatures. Do not exceed a temperature of 40 °C during its purification.

2.2.2 Synthesis of molecularly-imprinted polymers

Molecularly-imprinted polymers (MIP) were synthesized following the non-covalent approach adapted from Chapuis et al.[93] for imprinting terbuthylazine. The polymerization mixture consisted of 119.1 mg (1 mmol) 1*H*-benzotriazole (1H-BT) as template, 344.4 mg (4 mmol) methacrylic acid as a functional monomer, 3964 mg (20 mmol) ethylene glycol dimethacrylate as crosslinker, 39.4 mg (0.24 mmol) azobisisobutyronitrile as radical generator, and 5.6 mL dichloromethane as porogene. We dissolved the template in the functional monomer, cooled the solution to 0 ℃ for 15 minutes and added the crosslinker, the porogene, and the radical generator, sequentially. The polymerization mixture was purged with N_2 in a borosilicate glass tube (OD = 18 mm, ID = 15 mm), sealed with a screw-cap, and placed in an ice bath for 30 minutes.

Polymerization took place over 24 hours at 2 ± 0.2 ℃ by immersing the glass tubes in a merry-go-round photoreactor (DEMA model 125, Hans Mangels GmbH, Bornheim-Roisdorf, Germany). The photoreactor was centered with Heraeus Noblelight MP Hg lamp (model TQ 150) operating at 150 W and surrounded by a borosilicate glass jacket (see S2.4). Additionally, the photoreactor was filled with a nitrate filter solution 0.15 M to cut off wavelengths < 320 nm.

After polymerization, the tubes were removed and crushed to recover the polymer monoliths. The polymers were sequentially ground (Mixer Mill MM 301, Retsch GmbH, Germany) and sieved through 100 µm sieve (Retsch GmbH, Germany). The particle fraction < 100 µm was sedimented in methanol to obtain particle size distribution between 20 and 100 µm. We removed the template by ten repetitive cycles of Soxhlet extraction using mixtures of methanol and formic acid (90/10 vol%) until $\geq 98\%$ of the 1H-BT was recovered. Non-imprinted polymers were extracted in the identical manner. For the quantitative assessment of imprinting efficiency, the identical procedure was applied to synthesize a non-imprinted polymer (NIP) where the template was absent, as well as a MIP with 5,6-dimethyl-1*H*-benzotriazole as a template.

2.2.3 Sample preparation procedures using MISPE

The multi-steps procedure for extraction and cleanup of 1H-BT in (a) influent an effluent of waste water treatment plants (WWTP), (b) spiked river water, and (c) dishwasher tabs is shown schematically in Figure 2.1. Conceptually, sample preparation consisted of conventional solid-phase extraction (SPE, Figure 2.1, step **B**) and molecularly-imprinted solid-phase extraction (MISPE, Figure 2.1, step **D**) with different pre- and post treatments.

Extraction and cleanup of 1*H*-benzotriazole from waste water plant influent and effluent

In Step **A**, samples **1** in Figure 2.1 from WWTP influent (5L) and effluent (10 L) were filtered through 0.7 µm glass fiber filters (Whatman, GF/F 47mm) and acidified with HCl (32 %) to pH 2.0. Filtered samples **2** which contain 1H-BT were extracted by conventional SPE, in step **B**, using OASIS HLB cartridges (Waters, 6 g, 35 mL) and a 12-port vacuum extraction manifold (Supelco, Switzerland). Prior to sample loading, cartridges were conditioned with 100 mL hexane, 100 mL ethyl acetate, 100 mL methanol and 100 mL MiliQ water. Water samples **2** were percolated through the cartridges using a vacuum pump at a flow rate of $\leq$ 7.2 mL min^{-1} corresponding to a linear velocity of $\leq$ 1.6 cm s^{-1}. Subsequently, the cartridges were dried under vacuum overnight and eluted in 100 mL of ethylacetate. In step **C**, the SPE eluates **3** were dried using rotary vacuum evaporator (Büchi, Switzerland) at 40 ℃ under a gentle stream of N_2. The dry residues were reconstituted in 5 mL of aprotic organic solvent (**4**), that is a dichloromethane/toluene/acetonitrile mixture (55/40/5 vol%), in preparation for MISPE.

For 5 mL of sample **4** in step **E**, 3 g sorbent of the 1H-BT-imprinted polymer was packed in PP tubes (12 mL) and conditioned with 50 mL methanol/formic acid (90/10 vol%), 50 mL methanol, and 50 mL dichloromethane/toluene/acetonitrile (55/40/5 vol%). Following sample percolation, the sorbent was washed with 40 mL dichloromethane/toluene/acetonitrile (55/40/5 vol%). Thereafter, the sorbed analytes were eluted with 10 mL methanol. Throughout the sample percolation, wash, and elution steps, the flow rate did not exceed 0.5 mL min^{-1} or 0.25 cm s^{-1}. In step **F**, the MISPE eluate **5** was evaporated under a gentle stream of N_2 and reconstituted in 1 mL methanol, followed by a liquid-liquid extraction with *n*-hexane. The methanol extract was ex-

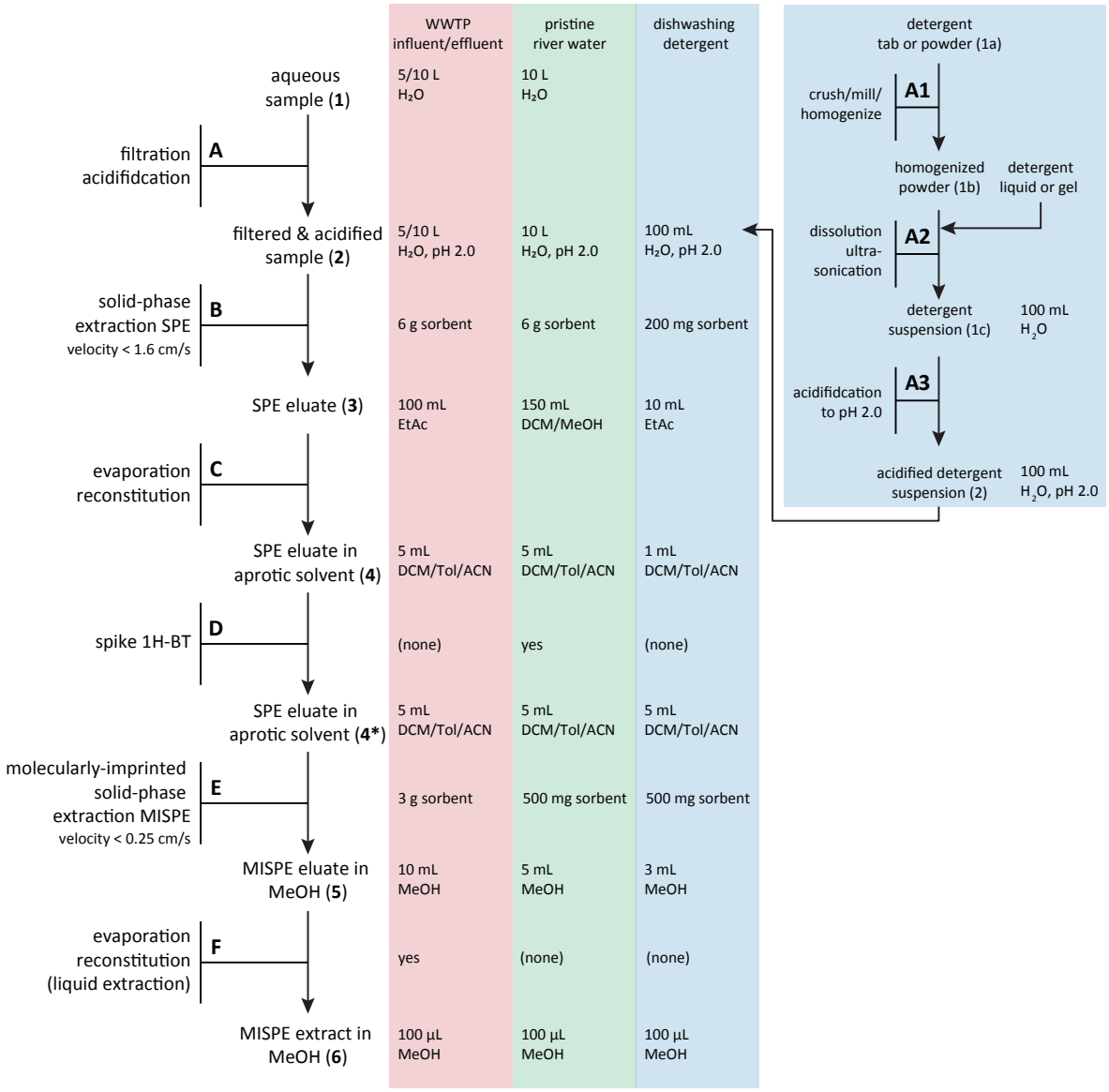

Figure 2.1: Sample preparation procedure for analysis of 1*H*-benzotriazole (1H-BT) from different water matrices (influent and effluent of waste water treatment plants (WWTP), spiked river water, and dishwasher detergents. Capital letters **A** to **F** stand for treatment steps, bold numbers **1** to **6** refer to samples obtained throughout the treatment sequence. Acronyms of organic solvents stand for acetonitrile (ACN), ethylacetate (EtAc), dichloromethane (DCM), methanol (MeOH), and toluene (Tol). Details on the specific initial processing steps of solid, gel-like, and liquid dishwasher detergents are shown in the upper-right box.

tracted five times with 1 mL *n*-hexane for each extraction step. The *n*-hexane extracts (5 mL) were evaporated again and reconstituted in methanol to obtain target analyte concentrations within the linear range of the gas chromatography coupled to isotope-ratio mass spectrometry (see below).

Cleanup of 1*H*-benzotriazole from spiked river water

Extraction of environmental matrix from 10 L river water followed the same procedure described above with some minor modifications (Figure 2.1). In step **B**, the cartridge was eluted with 150 mL of dichloromethane/methanol (97/3 vol %). In step **C**, the sample was evaporated and reconstituted in 5 mL dichloromethane/toluene/acetonitrile (55/40/5 vol %). Thereafter, step **D**, 50 µL of a 10 mmol L^{-1} solution of 1H-BT were spiked to SPE eluate **4**. The 1H-BT concentration in **4*** represents a river water sample **1** with 1H-BT concentration of 6.0 µg L^{-1}. The 5 mL of **4*** was purified with MISPE in step **E**, for which 500 mg of polymer was packed in PP tubes (6 mL), conditioned as described above and used with a flow rate of $\leq$ 0.3 mL min^{-1} or $\leq$ 0.25 cm s^{-1}. The MISPE eluate **5** was then evaporated under a gentle stream of N_2, in step **F**, to 100 µL without liquid-liquid extraction.

Extraction and cleanup of 1*H*-benzotriazole from dishwasher detergent

Samples from different dishwasher detergents required additional pre-treatment prior to SPE as illustrated in Figure 2.1, steps **A1** to **A3**. Detergent tabs were crushed using a mortar and pestle and then dried in the oven along with the powder detergents at 40 ℃ overnight. The crushed tabs and powders were then milled and homogenized in a ball mill with a frequency of 30 Hz for 2 mins (**A1**). One hundred milligram of the homogenized detergent powder or unprocessed liquids and gels (**1b**) were dissolved in 100 mL water and ultra-sonicated for 15 min in step **A2**. The detergent suspension **1c** was acidified in step **A3** to pH 2.0 using HCl 20% leading to an acidified detergent suspension (**2**). The latter was subsequently treated according to the steps outlined in Figure 2.1.

In step **B**, the acidified detergent suspensions were extracted using SPE on OASIS HLB cartridges (Waters, 200 mg, 6 mL) at flow rates $\leq$ 1.9 mL min^{-1} or $\leq$ 1.6 cm s^{-1}. The cartridges were eluted with 10 mL ethyl acetate. In step **C**, evaporation/reconstitution resulted in 1 mL dichloromethane/toluene/acetonitrile (55/40/5

vol%) mixture. Samples **4** were purified in step **E** using MISPE with 500 mg sorbent of 1H-BT-imprinted polymer which was packed in PP tubes (6 mL) and conditioned as described above. After sample percolation, the sorbent was washed with 8 mL of dichloromethane/toluene/acetonitrile (55/40/5 vol %). Elution of 1H-BT was carried out with 3 mL methanol. The evaporation/reconstitution in step **F** yielded 100 µL methanolic solution.

2.2.4 Isotope fractionation experiments

The extent of C and N isotope fractionation of 1H-BT from incomplete recovery during a MISPE procedure, step **E**, was tested in a three-steps procedure in the presence and absence of organic matrix from river water samples. (*a*) Two samples which contained 100 µmol L^{-1} 1H-BT in either 5 mL river water extract in dichloromethane or in neat dichloromethane were loaded onto two separate MIP-containing cartridges while the breakthrough was collected (F_1, "load" fraction). Thereafter, (*b*) the MISPE cartridges were washed with 5 mL dichloromethane leading to another set of 1H-BT-containing samples (F_2, "wash" fraction). Lastly, (*c*) the remaining 1H-BT on the MISPE cartridges was eluted using 5 mL methanol (F_3, "elute" fraction). The volume of all three fractions were blown down to 100 µL prior to quantification and stable-isotope analysis of 1H-BT.

2.2.5 Chemical and stable-isotope analyses

Quantification of analytes in aqueous and organic matrices

Quantification of benzotriazoles and other organic compounds in standard solutions were performed with high-performance liquid chromatography (HPLC) using a Dionex Ulti-Mate 3000 System (Thermo Scientific). Separation was performed on Supelcosil LC-18 column (250 x 4.6 mm, 5 µm, Supelco) with isocratic mixtures of water/methanol (70/30 vol%) at a flow rate of 1.0 mL min^{-1}. UV-Vis detection was carried out using photodiode array detector (PDA-3000, Thermo Scientific) at wavelengths of maximum absorption for each compound. Analyte concentrations in organic solvents were measured after evaporating the solvent to dryness and reconstituting the dry residues in water/methanol mixtures (70/30 vol%). Samples of 20 µL were injected using a temperature-controlled autosampler at 10°C.

Concentrations of benzotriazoles in river and waste water samples were determined

by liquid chromatography coupled to a linear ion trap-Orbitrap high-resolution mass spectrometer (LTQ-Orbitrap XL, Thermo, Waltham, MA) using electrospray ionization in the positive mode. The detailed method is described by Huntscha et al.[92]

Organic carbon measurements

Dissolved and total organic carbon concentrations (DOC, TOC) were measured using a total organic carbon analyzer (TOC-L, Shimadzu) equipped with a combustion catalytic oxidation unit (680 °C) and a non-dispersive infrared detector. DOC concentrations in river and waste water samples were carried out after filtration through a 0.45 µm filter. TOC concentrations in samples dissolved in organic solvents were determined on the TOC analyzer after evaporation of the solvent under a gentle stream of N_2 for 30 min followed by reconstititution of the dry residues in water using ultra-sonication for 15 min and homogenization for 10 min using stand dispersion unit (Polytron PT 3100, Kinematica).

Compound-specific isotope analysis

C and N isotope-ratio measurements of 1H-BT was carried out as described by Spahr et al.[94] using gas chromatography/isotope-ratio mass spectrometry (GC/IRMS) and a customized nickel/platinum reactor for analyte combustion at 1000℃. Liquid samples of 1 µL were injected into a split/ splitless injector coupled to a RTX-5 Amine GC column (30 m × 0.32 mm). Helium was used as a carrier gas at a constant pressure of 100 kPa. The temperature program was 1 min at 80 ℃, ramped by 15 ℃ min^{-1} to 180 ℃, held for 10 min, ramped by 40 ℃ min^{-1} to 250 ℃, and held for 5 min.

Isotope ratios are reported in per mil (‰) relative to the international reference materials Vienna PeeDee Belemnite ($\delta^{13}C_{VPDB}$) and air ($\delta^{15}N_{air}$). The reported values are arithmetic means of at least triplicate measurements with one standard deviation ($\pm\sigma$) as a measure of the uncertainty in the form of isotope signatures ($\delta^{13}C$ and $\delta^{15}N$) We used a suite of calibrated reference materials with $\delta^{13}C$ from −54.6‰ to +7.7‰ and $\delta^{2}H$ from −6‰ to +41‰[95,96] as well as repeated measurements of in-house standards (benzotriazoles) in a standard bracketing procedures to ensure accuracy of the measured $\delta^{13}C$ and $\delta^{15}N$ values.

2.2.6 Data evaluation

Selectivity of molecularly-imprinted polymers

The selectivity of the produced polymers were assessed by high-performance liquid chromatography (HPLC)[97] using a stainless-steel column (53.0 x 3.0 mm, Bischoff, Germany) connected to a pre-column (14 x 3.0 mm). Both pre-column and main column were dry-packed with either MIP or NIP and connected to an HPLC pump. Methanol at a flow rate of 2.0 mL min^{-1} was used as eluent to condition and to compress the sorbent in the column. Once a constant back-pressure was maintained in the HPLC system over at least 120 min, the eluent was stopped and the pre-column was removed leaving the main column for characterization of (a) capacity factors, (b) imprinting factors, and (c) enthalpies of analyte-polymer interaction.

(a) Capacity factors, k_i, of benzotriazoles and other organic compounds on the synthesized polymers were determined with eq. 2.1 using an HPLC system equipped with UV-Vis detector, an autosampler, and a column oven. Chromatographic conditions included acetonitrile as eluent at a constant flow rate of 0.1 mL min^{-1}, 50 µL injection volume of solutions containing the target compounds at concentrations between 5 and 7 mg L^{-1} in acetonitrile, UV detection at the corresponding wavelength of maximum absorbance.

$$k_i = \frac{t_i - t_0}{t_0} \tag{2.1}$$

where k_i is the capacity factor of the analyte i on the synthesized polymer, t_i and t_0 are retention times of the analyte and the conservative tracer (acetone), respectively.

(b) Imprinting factors, IF_i, are calculated with eq. 2.2 for each analyte i as the ratio of its capacity factors obtained using the imprinted polymer ($k_{i,\mathrm{MIP}}$) and non-imprinted polymer ($k_{i,\mathrm{NIP}}$), respectively.

$$IF_i = \frac{k_{i,\mathrm{MIP}}}{k_{i,\mathrm{NIP}}} \tag{2.2}$$

(c) Enthalpies of interaction between the analyte and the synthesized polymers, ΔH_i, were calculated from the slope of van't Hoff equation, eq. 2.3, where the natural logarithm of capacity factors at three temperatures (278, 288, and 298 K) were plotted versus the corresponding reciprocal absolute temperatures ($1/T$). See section S2.5 for

derivation.

$$\frac{d \ln k_i}{d\,(1/T)} = -\frac{\Delta H_i}{R} \tag{2.3}$$

where R is the gas constant.

Isotope fractionation during analyte cleanup with molecularly-imprinted solid-phase extraction

Comparison of the mass of 1H-BT in each of the three fractions, F_1 to F_3, of the isotope fractionation experiment with the initially added 0.5 µmol enabled determination of the mass fraction, m_i, of 1H-BT in each collected fraction. The mass fractions m_i were used in isotopic mass balances to assess the extent of possible isotope fractionation, Δ^hE, during the MISPE cleanup process in case of incomplete recoveries, referred as step **E** in Figure 2.1. The extent of C and N isotope fractionation, Δ^hE, was derived based on an isotopic mass balance using eq. 2.4.

$$\Delta^h\mathrm{E} = \delta^h\mathrm{E}_0 - \sum_{i=1}^{3} \left(m_i \cdot \delta^h\mathrm{E}_i\right) \tag{2.4}$$

where $\delta^h\mathrm{E}_0$ and $\delta^h\mathrm{E}_i$ are the C and N isotope signatures of 1H-BT measured in the stock solution as well as in the three sample fractions F_i, respectively, and m_i is the mass fraction of 1H-BT therein.

The operational N isotope enrichment factor, ε_N, for the MISPE cleanup step **E** was obtained through non-linear regression of eq. 2.5.

$$\frac{\delta^{15}\mathrm{N}_{i,\mathrm{MIP}} + 1}{\delta^{15}\mathrm{N}_0 + 1} = (f_{i,\mathrm{MIP}})^{\varepsilon_\mathrm{N}} \tag{2.5}$$

where $f_{i,\mathrm{MIP}}$ is the remaining fraction of 1H-BT associated with MIP after an elution step. $f_{i,\mathrm{MIP}}$ of the "load" and "wash" fractions (F_1 to F_2) were calculated with eq. 2.6. The N isotope signature of 1H-BT associated with the MIP after elution step i, $\delta^{15}\mathrm{N}_{\mathrm{MIP},i}$, was derived through a mass balance approach as in eq. 2.7. Note that eq. 2.7 that was applied to calculate $\delta^{15}\mathrm{N}_{i,\mathrm{MIP}}$ for F_1, whereas $\delta^{15}\mathrm{N}_{i,\mathrm{MIP}}$ of F_2 corresponded to the δ^{15}N-value of 1H-BT recovered in the methanolic extract. The N isotope enrichment factor, ϵ_N, was obtained through non-linear regression of eq. 2.5 and the corresponding

apparent kinetic isotope effect, ^{15}N-AKIE, from eq. 2.8.

$$f_{i,\mathrm{MIP}} = 1 - \sum_{i=1}^{i-1} m_i \tag{2.6}$$

$$\delta^{15}\mathrm{N}_{i,\mathrm{MIP}} = \frac{\delta^{15}\mathrm{N}_0 - \sum (m_i \cdot \delta^{15}\mathrm{N}_i)}{1 - \sum m_i} \tag{2.7}$$

$$^{15}\mathrm{N\text{-}AKIE} = \frac{1}{1 + \epsilon_\mathrm{N}} \tag{2.8}$$

The deviation of the measured δ^{15}N from the accurate value due to incomplete analyte recovery, Δ, was quantified with a modified form of eq. 2.5 as in eq. 2.9.

$$\Delta = \delta^{15}\mathrm{N}_0 - \theta^{\epsilon_\mathrm{N}}(\delta^{15}\mathrm{N}_0 + 1) + 1 \tag{2.9}$$

where Δ is the expected deviation of δ^{15}N and θ is the fractional analyte recovery.

2.3 Results and Discussion

2.3.1 Isotope analysis of 1*H*-benzotriazole after selective cleanup from spiked river water

The applicability of MIP for selective analyte cleanup was evaluated for CSIA in river water spiked with 1H-BT. Figure 2.2 shows the chromatograms for C isotope-ratio measurements of 1H-BT for a sample taken at selected treatment steps as illustrated in Figure 2.1. The top panel in Figure 2.2 corresponds to the SPE eluate **4***, to which the 1H-BT standard was added in an amount that would correspond to an aqueous concentration 6.0 µg L^{-1} in the original water sample (**1** in Figure 2.1). The retention time of 1H-BT is indicated with a dashed line and the chromatogram of 1H-BT standard in dichloromethane is shown at the bottom of Figure 2.2. The chromatogram illustrates that a conventional enrichment of micropollutants from aqueous samples with SPE procedures (steps **A** to **C**, Figure 2.1) is concomitant with the accumulation of organic matrix. The isotopic composition of the organic matrix is not known a priori and therefore the resulting background signals interfere with accurate C isotope-ratio measurements by GC/IRMS[19,40,43,44]. Qualitative evidence for the selectivity of 1H-BT

retention on the MISPE during sample preparation in step **E** was obtained from washing the MISPE with dichloromethane/toluene/acetonitril 55/40/5 vol% (Figure 2.2, SPE eluate (**4***) wash). Due to the specific interactions of the MIP with 1H-BT, the analyte is no longer found in the sample, whereas, the chromatogram of the organic matrix looks largely identical to the one of the loaded SPE eluate. Lastly, the MISPE eluate **5** obtained from washing the polymer with methanol contains primarily 1H-BT (green line in Figure 2.2). This observation further confirms the selectivity of the synthesized polymer. The excellent recovery of 1H-BT in the MISPE eluate **5** of $103 \pm 5\%$ was a prerequisite for accurate isotopic analysis. Indeed, the deviation of C and N isotope signatures from its original value $\Delta^{13}C$ and $\Delta^{15}N$ where $0.5 \pm 0.4‰$ and $0.6 \pm 0.4‰$ and thus within analytical uncertainty of typical GC/IRMS measurements[40,98].

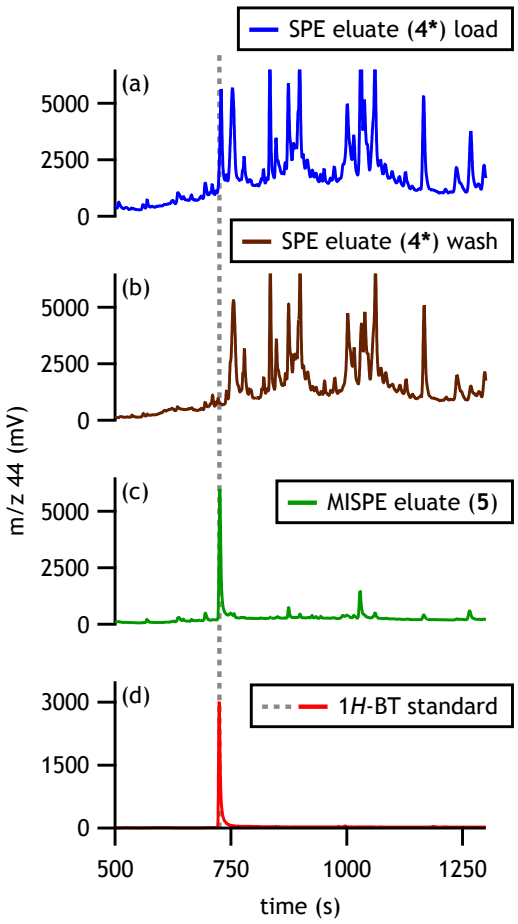

Figure 2.2: Comparison of GC/IRMS chromatograms for C isotope-ratio measurement through the operational procedure for cleaning up (a) SPE eluate of river water spiked with 1H-BT, (b) its eluate after washing the MISPE, (c) the MISPE extract **5** in methanol, and (d) a standard solution of 1H-BT.

2.3.2 Quantitative evaluation of imprinting efficiency

Selectivity of 1*H*-benzotriazole (1H-BT) retention on the produced molecularly-imprinted polymer (MIP) was assessed by quantifying imprinting factors (*IF*) using eq. 2.2, the enthalpies of interaction of 1H-BT with the MIP (ΔH_{MIP}), and with the non-imprinted polymer (NIP, ΔH_{NIP}). Those numbers are compared in Table 2.1 with a series of structurally-related compounds namely, methyl-substituted benzotriazoles (1-CH_3-BT, 5-CH_3-BT, 5-,6-$(CH_3)_2$-BT), as well as benzothiazole, naphthalene, and atrazine. *IF*-values > 1.0 were observed, which are indicative of selective binding of the target molecule to the MIP, for 1H-BT and the two aromatic ring substituted benzotriazoles, 5-CH_3-BT and 5-,6-$(CH_3)_2$-BT. No selectivity, that is $IF \leq 1.0$, were found for other compounds including *N*-substituted 1-CH_3-BT as well as benzothiazole, naphthalene, and atrazine. Note that the magnitude of *IF*-values not only depends on the interactions of analyte and polymer but also on that of the solvent used in the experiments[99]. Whereas the numbers shown in Table 2.1 may appear small, the precision of *IF*-values of < 0.1 (95% confidence intervals) are sufficient for comparison among different organic analytes here.

Imprinting factors of benzotriazoles were highest for the template molecule 1H-BT and decreased in the order 1H-BT > 5-CH_3-BT > 5-,6-$(CH_3)_2$-BT > 1-CH_3-BT. The observed sequence agrees with the notion that *IF* are highest for the template used for synthesis[100]. This outcome was verified by assessing *IF* of the same analytes on another custom-made MIP, where 5-,6-$(CH_3)_2$-BT was employed as a template instead of 1H-BT. The $IF_{(CH_3)_2-\mathrm{BT}}$-values are shown in Table 2.1 for the 5-,6-$(CH_3)_2$-BT-imprinted MIP and they are of similar magnitude as *IF*-values for 1H-BT imprinted polymers. $IF_{(CH_3)_2-\mathrm{BT}}$ decrease in the sequence 5-,6-$(CH_3)_2$-BT > 5-CH_3-BT > 1H-BT > 1-CH_3-BT confirming that the selectivity was highest for the template molecule. For both MIPs, no selective interactions was observed for 1-CH_3-BT. Absence of selectivity for *N*-substituted benzotriazole suggests that the interactions of analytes with the polymer was based on hydrogen-bonding of the triazole moiety with the carboxylic acid functional group of the monomer (methacrylic acid, Figure 2.3). Substitution at the 1*H* position on the triazole ring caused complete loss of selectivity towards 1-(CH_3)-BT on both polymers.

Further evidence for the selectivity of the MIPs was obtained from the comparisons of interaction enthalpies, ΔH_{MIP}, with different analytes, and interaction enthalpies of non-imprinted polymers, ΔH_{NIP} (Table 2.1). ΔH_{MIP} were most negative, that is

Table 2.1: Comparison of imprinting factors (IF) and enthalpies of interaction (ΔH) for 1H-benzotriazole (1H-BT), 5-methyl-1H-benzotriazole (5-CH_3-BT), 5,6-dimethyl-1H-benzotriazole (5-,6-$(CH_3)_2$-BT), 1-methyl-benzotriazole (1-CH_3-BT), benzothiazole, naphthalene, and atrazine

Parameter	1H-BT	5-CH_3-BT	5-,6-$(CH_3)_2$-BT	1-CH_3-BT	benzothiazole	napthalene	atrazine
IF [a]	**1.5**	**1.3**	**1.2**	1.0	0.9	0.9	1.0
$IF_{(CH_3)_2-BT}$ [b]	1.1	1.3	1.6	1.0	n.a. [c]	n.a.	n.a.
ΔH_{MIP} [d,e]	–13.5±0.2	–12.8±0.4	–12.2±0.1	–9.8±0.3	–10.8±0.1	–7.1±0.0	–16.3±0.7
ΔH_{NIP} [d,e]	–9.5±0.5	–10.5±0.1	–10.5±0.2	–9.5±0.2	–10.8±0.2	–7.0±0.1	-15.8±0.2
$\Delta H_{MIP} - \Delta H_{NIP}$ [d,e]	**–4.0±0.5** [d]	**–2.3±0.4**	**–1.7±0.2**	–0.3±0.3	0.0±0.2	0.1±0.1	–0.5±0.8

[a] MIP imprinted with 1H-BT as template, all values exhibit 95% confidence interval of $\pm \leq 0.1$; [b] MIP imprinted with 5-,6-$(CH_3)_2$-BT as template; [c] n.a. = not available; [d] in kJ/mol; [e] propagated uncertainties reflect 95% confidence intervals.

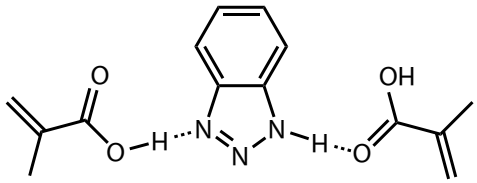

Figure 2.3: Hydrogen bonding between the template, 1H-BT, and the functional monomer, methacrylic acid, used for imprinting.

most favourable, for the template molecule 1H-BT and became less negative for the substituted benzotriazoles. ΔH_{MIP}-values ranged between 7.0 and 16 kJ/mol which is in the lower range of interaction enthalpies for hydrogen bonding (8-84 kJ/mol,[72,101]). Note that interactions of benzotriazoles with non-imprinted materials were also exothermic but the difference between MIP and NIP, $\Delta H_{\mathrm{MIP}} - \Delta H_{\mathrm{NIP}}$, revealed the larger selectivity of the MIPs. $\Delta H_{\mathrm{MIP}} - \Delta H_{\mathrm{NIP}}$ for benzotriazoles followed the same sequence reported for *IF*-values. However, the differences were close to zero for the remaining compounds showing the lack of selective interactions of the MIP with benzothiazole, naphthalene, and atrazine.

2.3.3 Isotope fractionation from incomplete analyte recovery

The extent of C and N isotope fractionation from analyte-MIP interactions was quantified in a separate experiment on MISPE cleanup in step **E** (Figure 2.1). Table 2.2 shows mass fractions, m_i, and the corresponding δ^{13}C and δ^{15}N-values of 1H-BT recovered in three sample fractions (F_i) and the total mass balance of 1H-BT. F_1 corresponds to the fraction of analyte collected after breakthrough during the cartridge loading with 1H-BT in dichloromethane and amounted to 41% of the total analyte mass. F_2 is the fraction of analyte obtained through washing of the cartridge with the identical solvent recovering 42%. F_3 reflects the remaining 16% of 1H-BT that were recovered from the MISPE through elution with methanol.

The C isotope signatures of 1H-BT in the presence and absence of organic matrix from river water samples varied only slightly (±1‰) in the three fractions. The extent of C isotope fractionation pertinent to the MISPE cleanup step, Δ^{13}C, was negligible regardless of the sample matrix (-0.6 ± 1.4‰ and 0.1 ± 1.1‰, Table 2.2). In contrast, δ^{15}N values of 1H-BT varied substantially (up to 13‰) between the three sample fractions. Due to the almost complete mass balance of the analyte, MISPE-induced N isotope fractionation is, nevertheless, negligible within uncertainty in both sample

matrices (-1.4 ± 1.3‰ and -0.2 ± 1.1‰).

These observations suggests that a non-stoichiometric recovery of the analyte after the MISPE cleanup step would not cause systematic C isotope fractionation whereas N isotope signatures could be biased towards more positive δ^{15}N values. We tentatively quantified an operational N isotope enrichment factor, ε_{N}, from the small data set for the MISPE cleanup step **E** in absence of organic matrix (eq. 2.5). Figure 2.4 shows the average N isotope signatures of 1*H*-BT that remained associated with the MIP ($\delta^{15}\mathrm{N}_{i,\mathrm{MIP}}$, eq. 2.7) after sequential loading step F_1 and F_2, respectively (blue and green areas). The most enriched fraction of 1*H*-BT, F_2, with a δ^{15}N of -18.1 ± 0.9‰, was eluted from the MIP through the change of solvent (red area in Figure 2.3). The N isotope fractionation trend was quantified with an ε_{N} of -5.0 ± 2.2‰ (eq. 2.5) and illustrates that the ^{15}N-containing 1*H*-BT is retained preferentially by the MIP. This isotopic preference corresponds to an isotope effect of 1.0054 ± 0.0022 under the chosen experimental conditions and confirms the above conclusion that the selectivity of the MIP is indeed based on H-bonding withe the triazole moiety of the analyte (Figure 2.3). Finally, the isotope effect implies that 1*H*-BT recoveries during the MISPE cleanup step of $\geq 81\%$ are sufficient to limit such shifts of δ^{15}N to ≤ 1.1‰ (eq. 2.8), that is to the typical precision of N isotope ratio measurements by GC/IRMS[40].

2.3.4 Application in waste water treatment plants

The sample preparation procedures shown in Figure 2.1 were applied to determine the C and N isotope signatures of 1H-BT in the influent and effluent of a WWTP, one of the frequently encountered matrices of the micropollutant with DOC contents of several mg C L^{-1}.[91,92] The outcome was verified through a comparison of δ^{13}C and δ^{15}N values with those form 1H-BT in dishwasher detergents sold in villages that discharge their sewer into the studied WWTP.

Figure 2.5 shows the δ^{13}C and δ^{15}N values of 1H-BT in the influent and effluent of the WWTP as well as in dishwasher detergents sold by retailers in the study area. δ^{13}C and δ^{15}N values of 1H-BT in dishwasher detergents span from -27‰ to -23‰ and -11‰ to 1‰, respecitvely. δ^{13}C cover a similar range observed previously by Spahr et al.[94] with a simplified approach whereas this work reveals an even wider distribution of δ^{15}N in 1H-BT. The waste water samples (**2** in Figure 2.1) contained substantial amounts of DOC that amounted to 7.3 and 28 mg C L^{-1} for effluent and influent, respectively. Substantial interferences on C isotope-ratio measurements were found after MISPe (**5** in

Table 2.2: Sample fractions of 1H-BT, F_i collected during the MISPE cleanup step **E** (Figure 2.1): mass fractions of 1H-BT, m_i, C and N isotope signatures, δ^{13}C and δ^{15}N, and extent of C and N isotope fractionation, Δ^{13}C and Δ^{15}N.

		reference	**no matrix**			**river water extract**		
F_i [a]			F_1	F_2	F_3	F_1	F_2	F_3
m_i	(-) [b]	1.00 ± 0.03	0.41 ± 0.02	0.42 ± 0.02	0.16 ± 0.03	n.d.	0.74 ± 0.02	0.26 ± 0.02
δ^{13}C	(‰) [b]	-26.1 ± 0.5	-25.4 ± 0.3	-25.8 ± 0.4	-24.9 ± 0.1	n.d.	-26.4 ± 0.2	-25.6 ± 0.6
δ^{15}N	(‰) [b]	-26.9 ± 0.2	-28.3 ± 0.1	-25.6 ± 0.2	-18.1 ± 0.9	n.d.	-30.5 ± 0.3	-17.5 ± 0.6
Δ^{13}C	(‰) [c]	0.0 ± 1.3		-0.6 ± 1.4			0.1 ± 1.1	
Δ^{15}N	(‰) [c]	0.0 ± 1.2		-1.4 ± 1.3			-0.2 ± 1.1	

[a] Data for F_1 and F_2 determined from 1H-BT in dichloromethane, F_3 in methanol;
[b] uncertainties are $\pm 1\sigma$ of triplicate measurements of concentrations or isotope ratios;
[c] porpagated uncertainties (95% confidence intervals).

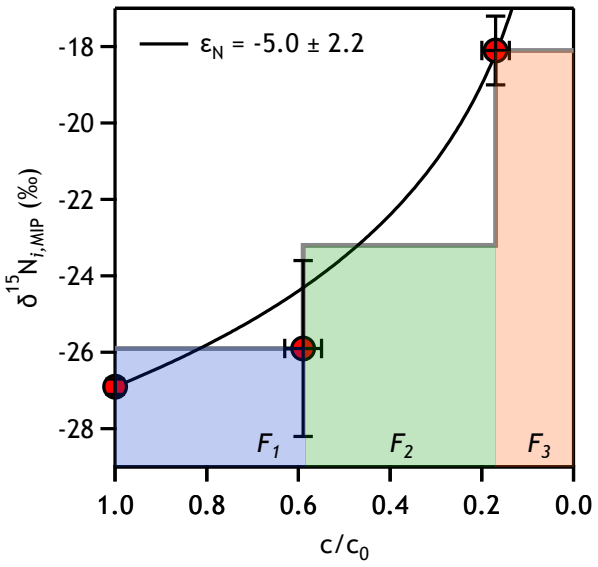

Figure 2.4: N isotope fractionation of 1*H*-BT through stepwise elution from the MIP. δ^{15}N values ($\pm 1\sigma$) stand for the fraction of remaining 1*H*-BT on the MIP using data from Table 2.1. F_1 corresponds to the fraction of 1*H*-BT that eluted during the loading procedure, whereas fraction F_2 eluted during the washing step (both conducted with dichloromethane). F_3 corresponds to the remaining MIP-bound 1*H*-BT that could be removed from the MIP by washing with methanol. The solid line was obtained through non-linear regression of eq. 2.5 with an ε_N of -5.0 ± 2.2‰.

Figure 2.1) and were reduced through an additional liquid-liquid extraction during step **F**. δ^{15}N values of 1H-BT in influent and effluent samples were identical (-4.5 ± 0.9‰ vs. -5.6 ± 1.3‰) within uncertainty whereas the difference of their δ^{13}C was only minimal (-26.8 ± 0.2‰ vs. -26.1 ± 0.4‰). Even though a quantitative analysis of the C and N isotope signatures in the WWTP and in dishwasher detergents is beyond the scope of this work, data in Figure 2.5 reveals some consistent trends which confirm the applicability of MISPE-based procedures for CSIA. Similar C and N isotope signatures of 1H-BT in influent and effluent agree with the frequently made observation that this micropollutant is not degraded during the waste water treatment process[91,92]. Moreover, those values are also within the range of δ^{13}C and δ^{15}N values found in dishwasher detergents that are sold in the study area and they are within less than 1‰ of their average values.

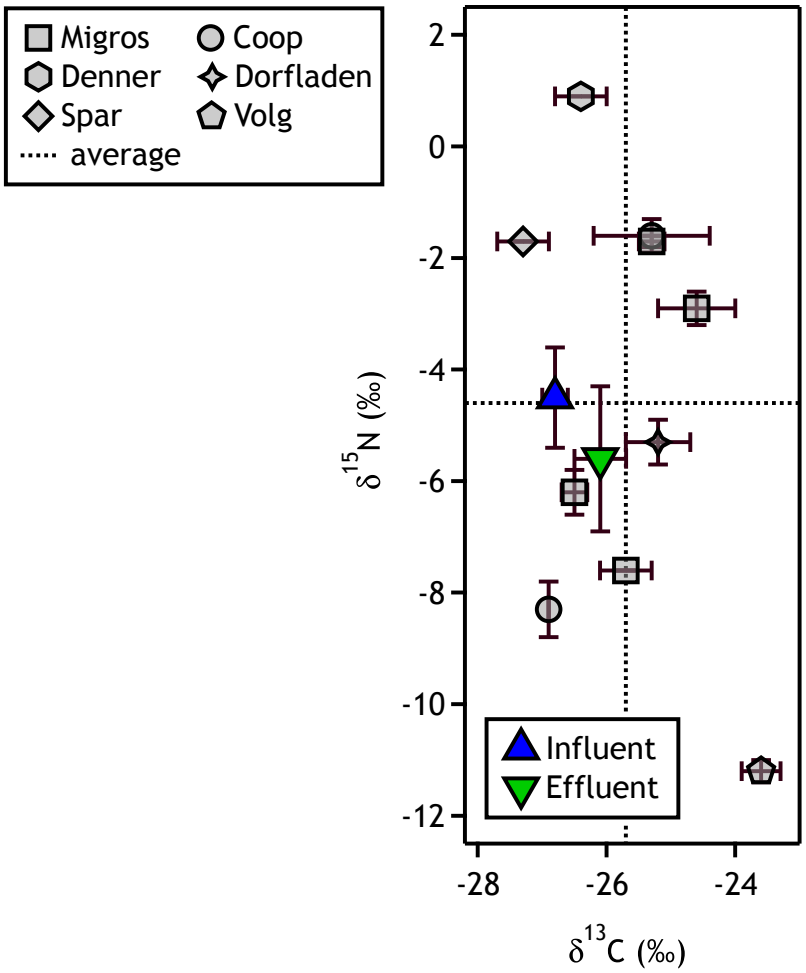

Figure 2.5: C and N isotope signatures of 1H-BT in the influent and effluent of a WWTP (coloured triangles) as well as in various solid, liquid, and gel-like dishwasher detergents sold by retailers in the study area (grey symbols). The dashed lines correspond to the arithmetic mean of δ^{13}C and δ^{15}N of 1H-BT in detergent samples. Error bars represent $\pm 1\sigma$.

2.4 Conclusion

This work illustrates that a generic imprinting technique of 1H-BT using non-covalent approach is successful at enhancing the selectivity of sample preparation procedures for CSIA. Extractions of organic micropollutants in large volume samples by conventional SPE are an essential step to enrich adequate amounts of analytes for isotope-ratio mass spectrometry but they will inevitably lead to concomitant enrichment of organic matter. The matrix can be removed selectively in organic extracts with the MIP. The application of MIP to CSIA of 1H-BT in rive water extracts revealed sufficient efficiency in removing the organic matrix interferences. Influent and effluent samples from WWTPs showed, however, that some of the organic matrix interferences can bind to the MIP. This suggests that the impact of dissolved organic carbon (DOC) on MIP selectivity should be investigated for CSIA, particularly for measurements of C isotope ratios. In fact, the C-normalized DOC:1H-BT ratio decreased systematically as a consequence of the series of treatment of WWTP samples. Whereas the DOC:1H-BT ratio in the aqueous WWTP influent was 11000 (**1**,in Figure 2.1), it decreased to 860 in sample **3** after SPE and 340 in sample **5** after MISPE. In WWTP effluent, the DOC:1H-BT ratio decreased from 3200 in the aqueous effluent (**1**) to 190 after SPE (**3**) and 76 (**5**) after MISPE. Whereas liquid-liquid extraction was implemented in order to further reduce DOC:1H-BT ratios in WWTP samples, alternative approaches such as preparative HPLC on sample **5** can be applied successfully[83]. A systematic and quantitative assessment of the acceptable ratio of matrix:micropollutant is necessary to assess feasibility of MISPE sample preparation for CSIA more generally.

Supporting Information to Chapter 2

S2.1 Chemicals

Chemicals used including their purities and suppliers follow: 1*H*-benzotriazole (99%), 5-methyl-1*H*-benzotriazole (98%), 5,6-dimethyl-1*H*-benzotriazole monohydrate (99%), ethyl acetate ($\geq$ 99.7% Chromasolv®), 2,2'-azobisisobutyronitrile (AIBN) ($\geq$ 98.0% purum), methacrylic acid (MAA) (99%), and ethylene glycol dimethacrylate (EGDMA) (98%) were purchased from Sigma-Aldrich. Sodium hydroxide ($\geq$ 99%), hydrochloric acid (32%, for analysis), sodium sulfate anhydrous ($\geq$ 99% for analysis), acetone ($\geq$ 99.8% for analysis EMSURE®), formic acid ($98 - 100\%$ for analysis EMSURE®), dichloromethane ($\geq$ 99.8% for analysis EMSURE®), toluene ($\geq$ 99.9% for analysis EMSURE®), and $n-$hexane ($\geq$ 99.9% for analysis EMSURE®), were purchased from Merck. Benzothiazole (96%), and naphthalene ($\geq$ 99%) were purchased from Aldrich. 1-methyl-benzotriazole ($\geq$ 98%) from Alfa Aesar. Methanol ($\geq$ 99.9% Optima® LC/MS), and acetonitril ($\geq$ 99.8% for HPLC ACROS Organics™), from Fisher Sienteific. An in-house standard of 1*H*-benzotriazole ($\geq$ 99% puriss. p.a.) was purchased from Fluka.

All chemicals were used as received except for MAA, EGDMA, and AIBN. AIBN was purified by recrystallization from methanol. MAA was distilled at reduced pressure between 1 and 2 mbar and temperature between 33 and 35. EGDMA was subjected to sequential extractions with aqueous solution of sodium hydroxide 10%, water, and saturated aqueous solution of sodium chloride. The purified EGDMA was subsequently dried with anhydrous sodium sulfate, filtered, and distilled between 1 and 2 mbar at 85 to 90 °C.

Carrier and reference gases for GC/IRMS were helium (99.999%), N_2 (99.9999%), CO_2 (99.999%), and H_2 (99.999%) from Carbagas (Rümlang, Switzerland). Aqueous solutions were prepared with deionized water (18.1 MΩ·cm, Barnstead NANOpure Diamond Water Purification System).

S2.2 Dishwasher detergents

Table S2.1: List of dishwasher detergents purchased from retailers in the catchment area of WWTP Aadorf along with their measured contents of 1*H*-benzotriazole.

Retailer	**Brand name**	**Sample type**	**Sample No.**	**1H-BT concentration** (mg 1H-BT/g detergent)
Coop	Sun	tabs	A1	0.18
	Somat	tabs	A2	0.91
	Prix Garantie	tabs	A3	n.d.
	Finish powerball	tabs	A4	n.d.
	Qualité & Prix	tabs	A5	n.d.
Migros	M-Budget	tabs	B1	0.10
	M Classic	tabs	B2	0.34
	Handy matic	tabs	B3	0.18
	Handy matic	gel	B4	0.55
	Handy matic	machine care liquid	B5	n.d.[a]
Spar	Splendid	tabs	C1	0.14
	Splendid	machine care liquid	C2	n.d.
	Sun	gel	C3	n.d.
Denner	Denner	tabs	D	0.39
Volg	Volg	powder	E	0.14
Village store	Splendid	tabs	F	0.08
Held ecover	Held ecover	powder	G	n.d.

[a] n.d. not detected with limit of detection of 0.003 mg 1H-BT/g detergent (95% confidence interval)

S2.3 Field site and sampling

For pristine river water, we sampled river Bünz in Muri AG, Switzerland, on September 23, 2014, 100 m upstream of the municipal waste water treatment plant (WWTP). Samples were collected in a 55 L bottle that had been rinsed with methanol, deionized water, and river water prior to sampling. River water aliquot of 100 mL was separated from the 55 L sample and kept in the freezer at −20 °C for chemical analysis of micropollutants and dissolved organic carbon (DOC) The remaining water were subject to the sample preparation procedures described below.

For waste water, we sampled 25 L influent and 50 L effluent of a municipal WWTP in Aadorf, TG, Switzerland, on June 10, 2015. The Aadorf WWTP consists of a sand channel, a primary clarifier, and a biological treatment step combined with a secondary clarifier. The hydraulic retention times for the WWTP were between 7 and 11 h on the day of sampling and the flow rate amounted to 7050 m^3/d. The influent water was sampled right after the bar screen before entering the sand channels, whereas the effluent water was sampled before discharge from the WWTP into the nearby creek (Lützelmurg). Aliquots for concentration measurements of micropollutants and DOC were again treated identically to river water samples while the remaining samples were processed as shown below.

Seventeen different brands of dishwasher detergents were purchased from 7 retailers in the catchment area of the WWTP Aadorf. A list of the purchased detergents, their measured contents of 1H-BT can be found in Table S2.1.

S2.4 Reactor for synthesis of molecularly-imprinted polymers

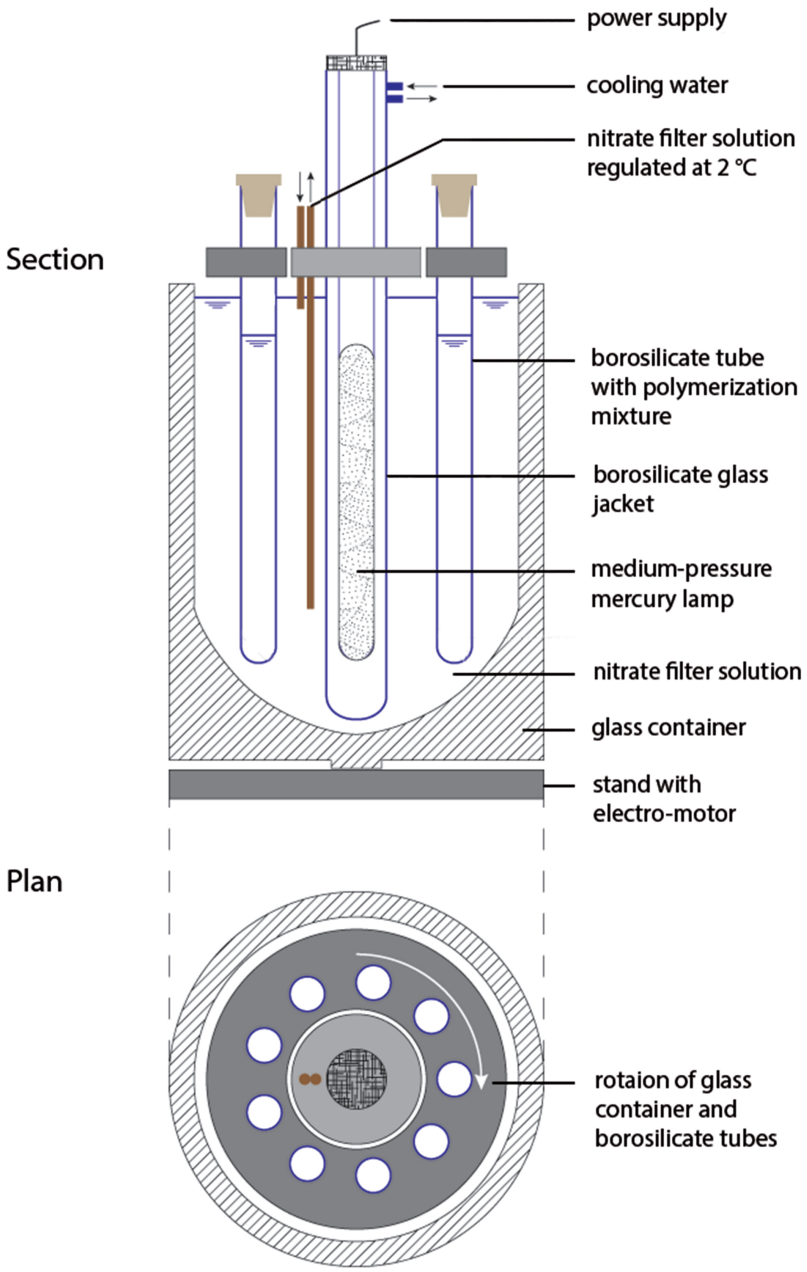

Figure S2.1: Layout of the merry-go-round photoreactor used for synthesis of molecularly-imprinted polymers as well as non-imprinted polymers, adopted and modified from Wegelin et al.[102]

S2.5 Derivations of interaction enthalpies for assessment of molecularly-imprinted polymers

The enthalpies of interaction between the analyte and the synthesized polymers, ΔH_i, were calculated from the slope of van't Hoff equation, eq. S2.3, where the natural logarithm of capacity factors at variant temperatures of 278, 288, and 298 K were plotted versus the corresponding reciprocal absolute temperatures ($1/T$). Derivation of eq. S2.3 is shown below.

The capacity factor, k_i, correlates with the equilibrium distribution coefficient, K_i, according to eq. S2.1[103,104]:

$$k_i = K_i \frac{V_s}{V_m} \tag{S2.1}$$

where V_s and V_m are volumes of the solid phase and the mobile phase, respectively. The van't Hoff equation can be written as shown in eq. S2.2. Assuming that the ratio V_s/V_m in eq. S2.1 is independent of temperature, the capacity factor k_i may be written for K_i as shown in eq. S2.3[103,104].

$$\frac{d \ln K_i}{d\frac{1}{T}} = -\frac{\Delta H_i}{R} \tag{S2.2}$$

$$\frac{d \ln k_i}{d\frac{1}{T}} = -\frac{\Delta H_i}{R} \tag{S2.3}$$

where R is the gas constant.

Chapter 3

Impact of natural organic matter on δ^{13}C of triazines analyzed by offline molecularly - imprinted solid-phase extraction coupled to gas chromatography / isotope-ratio mass spectrometry

3.1 Introduction

Degradation of pesticides in the environment is difficult to assess due to the different processes that simultaneously influence their concentration dynamics.[11] In contrast, changes in isotopic signatures within a single organic molecule, measured by compound-specific isotope analysis (CSIA), provides a conclusive indicator of its degradation.[12,13,16,17,40,75]. Successful applications of CSIA to pesticides have been seen in a large number of studies covering development of analytical methods[83,105–108], source identification,[109–111] assessment of degradation[33,112–115], and elucidation of transformation pathways[116,117]. Nevertheless, due to poor sensitivity of CSIA techniques, most of these works have been limited to lab-scale studies or simulated systems where the pesticide occurrence can be designed to suit the stable-isotope analytical method.

Environmental samples with pesticides at low occurrence, in the range ng L^{-1}-µg L^{-1}, requires extraction of large volumes of water ($\geq$ 10 L) which consequently leads to inevitable interferences from the matrix[16,83]. On the other hand, acquisition of accurate isotopic data using gas chromatography coupled to isotope-ratio mass spectrometer (GC/IRMS) critically relies on the chromatographic performance such as complete peak separation from interferences and correct integration of the entire peak from baseline to baseline[19,40,43,44]. In CSIA, there is no substitute for good chromatography because the inherent isotope signatures of individual compounds can not be acquired in presence of unresolved interferences of unknown signatures. To this end, careful sample preparation of environmental samples play a key role for transferring the analytes from the environmental sample to a clean extract with as less interfering matrices as possible.

Preparative chromatography of environmental extracts using reversed-phase high-performance liquid chromatography (RP-HPLC) has been successfully applied to obtain clean chromatograms for desethyl-atrazine and atrazine in ground water at the sub-microgram per liter range.[83] Nevertheless, implementation of this cleanup step in the analytical workflow for CSIA is time-consuming and intricate. For example, the use of RP-HPLC requires reconstitution of the atrazine-containing extract in HPLC-compatible eluent which typically comprises high contents of water. Given the minimum atrazine concentration needed in the extract to measure on GC/IRMS[116] (i.e. 90-600 mg L^{-1}) and the limited solubility of atrazine in water (i.e. 35 mg L^{-1})[118], solubility limits of the analyte might be exceeded. In such a case, significant losses of the analyte may occur due to different processes such as deposition onto glassware walls, or sorption to co-present matrix. Alternatively, a cleanup step from organic solvents using

offline molecularly-imprinted solid-phase extraction (MISPE) offers a simple approach for sample preparation of environmental samples for CSIA (see chapter 2).

Specific recognition offered by molecularly-imprinted polymers (MIP) relies on the formation of definable interactions between a template molecule and a functional monomer. Subsequent removal of the template from the produced polymer results in a complementary binding site with high affinity towards the template molecule and closely-related structures. Selective extraction of organic compounds from different matrices using MISPE is, in fact, well-established in analytical chemistry,[47,73,84,88,93,119–125] and particularly for triazines (see Figure 1.2). Isotope analysis of 1*H*-benzotriazole using GC/IRMS in different environmental extracts illustrated the use of MIP to reduce the interfering matrix from natural organic matter while retaining the analyte (see Figure 2.2). However, the impact of natural organic matter loads on the MIP selectivity is unknown, neither the maximum loads of natural organic matter that GC/IRMS may handle without compromising the acquired isotope ratios for the analytes.

The overall objective of this chapter was to investigate the impact of different loads of natural organic matter from river water (matrix) on carbon-isotope measurements of triazines using offline MISPE-GC/IRMS. The work focused mostly on atrazine, a herbicide that is still frequently detected in natural waters, and two of its transformation products, namely desethyl-atrazine and desisopropyl-atrazine. The work detailed goals were to (a) explore the maximum acceptable limit of C-normalized matrix:analyte ratio for GC/IRMS and the impact of MISPE on this ratio, (b) C and N isotope integrity of analytes after MISPE cleanup for atrazine and desethyl-atrazine, and lastly (c) study the effects of sorbent masses and protic solvents on implementation of MISPE in CSIA using established pre-enrichment procedures.

3.2 Experimental section

3.2.1 Chemical and materials

A list of used chemicals and materials along with the suppliers are listed in the supporting information.

3.2.2 Sample preparation of matrix from river organic matter

Pristine river water from river Bünz in Muri AG, Switzerland was collected, in 55 L glass bottle, 100 m upstream of the first WWTP the discharges its effluent into the river. Concentration of DOC was 2 mg C/L, which was analyzed using an aliquot of 50 mL before any treatment of the collected sample (sample **1** in Figure 3.1). Preservation of the sample (step **A**) was done on the same day of sampling through acidification to pH 3 using hydrochloric acid 32% and filtration through 0.7 µm glass fiber filters (Whatman, GF/F 47mm) and the acidified filtrate sample (**2**) was stored at 4 °C until further processing.

In step **B**, a total of 40 liters of sample **2** was extracted using 4 parallel Oasis HLB cartridges (Waters, 6g, 35 mL) and a 12-port vacuum extraction manifold (Supelco, Switzerland). The cartridges were conditioned with 100 mL methanol and 300 mL pure water. Water samples **2** were percolated through the cartridges using a vacuum pump at a flow rate of $\leq$ 7.2 mL min^{-1} corresponding to a linear velocity of $\leq$ 1.6 cm s^{-1}. Subsequent drying of the cartridges was performed under vacuum overnight and the dried cartridges were eluted in 150 mL of dichloromethane/methanol (97/3 vol%). In step **C**, the SPE eluates **3** were dried using rotary vacuum evaporator (Büchi, Switzerland) at 40 ℃ under a gentle stream of N_2. The dry residues were reconstituted in 3 mL pure dichloromethane (**4**). An aliquot of the dichloromethane extract was taken for determination of total organic carbon of the extracted matrix after evaporation of the solvent and resuspension in pure water.

3.2.3 Molecularly-imprinted solid-phase extraction

In steps **E**, Triazine-imprinted polymers (750 mg) were packed in empty PP SPE cartridges (Supelco, 12 mL) sandwiched with two PE frits for which MISPE was conducted using a 12-port vacuum extraction manifold. The cartridges were sequentially conditioned with 2 x 5 mL methanol, 2 x 5 mL methanol:formic acid (9:1 v/v), and 2 x 5 mL dichloromethane. After conditioning, the sample (1.5 mL) was loaded on the cartridge and allowed to percolate through. The cartridges were washed with 25 mL dichloromethane and eluted with 6 mL methanol. Steps of loading, washing and elution were all kept at a flow rate equal or less than 0.5 mL min^{-1}. The methanolic extract were evaporated to dryness under a gentle stream of nitrogen and reconstituted in the original volume using methanol 30 vol% in water and measured on high-performance

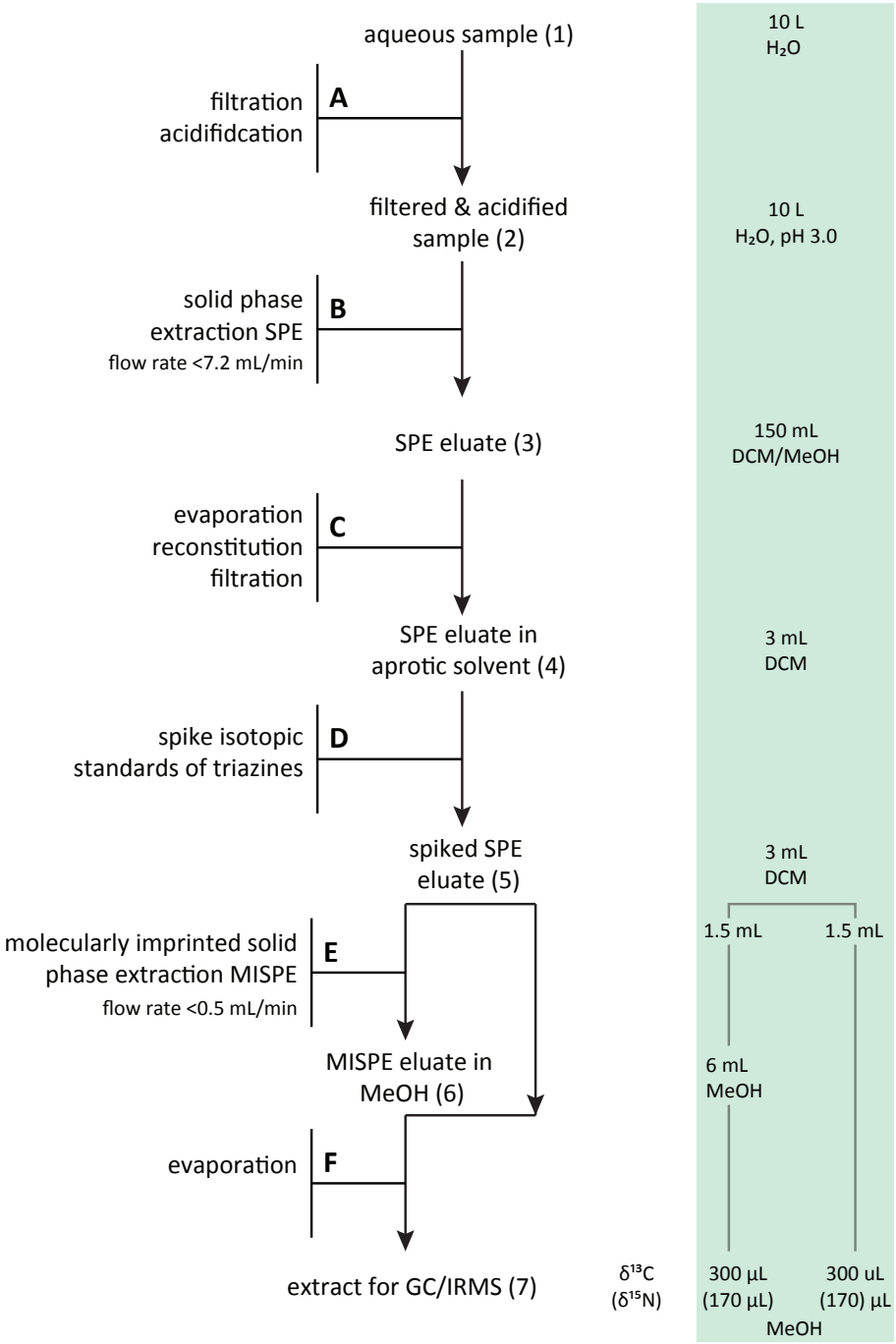

Figure 3.1: Sample preparation for pristine river water comprising (A, B) enrichment of matrix, (C) change to aprotic solvent, (D) spike isotopic standards of triazines, (E) selective cleanup using MISPE, and (F) reduction of volume to 300 µL and 170 µL for measurements of δ^{13}C and δ^{15}N, respectively.

liquid chromatography.

3.2.4 Experiments

Impact of matrix-to-analyte ratio on GC/IRMS and role of MISPE

In step **D**, samples with different C-normalized matrix:atrazine ratios were prepared from sample **4** which were obtained from 30 L of river water samples processed as described in 3.2.2. SPE eluates in dichloromethane (**4**) contained 10% of the DOC that was initially in the river water sample **1**. A calibration series of different matrix amounts was prepared by transferring aliquots of different volumes of the SPE eluate **4** into separate vials and evaporate the solvent to dryness. The dried samples were then reconstituted with a standard solution of atrazine of known isotopic signatures and concentration of 0.2 mmol L^{-1} atrazine in each sample with different matrix contents. Ratios of C-normalized matrix:atrazine in the prepared samples ranged between 1 and 800 (mg C_{matrix} L^{-1})/(mg $C_{atrazine}$ L^{-1}). The samples **5** were then either treated with MISPE, as described in step **E**, or skipped the MISPE treatment to the next step. The MISPE- treated and untreated eluates, samples **6** and **5**, were evaporated and reconstituted in dichloromethane/methanol (50/50 vol%) to obtain the final atrazine concentration of 0.2 mmol L^{-1} which was above the method limits of quantification for carbon-isotope ratio measurements (0.04 mmol L^{-1}). Carbon-isotope ratio of atrazine was measured with GC/IRMS and was reported as deviation from a reference

Integrity of δ^{13}C and δ^{15}N for atrazine and desethyl-atrazine after MISPE

Ten liters of river water was extracted as described in 3.2.2 to obtain the SPE eluate **4** that was spiked with desethyl-atrazine and atrazine to check for isotopic fractionation. The final concentration of desethyl-atrazine and atrazine in SPE eluate **5** was 0.15 and 0.12 mmol L^{-1} (27 and 26 mg L^{-1}), respectively. The latter concentrations correspond to 0.045 and 0.036 µmol L^{-1} (8.1 and 7.8 µg L^{-1}) in the original aqueous sample **1**, for desethyl-atrazine and atrazine, respectively. The C-normalized ratio of matrix:analyte in sample **4** corresponded to 62 and 58 for desethyl-atrazine and atrazine, respectively. In step **E**, a selective cleanup on MISPE was performed using only 1.5 mL sample **5** as described in 3.2.3. Both samples, the MISPE eluate no. **6** and the untreated eluate no. **5**, were further evaporated and reconstituted in methanol. The reconstitution volume for sample **7** was set to 300 µL for carbon isotope-ratio measurement which corresponded to 0.74 and 0.59 mmol L^{-1} desethyl-atrazine and atrazine in extract **7**, respectively. For nitrogen isotope ratio, the volume was further blown down to 170 µL which corresponded

to 1.25 and 0.99 mmol L^{-1} desethyl-atrazine and atrazine, respectively.

Effects of sorbent mass and protic solvents on retention

Atrazine, desethyl-atrazine, and desisopropyl-atrazine were used as target analytes, whereas acetochlor and metolachlor were used as proxy for interfering compounds. Breakthrough curves over MISPE were developed using standard solutions of the mentioned compounds in dichloromethane at a concentration 1.5 mmol L^{-1} each, and variant amounts of triazine-imprinted polymers (25, 200, and 750 mg). The cartridges were sequentially conditioned with 2 x 5 mL methanol, 2 x 5 mL methanol:formic acid (9:1 v/v), and 2 x 5 mL dichloromethane. After conditioning, the sample was loaded on the cartridge and allowed to percolate through. The cartridges (25, 200, and 750 mg) were washed with dichloromethane (1.5, 15, and 25 mL) and eluted with methanol (1.5, 4.5, and 6 mL), respectively. For effect of protic solvents, 25 mg of the sorbent was used with 5 mL standard solution that was additionally spiked with 1% methanol. All the volumes that broke through the cartridges were collected in fractions of 0.15, 0.75, or 1 mL. The collected fractions were evaporated to dryness under a gentle stream of nitrogen and reconstituted in the original volume using methanol 30 vol% in water and measured on HPLC for quantification of the analytes.

3.2.5 Chemical and isotope analysis

Organic carbon measurements

Dissolved and total organic carbon concentrations (DOC and TOC) were measured using a total organic carbon analyzer (TOC-L, Shimadzu) equipped with a combustion catalytic oxidation unit (680 °C) and a non-dispersive infrared detector. DOC concentrations in river water samples were carried out after filtration through 0.45 µm filter. TOC concentrations in samples dissolved in organic solvents were determined on the TOC analyzer after evaporation of the solvent under a gentle stream of N_2 for 30 min followed by reconstitution of the dry residues in water using ultra-sonication for 15 min and homogenization for 10 min using stand dispersion unit (Polytron PT 3100, Kinematica). The latter method was validated for variant solvents (methanol, dichloromethane, n-hexane, toluene, and ethylacetate) and showed accurate results with no residues of the investigated organic solvent after evaporation and reconstitution.

Concentration measurements

An HPLC Dionex UltiMate 3000 System (Thermo Scientific) was used to analyze concentrations of the investigated triazines and chloracetanilides in organic extracts after reconstitution in water/methanol 70/30 %vol. Injections of 20 µL from each sample was performed using an autosampler. Separation was carried out on Supelcosil LC-18 column (250 x 4.6 mm, 5 µm, Supelco) at a flow rate of 1 mL min^{-1} using a gradient of methanol and water: 0-7 min methanol 30 vol%, 7-17 min methanol 95 vol%, followed by re-equilibration with methanol 30 vol% for 5.5 min. Detection was carried out using UV-vis detector at wavelength 220 nm. An external calibration of the investigated compounds in a mixture was used for quantification.

Carbon- and nitrogen isotope-ratio measurements

Compound-specific isotope analysis of desethylatrazine and atrazine were performed for the elements carbon and nitrogen following a modified procedure from Meyer et al.[116] The GC was equipped with 1 m deactivated fused-silica guard column (530 µm ID, 660 µm OD, BGB Analytik) and a 30 m x 0.25 mm RTX-1 column (Crossbond dimethyl polysiloxane, 1 µm df, Restek). Samples (3 µL in methanol, dichloromethane, or methanol/dichloromethane 50/50 vol%) were injected in a split/splitless injector operated for 1 min in splitless mode and then in split mode with a split flow of 50 mL/min at 230 ℃. As a carrier gas, helium was used at constant pressure (120 kPa). The temperature program was 1 min at 80 ℃, 40 ℃/min to 220 ℃, 5 ℃/min to 230 ℃ (3 min), 10 ℃/min to 250 ℃ (5 min), 10 ℃/min to 270 ℃ (22 min). The Ni/Pt reactor was again re-oxidized after every measurement for 20 min with O_2. Method quantification limits (MQL) of GC/IRMS was calculated according to Jochmann et al.[126] and is presented in the supporting information (see S3.3).

Data evaluation

Isotope ratios are reported in per mil (‰) relative to the international reference materials Vienna PeeDee Belemnite ($\delta^{13}C_{VPDB}$) and air ($\delta^{15}N_{air}$). The reported values are arithmetic means of at least triplicate measurements with one standard deviation ($\pm\sigma$) as a measure of the uncertainty in the form of isotope signatures ($\delta^{13}C$ and $\delta^{15}N$) Shifts in isotopic signatures for processed samples spiked with in-house isotopic standards are reported as the deviation of isotope ratio measured for the sample ($\delta^h E_{sample}$) from the

value measured for a standard solution of the same isotopic standard ($\delta^h E_{ref}$, Eq. 3.1).

$$\Delta\delta^h E(‰) = \delta^h E_{sample} - \delta^h E_{ref} \tag{3.1}$$

Both $\delta^h E$ and $\Delta\delta^h E$ values are reported as arithmetic mean of replicate measurements with $n = 3$ with one standard deviation ($\pm\sigma$) as a measure of the uncertainty unless specified otherwise. The errors for the $\Delta\delta^h E$ values were propagated from the standard deviations of $\delta^h E_{sample}$ and $\delta^h E_{ref}$ measurements according to eq. 3.2

$$\sigma_{\Delta\delta}(‰) = \sqrt{(\sigma_{sample})^2 + (-\sigma_{ref})^2} \tag{3.2}$$

Evaluation of the baseline associated with atrazine peaks in GC/IRMS was done automatically by Isodat software (Thermo, Switzerland) according to the individual background algorithm. Shifts in baseline for the measured samples were given in mV for mass 44, and are reported after subtracting the baseline measured for a standard solution of the same isotopic standard.

3.3 Results and discussion

3.3.1 Matrix-dependent limits of GC/IRMS and MISPE

The dissolved organic carbon (DOC) in an environmental aqueous sample can bias the isotopic signatures of the lower-abundant target analyte present in the same sample when separation of the target analyte from the interfering DOC is not efficient. Such biases occur when the isotopic composition of the interfering DOC, referred to as matrix, differs from that of the analyte. Corrections of such biases, through construction of an isotopic mass balance of the interfering DOC and the target analyte, can in principle be possible if the isotopic composition of the interfering DOC and its amount are known. Although isotopic composition of DOC in riverine and coastal waters have been investigated for decades, such values unfortunately cannot be used for bias corrections. The reason is that isotopic composition of DOC are typically measured by means of bulk-sample isotope analysis (BSIA) techniques where all the organic carbon in the sample is combusted into the measurement gas CO_2 before measurement on IRMS. As such, the acquired isotopic signatures of DOC represent the average isotopic composition of all molecular components constituting the DOC. By contrast to BSIA, the DOC compo-

nents in a sample undergo sequential separation and fractionation in CSIA throughout sample preparation and separation on gas chromatography prior to combustion and measurement. Therefore, the influence of natural organic matter on accuracy of isotopic measurements of target analytes are studied in this work for environmental samples that are subjected to the same sample preparation procedures and chromatographic separation optimized for measurements of the target analyte.

The influence of interfering matrix from natural organic matter on δ^{13}C of atrazine was assessed in samples that contained constant concentration of atrazine (0.2 mmol L^{-1} or 43.1 mg L^{-1} or 19.2 mg C L^{-1}) and different loads of matrix. The different loads of matrix compared to atrazine is expressed as a C-normalized ratio, matrix:atrazine, which ranged from 1 to 800. The relatively low peak amplitude of atrazine (2250 mV at m/z 44) will be readily influenced by the co-present matrix, which simulate realistic conditions of micopollutants where the abundance of the target analyte in the extract is typically not high. The results shown in Figure 3.2(a) compare carbon isotopic shifts for atrazine, $\Delta\delta^{13}C$, for samples treated with molecularly-imprinted solid-phase extraction (w MISPE) to those without treatment (w/o MISPE), whereas Figure 3.2(b) shows the baseline attributed to the matrix presence. Prior to the cleanup, the GC/IRMS method could measure precise δ^{13}C values for the analyte up to a matrix:analyte ratio of 10 which was associated with an increase in the baseline by 46 mV due to the interfering matrix. Above a ratio of 10, δ^{13}C for atrazine was shifted and a progressive increase in the baseline was also observed which ranged from 80 to 212 mV. The results suggests that a minimum increase in the baseline by 80 mV biases the carbon isotope ratio of atrazine by approximately 2‰. Although the processing software implements algorithms to correct for the background for each peak, a precise δ^{13}C for these samples could not be measured within ±0.7 ‰.

After the cleanup of samples with ratios of 20 to 50 on MISPE, precise and accurate δ^{13}C were acquired using the same GC-IRMS setup. Removal of the interfering matrix is also visible for these samples in Figure 3.2(b) which could reduce the baseline by 69 to 165 mV. Further samples that contained higher ratios of matrix:analyte (i.e. 100-800) were only measured after the cleanup to avoid substantial damage to the GC column. A systematic progressive shift towards heavier carbon isotopic ratios was observed for these samples where accurate δ^{13}C could not be measured above the ratio 100 and the associated matrix baseline were in the range from 222 to 893 mV. The previous results shows that the GC/IRMS performance can be enhanced by approximately one order of magnitude by subjecting the triazine-containing organic extract to a selective cleanup

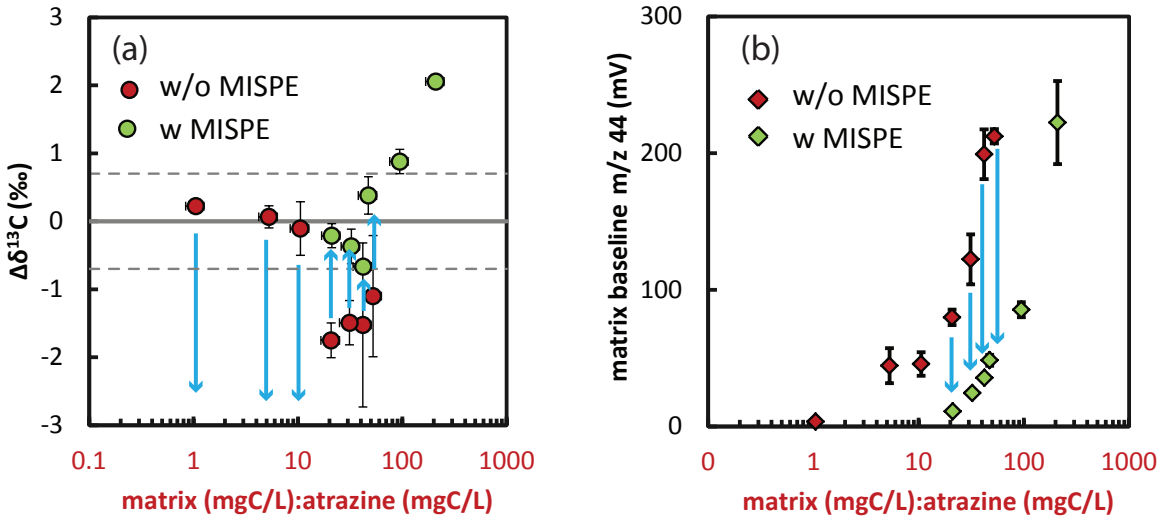

Figure 3.2: The ratio of C-normalized matrix to atrazine as a function of (a) observed deviations of carbon isotopic signature for atrazine, and (b) increase in background for mass 44 due to matrix. Green points stand for samples with MISPE treatment, red for samples without MISPE treatment, and numbers for samples names. Dashed grey lines in (a) represent a calculated limit of $\pm 0.7‰ = \sqrt{(0.5)^2 + (0.5)^2}$. The x-axis indicates the matrix:atrazine ratio for only the samples without MISPE treatment.

using triazine-imprinted MIP.

3.3.2 Integrity of δ^{13}C and δ^{15}N for atrazine and desethyl-atrazine after MISPE

The chromatograms shown in Figure 3.3 depict a comparison of the acquired isotopic measurements for atrazine and desethyl-atrazine in presence of matrix before and after the specific cleanup on MISPE. Prior to cleanup, the sample clearly showed a substantially noisy background in the carbon mode (A), whereas such a noise was not visible in the nitrogen mode (B) . Notably, the noisy background was completely removed after the sample cleanup with the traizine-imprinted polymer. These observations of apparent interferences prior to cleanup for C measurements are in accordance with the higher abundances of C relative to N in riverine natural organic matter[127], which makes C isotope measurements more prone to interferences. The absence of a noisy background in N isotope measurement may suggest the possibility to measure nitrogen isotope ratios without cleanup for such a sample. However, excess loads of C in the sample are known to cause adverse effects on N isotopic measurements. For example, exhaustion of oxidation and reduction reactors may occur as a result of the excess C impeding

thereby quantitative conversion of N-bearing compounds into the measurement gas N_2 which is necessary for accurate $\delta^{15}N$[128] Additionally, the incomplete oxidation of excess C-bearing compounds is known to introduce isobaric interferences in the ion source to masses m/z 28 and 29 needed for calculation of $\delta^{15}N$[129–131]. Therefore, removal of excess carbon from the sample matrix is necessary not only for C but also for N measurements in order to avoid a damage to the system or a bias of the measurements.[132] Deviations of carbon isotopic signatures from pure standards after MISPE ($\Delta\delta^{13}C$ and $\Delta\delta^{15}N$) amounted, respectively, to -1.1±0.9 and -0.1±0.1‰for desethyl-atrazine and 0.1±0.1 and 0.0±0.2‰for atrazine (see Table 3.1). The accurate and precise isotopic measurements indicate that the application of MISPE to environmental samples can be used with the advantage of acquiring clean chromatograms without introducing isotopic fractionation.

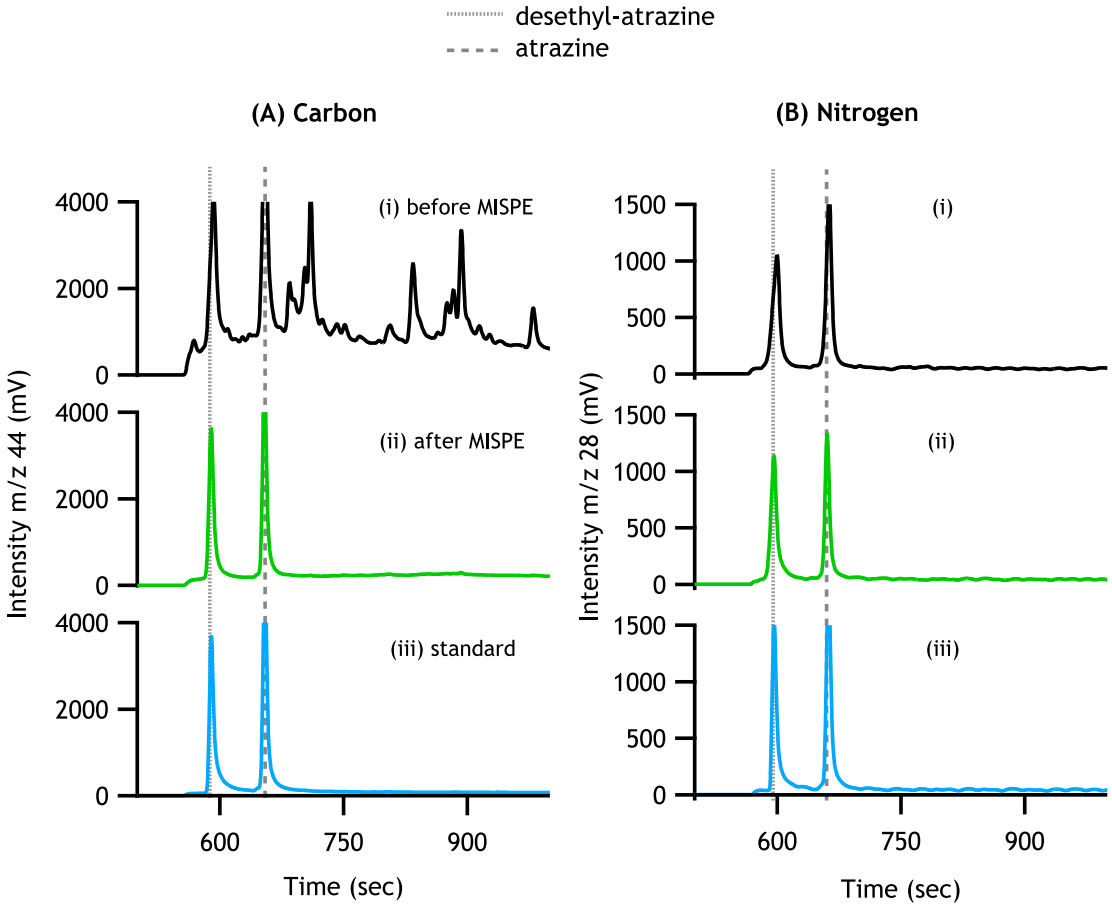

Figure 3.3: Carbon (A) and nitrogen (B) isotopic measurements of desethyl-atrazine and atrazine in (i) presence of river water matrix before MISPE treatment, (ii) in presence of river water matrix after MISPE treatment, and (iii) a standard solution in absence of any interferences.

Table 3.1: Deviation of carbon and nitrogen isotopic signatures for desethyl-atrazine and atrazine after MISPE compared to the isotopic signatures of the pure standards[a]

triazine	$\Delta\delta^{13}$C $\pm\sigma$ (‰) [b]	$\Delta\delta^{15}$N $\pm\sigma$ (‰) [b]
desethyl-atrazine	–1.1 ± 0.9	–0.1 ± 0.1
atrazine	0.1 ± 0.4	–0.0 ± 0.2

[a] 4.6 μmol triazines and 4.6 μmol chloracetanilides in 1.5 mL dichloromethane applied to 750 mg MIP sorbent with 25 mL wash prior to elution with 6 mL of methanol. [b] $n = 5$, propagated error indicates one standard deviation uncertainty ($\pm\sigma$)

3.3.3 Implications to whole sample preparation workflows for CSIA

Solid-phase extraction (SPE) using reversed-phase sorbents is the most used method for preparation of water samples for triazine analysis which yields an extract of the enriched triazines in organic solvent(s) such as methanol, dichloromethane, or ethyl acetate. While the organic extracts from SPE can be applied to MISPE for the cleanup step, attention must be paid to the (1) compatibility of the SPE elution solvent with MISPE, and (2) avoidance of breakthrough of the triazines over the MISPE due to high analyte mass required by CSIA. Therefore, breakthrough curves over MISPE were constructed in dichloromethane (1) in absence and presence of 1% methanol as a representative of protic solvents (Figure 3.4), and (2) using different amounts of MISPE sorbent (25, 200, and 750 mg, see Figure 3.5) for atrazine, desethyl atrazine, and desisopropyl atrazine. Acetochlor and metholachlor were used as conservative tracers.

The results show that 1% of methanol in the extract led the triazines to breakthrough the MISPE cartridge with chloracetanilides (Figure 3.4). This suggests that solvent reconstitution would be necessary before MISPE if any amount of protic solvents such as acetone or methanol were used for the SPE elution. Comparison of breakthrough volumes shows that ACE and MET did not show significant retention on the different sorbent masses and started to breakthrough at volumes very close to the dead volume (see Table 3.2). In comparison with ACE and MET, the three triazines demonstrated selective retention on the MISPE in the following order: DIA > DEA > ATZ. While

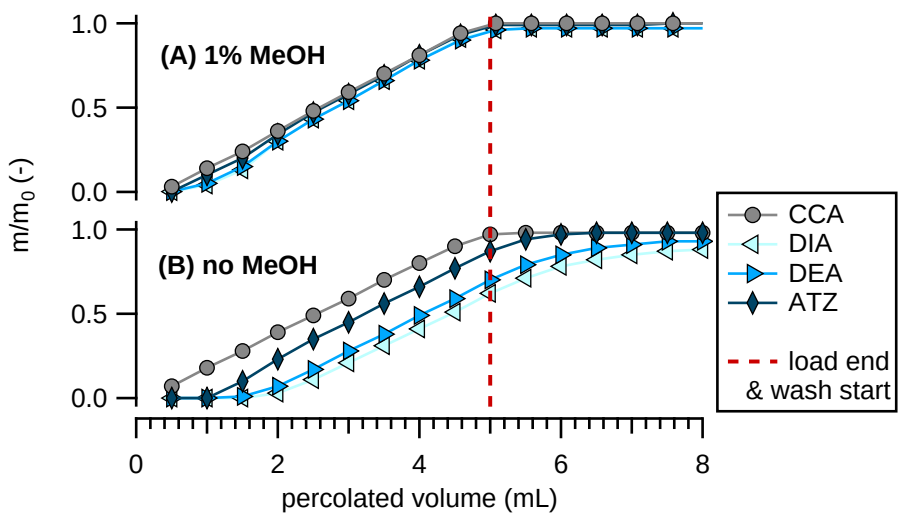

Figure 3.4: Breakthrough curves of chloracetanilides (CCA), atrazine (ATZ), desethyl-atrazine (DEA), and desisopropyl-atrazine (DIA) on molecularly-imprinted solid-phase extraction in (A) dichloromethane containing 1% methanol, and (B) pure dichloromethane.

a slight retention of DIA, DEA, and ATZ was observed for sorbent mass of 25 mg, more pronounced retention was observed for higher masses 200, and 750 mg. The early breakthrough observed for 25 and 200 mg sorbent mass is caused by high contents of the analytes in the extracts which is required for CSIA (2.3 µmol absolute mass each or 1.5 mmol L^{-1}). The amounts of the loaded triazines relative to the sorbent mass are 5.2, 0.6, and 0.2% for 25, 200, and 750 mg sorbent, respectively.

The available sample preparation procedures in literature using MISPE are often for the purpose of trace analysis of triazines and no procedures are available to our best knowledge for CSIA applications. Thus, attention must be paid to develop MISPE procedures specific for CSIA in order to allow a thorough wash of the MISPE phase to remove interferences. While the current set of data presented relative retention behavior of only three triazines, extension of the methodology to other members of the triazine class, such as terbuthylazine and prometryn, is possible. A systematic and quantitative assessment of partition coefficients between the MISPE and different compounds would be necessary to provide a tool for predicting the required amount of sorbent for a certain analyte. For this purpose, chromatographic methods can be used to derive partition coefficients from breakthrough curves[133–136]. The breakthrough curves presented in this study cannot unfortunately be used to derive partition coefficients for the investigated compounds due to lack of complete breakthrough for some compounds during the wash step which is necessary for calculating capacity factors. Additionally,

measurements of porosity and bulk density of the MISPE polymer are needed for this type of investigations.[137]

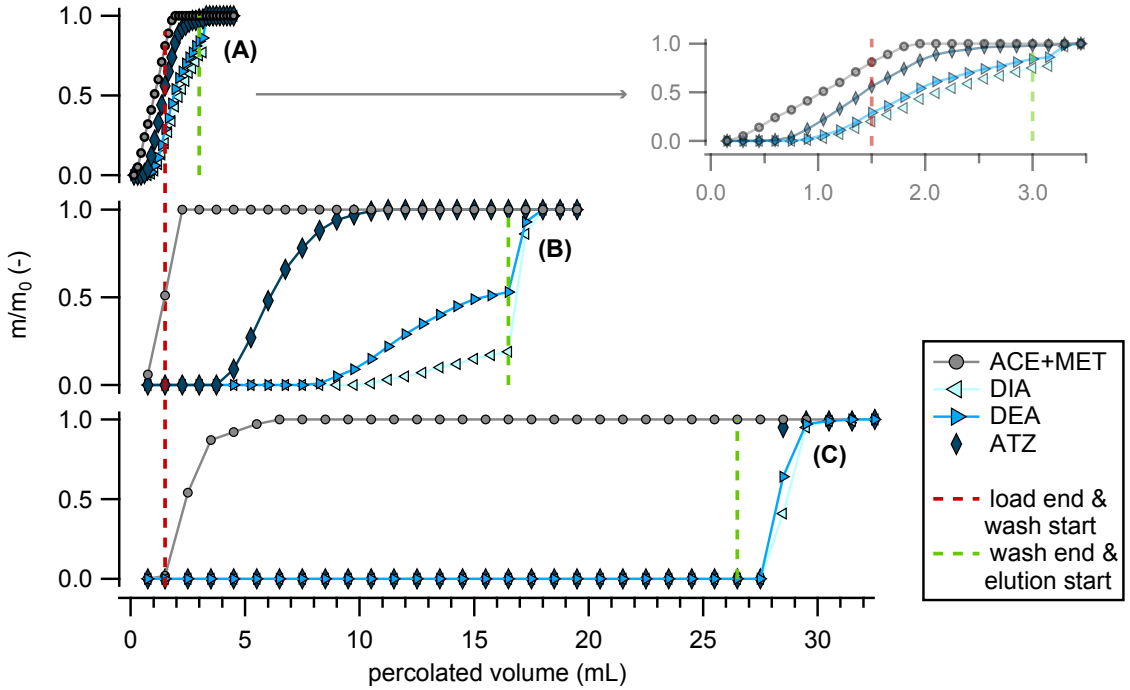

Figure 3.5: Comparison of breakthrough curves of chloracetanilides (ACE+MET) and triazines (DIA, DEA, and ATZ) on (A) 25, (B) 200, and (C) 750 mg of of triazine-imprinted polymers.

Table 3.2: Breakthrough volumes of triazines and chloracetanilides determined for different amounts of triazine-imprinted polymer.

MIP (mg)	dead volume (mL)	sample volume (mL)	breakthrough volume (mL) [a]			
			DIA [b]	DEA [c]	ATZ [d]	CAA [e]
25	0.2	1.5	0.9	0.75	0.6	0.3
200	0.65	1.5	14.25	9	4.5	0.75
750	1.5	1.5	>26.5	>26.5	>26.5	2

[a] Breakthrough volume is defined as the first fraction in which the analyte could be detected.

3.4 Conclusion

A simple and reliable method was developed to cleanup environmental samples for CSIA which is less laborious than the standard preparative chromatography method. The

molecularly-imprinted solid-phase extraction (MISPE) procedure is not only selective towards atrazine but also towards transformation products such as desethyl-atrazine and desisopropyl-atrazine. Given the selectivity of the polymer towards the class of triazines, the method has the potential to be extended to other class members such as terbuthylazine, simazine, propazine, prometryn, and their transformation products. Good chromatography remains an essential prerequisite for CSIA of environmental samples whereby contribution of interfering background is the main hurdle before reliable carbon isotope-ratio measurements. Quantitative assessment of GC-IRMS limitations as a function of matrix abundance in the sample was successful and showed that GC-IRMS could not resolve interfering dissolved organic carbon (DOC) when its abundance is higher than 10 times of the micropollutant and as a result accurate and precise carbon isotope-ratio measurements were compromised beyond a ratio of 10 for DOC:micropollutant. The selective cleanup of river water extracts using MISPE was successful at extending the GC-IRMS limits by one order of magnitude within an uncertainty of 0.7‰enabling thereby stable-isotope analysis of atrazine in river water matrices with a DOC:atrazine ratio of 100. The methodology of applying MISPE protocols for a selective cleanup of environmental extracts can be extended to other compounds for source apportionment and tracking transformation reactions of micropollutants in the aquatic environments using CSIA. Lastly, the DOC:micropollutant ratio can be a promising parameter to use as a priori indicator for feasibility of CSIA for a certain environmental sample.

Supporting Information to Chapter 3

S3.1 Chemicals

All chemicals were used without any further treatment. Analytical standards for quantification included atrazine (Pestanal®, 99.2%), desethyl-atrazine (Pestanal®, 99.9%), and desisopropyl-atrazine (Pestanal®, 96.3%), which were purchased from Riedel de Haën (Seelze, Germany). Metolachlor (Pestanal®, 97.6%) and acetochlor (Pestanal®, 96.0%) were purchased from Fluka (Buchs, Switzerland). In-house standards for stable isotope analysis included atrazine (98.8%) which was obtained from Sigma-Aldrich (Steinheim, Germany), atrazine (purity not provided) from Oskar Tropitzsch (Marktredwitz, Germany), desetheyl-atrazine (99.9%) from Riedel de Haën (Seelze, Germany), metolachlor (96.2%) and acetochlor (96.3%) from Chemos (Regenstauf, Germany).

Methanol (99.9%), dichloromethane ($\geq$ 99.8% for analysis EMSURE®), formic acid (98-100% for analysis EMSURE®), and hydrochloric acid (32%) were supplied by Merck (Darmstadt, Germany). Pure reagent water (18.2 MΩ) was produced using Barnstead™ Nanopure™ (Thermo Scientific, Basel, Switzerland) water purification system. Gases used for GC/IRMS analysis were supplied by Carbagas (Rümlang, Switzerland): helium (He, 99.999%) as a carrier gas, CO_2 (99.999%) and N_2 (99.999%) as reference gases.

S3.2 Materials

Oasis HLB sorbent (6 g, 35 cm^3 cartridges) was purchased from Waters (Milford, MA, USA). Triazine-imprinted polymers were supplied by MIP Technologies AB (Lund, Sweden) as bulk materials with average particle diameter 50 - 65 µm. Empty polypropylene SPE cartridges (6 cm^3) and polyethylene frits (porosity 20 µm) were purchased from Sigma-Aldrich (Buchs, Switzerland).

S3.3 Method quantification limit of GC/IRMS

The minimum mass required for accurate C and N isotope ratio analysis was quantified according to the moving mean procedure after Jochmann et al.[126]. The method quantification limit for atrazine and desethyl-atrazine was determined with standard solutions containing a mixture of both compounds.

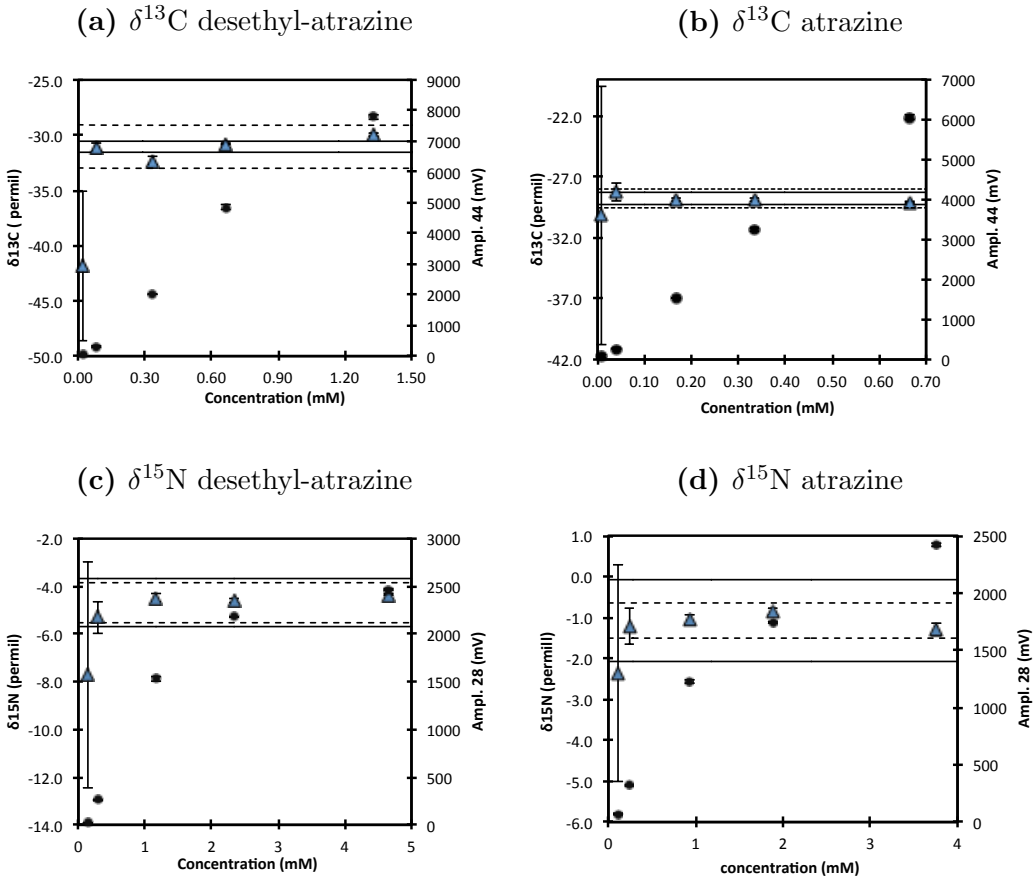

Figure S3.1: Linear range of GC/IRMS method for carbon isotopic signature of desethyl-atrazine (a) and atrazine (b) and for nitrogen isotopic of desethyl-atrazine (c) and atrazine (d). The triangles represent the the triazines isotopic signature. The circles represent the peak amplitudes. Both measurements with error bars for one standard deviation (σ for $n = 5$). The solid lines indicate the uncertainty limit of ± 0.5 and ± 1.0 for C and N, respectively. The dashed lines indicate the uncertainty limit of 2σ of the calculated moving mean.

Table S3.1: The method quantification limit for desethyl-atrazine and atrazine on GC/IRMS determined with uncertainties of 0.5 and 1.0 ‰ for C and N, respectively (MQL). The method quantification limit determined for uncertainty of 2σ calculated for the mean isotopic signature ($MQL_{2\sigma}$) [a]

compound	MQL [b]		$MQL_{2\sigma}$		2σ	
	carbon (nmol C)	nitrogen (nmol N)	carbon (nmol C)	nitrogen (nmol N)	carbon (‰)	nitrogen (‰)
desethyl-atrazine	n.a.[c]	4.4	1.5	4.4	2	0.8
atrazine	1.0	3.5	1.0	3.5	0.8	0.4

[a] calculated for $n = 5$ with an injection volume of 3 μL

[b] for uncertainty limit of ±0.5‰ and ±1‰ for C and N, respectively

[c] not applicable, uncertainty limit exceed for the first mean calculated.

Chapter 4

Matrix effects associated with direct enrichment of glyphosate and AMPA from natural waters on water-compatible molecularly-imprinted polymer

4.1 Introduction

Glyphosate, N-(phosphonomethyl)glycine, is the active ingredient of the herbicide Roundup which is the worldwide most-widely applied weed-control formulation in agricultural and urban areas[138–140]. While glyphosate had been considered for long time as non-toxic and environmentally-safe, public concerns have been raising in recent years. Such concerns have been driven by discovery of dozens of glyphosate-resistant weeds over the last 20 years[141], alteration of plant physiology[142], and the more persistent nature of its major transformation product aminomethyl phosphonic acid (AMPA)[143]. Furthermore, a number of studies refers to a frequent contamination of surface water and soils with glyphosate and AMPA[144–146]. Most recently, some authorities have listed glyphosate as carcinogen following the conclusion of the World Health Organization's International agency for Research on Cancer that "glyphosate is probably carcinogenic to humans"[147]. Addressing all these growing concerns requires analytical methods that are not only reliable but also simple in order to enable high throughput analysis of glyphosate and AMPA in the environment using different analytical techniques.

Since its introduction in the early 1970s, numerous reliable methods have been published on detection and quantification of glyphosate and AMPA. A comprehensive overview is provided in detailed reviews.[148–150] Analytical methods for compound-specific isotope analysis (CSIA) have also been developed for source identification and elucidation of degradation.[106,151] Nevertheless, the majority of these methods employ a derivatization step to amend the zwitterionic nature of the analytes that render their analysis challenging.[152] Derivatization procedures are practically, on the one hand, complex, time-consuming, and tedious due to the several steps involved in the derivatization and purification. For example, a widely-used derivatization procedure for glyphosate and AMPA requires preparation of the derivatizing agent, fluorenylmethyloxycarbonyl chloride, on the day of analysis in addition to 3 hours of waiting time that is necessary for maintaining the reaction time at the optimal pH value.[153] Additionally, solid-phase extraction (SPE) of the derivatized analytes requires thorough wash procedures of the SPE materials to remove interfering derivatization by-products. On the other hand, derivatization is not suitable for all analytical techniques such as carbon-isotope ratio measurements where pre-concentration of the unmodified analytes is warranted for large enrichment factors.

Elimination of the laborious derivatization step can in principle be achieved by direct pre-concentration of glyphosate and AMPA from the sample. Such an approach would

offer an extract with the unmodified analytes suitable to different analytical techniques and relatively easy to scale. For instance, given an average instrumental detection limit for direct spectrometric methods (i.e. $\geqslant$ 1 µg/L glyphosate and AMPA) and environmental occurrences (i.e. 0.11 and 0.20 µg/L, respectively[144]) , an enrichment factor $\geq$ 10 would be sufficient to detect the analytes in the extract. CSIA for forensic environmental applications may also benefit from such an approach where enrichment factor $\geq$ 10000 is typically an inevitable prerequisite for reliable isotope-ratio measurements. Since the direct enrichment can in principle be simply scaled up, the larger enrichment factors (i.e. $\geq$ 10000) needed for CSIA can be achieved.

Pre-concentration approaches, such as SPE packed with ion-exchange resins, have in fact been investigated for the direct enrichment of underivatized glyphosate and AMPA.[154–156] However, the small capacity of ion-exchange resins to efficiently retain glyphosate and AMPA along with the strong competition with other ions in the sample make these sorbents not suitable for efficient pre-concentration. For example, Mallat et al.[154] investigated the use of Amberlite IRA 410 but enrichment factors of the analytes were smaller than 5 and the method still employed post-column derivatization with o-phthalaldehyde for fluorescence detection. While larger enrichment factors, up to 65, were achieved using Amberlite IRA-900,[156] extraction efficiencies were found to be strongly dependent on the ion concentrations in the sample which in particularly resulted in poor extraction of AMPA. Similarly, a strong impact of the ionic compounds in the sample on extraction was reported by Patsias et al 2001 using PRP-X100 poly(styrene-divinylbenzene)-trimethylammonium anion-exchange cartridges.[155] Novel and more sophisticated pre-concentration technique used supported-liquid membrane extraction but enrichment factors did no exceed 10.[157] To achieve high enrichment factors typically required for CSIA using liquid chromatography / isotope-ratio mass spectrometry, Mogusu investigated the use of commercial activated alumina with high adsorption capacity of 85 mg glyphosate/g alumina.[158] Desorption of glyphosate, however, was found to be challenging where recoveries of glyphosate from alumina did not exceed 40% of the adsorbed fraction even after 24 hours of contact time with the elution solution of ammonium hydroxide 1 mol L^{-1}.

In the last few years, imprinting-techniques have enabled production of water-compatible molecularly-imprinted polymers (MIP) based on ionic interactions of oxyanions with substituted urea monomers,[159] which are capable of direct and selective extraction of glyphosate and AMPA from water without derivatization[160–165]. Although MIPs have been investigated for long time as SPE materials in analytical chemistry, the employed

interactions had mostly been based on H-bonding which impeded their application to water samples. In contrast, the advantage of using ionic interactions as a retention mechanism is that water molecules do not compete with the analytes for occupation of the active interaction sites within the MIP. Recently, Berho et al. have demonstrated a successful application of using such a MIP as a polar organic chemical integrative sampler for pre-concentration of glyphosate and AMPA from water.[165] Using the same MIP, Claude et al. showed that Cd^{2+}, Pb^{2+}, and Zn^{2+} present in ground water up to 5, 91, and 180 µg L^{-1}, respectively, did not reduce the extraction efficiency of glyphosate and AMPA.[164]. Moreover, glyphosate and AMPA could efficiently be extracted from a water sample of a volume of 500 mL,[164] which can offer an enrichment factor of up to 500 sufficient for reliable quantification using mass spectrometry as a detector. Despite the promising extraction efficiencies shown by these two studies,[164,165] a derivatization step with fluorenylmethyloxycarbonyl chloride was still implemented for detection by mass spectrometry. We believe that matrix effects are associated with the use of MIPs that significantly limit the analysis of the underivatized analytes in the extract.

Therefore, the general goal of this work was to develop sample preparation method using water-compatible MIP to enable concentration- and stable-isotope analysis of underivatized glyphosate and AMPA in natural waters. Ion-chromatography-electrospray ionization-tandem mass spectrometry (IC-ESI/MS-MS) was used for quantification and liquid-chromatography / isotope-ratio mass spectrometry (LC-IRMS) for measurements of $\delta^{13}C$. The work investigated more specifically matrix effects that lead to any loss of the analyte response or recovery throughout sample preparation which included (i) matrix effects caused by the MIP materials, which are termed throughout the work as bleed matrix effect, (ii) matrix effects caused by the environmental samples, which are referred to as sample matrix effects, (iii) development of approaches to mitigate the different matrix effects, and lastly (iii) assessment of recoveries and method quantification limits in surface-, ground-, and wastewater.

4.2 Experimental section

4.2.1 Reagents, standards, and sorbents

The chemicals and reagents used in this work included formic acid (98-100%), acetic acid (100%), 2-propanol ($\geqslant$ 99.5%), and hydrochloric acid (32%), which were purchased from Merck (Darmstadt, Germany). Sodium hydroxide solution (50-52%), sodium persulfate (99%), phosphoric acid (85%), analytical standards of glyphosate and AMPA ($\geqslant$ 99%), EPA 547 glyphosate solution (1000 mg L^{-1}), and AMPA ^{13}C,^{15}N,D_2 (100 mg L^{-1}) were all purchased from Sigma-Aldrich (Buchs, Switzerland). Glyphosate 1,2-$^{13}C_2$,^{15}N (100 mg L^{-1}) was supplied by Dr. Ehrenstorfer (Augsburg, Germany).

Pure reagent water (18.2 MΩ) was produced using Barnstead™ Nanopure™ (Thermo Scientific, Basel, Switzerland) water purification system. Stock solutions of glyphosate and AMPA (1000 mg L^{-1}) were prepared in pure reagent water and standardized using a certified reference solution when available.

Molecularly-imprinted polymers for glyphosate and AMPA enrichment, AFFINIMIP™ were purchased from Affinisep S.A.S. (Petit-Couronne, France). Oasis® HLB were purchased from Waters (Milford, MA, USA).

4.2.2 Sample preparation

Water samples (**A**) were filtered through 0.7 µm glass fiber filter (Whatman, GF/F 47 mm, Sigma-Aldrich, Switzerland). Molecularly-imprinted solid-phase extraction (MISPE) was performed using a 12-port vacuum extraction manifold (Visiprep™, Supelco, Switzerland). The cartridges (250 mg, 3 mL, Affinisep S.A.S.) were conditioned with 6 mL pure water unless specified otherwise. In step **1**, a volume of 100 mL of the water sample was percolated through the AFFINIMIP cartridge at a flow rate of 1.5 mL min^{-1} (linear velocity 2.4 cm s^{-1}).

After sample percolation, the cartridges were washed with 3 mL pure water and then eluted over Oasis HLB (60mg, 3 mL, Waters) using 3 mL aqueous solutions of hydrochloric acid 0.1 mol L^{-1} (step **2**). For concentration measurements, the chloride contents interfere with the IC-ESI-MS/MS and needed hence removal. Aqueous hydrochloric acid extracts (**B**) were evaporated to dryness at 65 °C under a gentle stream of N_2 to get rid of hydrogen chloride (step **3**). In step **4**, the dry residues (**C**) were reconstituted

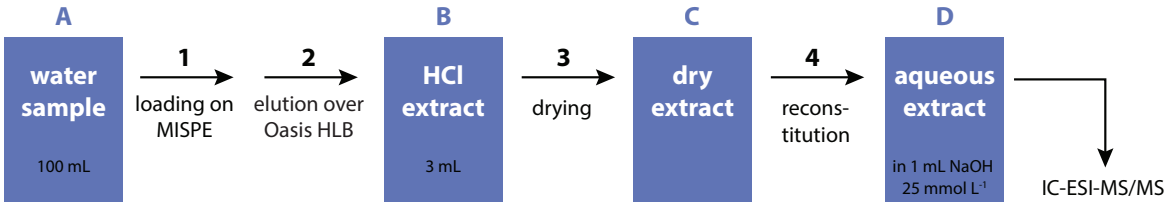

Figure 4.1: Procedural stages of molecularly-imprinted solid-phase extraction of glyphosate and AMPA from environmental aqueous samples

in 1 mL sodium hydroxide 25 mmol L^{-1} to obtain sample **D** that can be measured on IC-ESI-MS/MS. Figure 4.1 gives an overview of the procedure.

4.2.3 IC-ESI-MS/MS

Glyphosate and AMPA were measured by capillary ion chromatography (Thermo Dionex ICS-4000) coupled to tandem mass spectrometry (Thermo TSQ-Vantage) (IC-MS/MS). The capillary IC was equipped with an anion exchange column (IonPac™AS19-4µm, 0.4x250 mm, Dionex) and a guard column (IonPac™AG19-4µm, 0.4x50 mm, Dionex), which were both temperature-controlled at 35 °C. The capillary IC was run at a 12 µL min^{-1} flow rate using KOH eluent generator in gradient mode from 7 to 150 mmol L^{-1} (see gradient program in S4.1). An additional pump was used to run neat isopropanol at a flow rate of 12 µL min^{-1} which joined the capillary IC effluent in a mix-T that afterwards entered the tandem MS. The tandem MS analysis was performed using electrospray ionization in the negative mode with ESI probe equipped with a fused-silica capillary, sheath gas pressure of 40 (unitless), transfer capillary temperature of 250 °C, spray voltage of 2150 V. Two ion transitions, quantifier and qualifier, were acquired for each analyte in the selected reaction monitoring (SRM). Transition 168 to 150 for glyphosate and 110 to 63 for AMPA were assigned as quantifiers, whereas 168 to 63 and 110 to 79 were qualifiers for glyphosate and AMPA, respectively Values for parent and product masses, collision energies, and S-lens RF amplitude are listed in S4.2. Divert valve was used to direct the capillary IC effluent either to (i) waste at retention times < 17.5 min and > 25 min or to (ii) the tandem MS at retention times from 17.5 to 25 min.

Table 4.1: Sample preparation procedures for the optimized method and the experiments that investigated different matrix effects.

	sample preparation steps[a]							spike and measurements		
experiment	**A**	**1** loading	**2** elution[b]	**B**	**3** evaporation	**C**	**4** reconstitution	**D**	STD spike[c] (ISTD spike)[c]	STD conc. (ISTD conc.)	instrument
Optimized method, absolute recoveries and total matrix effects	water sample	any sample 100 mL	w Oasis	hydrochloric acid extract	yes	dry extract	NaOH 25 mM 1 mL	aqueous extract	none (D)	none (10 µg/L)	IC-ESI-MS/MS
		any sample 100 mL	w Oasis		yes		NaOH 25 mM 1 mL		A (D)	100 or 250 ng/L (10 or 25 µg/L)	IC-ESI-MS/MS
Investigation of MISPE-bleed effects on quantification		pure water 100 mL	w/o Oasis		yes		pure water 3 mL		D (D)	50 µg/L (50 µg/L)	IC-ESI-MS/MS
Mitigation of MISPE-bleed effects on quantification		pure water 100 mL	w or w/o Oasis		yes		pure water or NaOH 25 mM 3 mL		D (D)	50 µg/L (50 µg/L)	IC-ESI-MS/MS
Investigation of sample matrix effects on quantification		pure water 100 mL	w/o Oasis		yes		NaOH 25 mM 0.5 mL		A (A)	500 ng/L (500 ng/L)	IC-ESI-MS/MS
		env. sample 100 mL	w/o Oasis		yes		NaOH 25 mM 0.5 mL		A (A)	500-1500 ng/L (500-1500 ng/L)	IC-ESI-MS/MS
Impact of MISPE bleed onδ^{13}C of glyphosate and AMPA		pure water 100 mL	w/o Oasis		yes		pure water 3 mL		D (none)	55-120 mg/L (none)	LC/IRMS
Impact of hydrochloric acid on δ^{13}C of glyphosate and AMPA		no MISPE, HCl or pure water 1 mL			no for pure no for HCl yes for HCl		- - pure water, 1 mL		A (none)	55-120 mg/L (none)	LC/IRMS

[a] the blue letters A, B, C, and D represent the sample at different stages of preparation, whereas, numbers 1, 2, 3, and 4 represent the sequential preparation steps throughout the sample preparation process;
[b] Elution was always carried out with 3 mL hydrochloric acid 0.1 mol/L. The elution was carried out directly and the eluate was collected (designated w/o Oasis) or the eluate of the MISPE cartridge was allowed to pass over Oasis cartridge (designated w Oasis);
[c] The step at which the standard analytes (STD) and/or the internal standards (ISTD) were spiked.

Quantification of analytes

Isotope-labeled internal standards were used for quantification of glyphosate and AMPA. Analytes concentrations were calculated by comparing the peak area ratio of the product ion and its assigned internal standard to the corresponding ratio in a calibration curve. To assess the absolute recoveries of sample preparation using MISPE as well as matrix effects caused by the materials bleed, external calibration curves in pure water were prepared in a range that includes the predicted concentrations of the sample and were used to determine unknown concentrations.

Absolute recoveries

Natural and engineered waters were all grab-sampled in Switzerland and were river Rhine sampled in Basel, creek Chriesbach sampled in Dübendorf, groundwater sampled from a piezometer next to the creek Chriesbach, and wastewater from a municipal wastewater treatment plant after biological treatment. Characteristic parameters of the sampled waters are given in S4.3. To evaluate the effectiveness of sample preparation over MISPE, absolute recoveries were calculated.

One-hundred milliliter of pure-, river-, creek-, ground-, and treated wastewater were subjected to the sample preparation as summarized in Table 4.1. Two samples were used: as a control without spiking any analyte to determine naturally-occurring concentrations or as a spiked sample with 100 ng L^{-1} for pure-, river-, creek-, and ground-water, and with 250 ng L^{-1} for waste water. Isotopic-labeled internal standards were spiked into the aqueous extracts, sample **D**, for a final concentration of 10 µg L^{-1} in the aqueous extract for pure-, river-, and creek water or 25 µg L^{-1} for the wastewater extract. Absolute recoveries were calculated according to equation 4.1

$$R_{abs} = \frac{C_{sample,spk} - C_{sample,none}}{C_{spk}} \times 100\% \tag{4.1}$$

where R_{abs} is absolute recovery given in %, $C_{sample,spk}$, $C_{sample,none}$, and C_{spk} is the determined analyte concentrations in the spiked sample, the unspiked sample, and the corresponding spiked concentration, respectively, given in µg L^{-1}.

Matrix effects

Depending on the experimental design, different types of matrix effects were measured according to their origin. These matrix effects, ME, included those caused by the MISPE materials, ME_{bleed}, or caused by the environmental sample, ME_{sample}. For the optimized method, the total matrix effects, ME_{tot}, represents the combination of both ME_{bleed} and Me_{sample}. Equation 4.2 was used to calculate matrix effects by comparing internal standard peak areas in the extracted sample with that in a control.

$$ME = (\frac{A_{sample}}{A_{control}} - 1) \times 100\% \tag{4.2}$$

It means response suppression for $ME < 0$, response enhancement for $ME > 0$, or no matrix effect for $ME = 0$. A_{sample} is the peak area of the internal standard in the extracted sample. $A_{control}$ is the peak area of the internal standard in pure water that was not subjected to sample preparation when calculating ME_{tot} and ME_{bleed}, and the peak area of the internal standard of pure water that was subjected to sample preparation when calculating ME_{sample}.

Instrument quantification limits (IQL) and method quantification limits (MQL)

Instrument quantification limits (IDL) were determined according to DIN 32645[166] using triplicate measurements of a calibration series comprising 7 equidistant levels in pure water between 2 and 14 µg L^{-1} (see S4.4). Accordingly, IQL of glyphosate and AMPA were 1.8 ± 0.4 and 1.2 ± 0.3 µg L^{-1}, respectively. An estimation of method quantification limit, MQL_e, was calculated using Equation 4.3.

$$MQL_e = (100 - ME_{tot}) \times \frac{IQL}{EF \times R_{abs}} \tag{4.3}$$

where IQL is the instrumental quantification limit given in the same unit as MQL_e, R_{abs} and ME_{tot} are absolute recovery and matrix effect in %, and EF enrichment factor of MISPE.

4.2.4 LC/IRMS

Carbon isotope-ratio measurements, $\delta^{13}C$, for glyphosate and AMPA were performed using liquid chromatograph (LC) Dionex UltiMate 3000 system hyphenated, through a wet chemical oxidation interface Finnigan LC IsoLink, to an isotope-ratio mass spectrometer (IRMS) Delta V Plus IRMS (All from Thermo Scientific). The detailed method was adopted from Kujawinski et al.[106] with the only difference that a Hypercarb™ column with dimensions of 100×2.1 mm was used instead of 100×4.6 mm, and a flow rate of 0.15 mL min^{-1} instead of 0.30 mL min^{-1}. Flow injection analyses of individual compounds were also performed as described by Kujawinski et al.[106].

4.2.5 Experiments

Table 4.1 gives an overview of the procedural details for all experiments done in this work.

Investigation of MISPE-bleed effects on quantification

Soluble substances that bleed from the MISPE cartridges were obtained by following step **1** & **2** in Figure 4.1 for few cartridges except for replacing the sample **A** with pure water. All HCl extracts were combined and a 4 mL aliquot was taken to measure DOC value. After evaporation of HCl extract (sample **B**) to dryness (step **3**), the dry residues (**C**) were reconstituted in the original volume using pure water (step **4**) to obtain an aqueous extract (**D**) that contained bleeding substances from the MISPE cartridge. A calibration series of the bleed in pure water was prepared by sequential dilution of the obtained bleed-containing solution (**D**). The calibration covered a range of 0.1-100% relative to the prepared bleed-containing solution which corresponds to organic carbon bleed of 0.0036-3.6 mg C L^{-1}. All bleed standards were spiked with glyphosate and AMPA 50 µg L^{-1} each along with identical concentration of internal standards.

Measurements of the prepared standards were carried out on IC-ESI-MS/MS with each standard followed by 5 subsequent blank injections of pure water to estimate any potential carryover. Equation 4.2 was used to calculate bleed matrix effects, ME_{bleed}, where observed peak areas of glyphosate and AMPA in a bleed-containing sample, A_{sample}, were extracted from the standards or internal standards and compared to peak areas of glyphosate and AMPA in pure water that did not undergo sample preparation, $A_{control}$.

Peak areas in the first- or five-subsequent blank injection(s) were used to estimate the magnitude of carryover (see Equation 4.4). The standard was used for calculations when deviations from the internal standard did not exceed 20%.

$$CO = \sum_{i}^{5} \left(\frac{A_{blk,i}}{A_{sample}} \right) \times 100 \tag{4.4}$$

where CO is the carryover observed in the first subsequenct blank injection(s) where it is CO when $i = 1$ or CO_{total} when $i > 1$, whereas $A_{blk,i}$ is the observed peak area of the standard in the corresponding blank injection.

Mitigation of MISPE-bleed effects on quantification

Three approaches were tested for effectiveness to mitigate the influence of the MISPE bleed on IC-ESI-MS/MS sensitivity and carryovers.

- Pre-wash procedures of the MISPE cartridges prior to the sample loading step (step **1** in Figure 4.1) were tested to minimize the amount of the leaching bleed in the eluate. These procedures were **(i)** pre-wash with 6 mL of pure water as recommended by the materials manufacturer which was used for comparison, **(ii)** 100 mL pure water in addition to pressure exertion on the cartridge, **(iii)** sequential washing with 100 mL pure water, 100 mL HCl 0.1 mol L^{-1}, and 100 mL pure water, and **(iv)** sequential washing with 100 mL pure water, 100 mL HCl 0.1 mol L^{-1}, 100 mL methanol 20 vol %, and 100 mL water. In step **2**, 3 mL HCl 0.1 mol L^{-1} was used to elute the cartridges. The last 5-6 mL of water that broke through the MISPE was collected in addition to the HCl eluate.

- This approach relied on the use of reversed-phase sorbent to remove the bleed. Percolation of the already reconstituted aqueous extract (sample **D** in Figure 4.1) over Oasis® HLB cartridge was carried out followed by a wash step with 1 mL pure water to avoid loss in the dead volume. Alternatively, percolation of the 3 mL HCl extract (sample **B** in Figure 4.1) over Oasis® HLB cartridge was done followed by a wash step with 1 mL HCl 0.1 mol L^{-1}, and steps 3 and 4.

- In the third approach, disruption of interactions between the bleed and the analytes was tested. Thereof, reconstitution of the dry residues (**C**) in aqueous sodium hydroxide solution 25 mmol L^{-1} was tested.

The collected samples from the first approach were analyzed for dissolved organic carbon (DOC) as described in S4.7, whereas the samples from the second and third approaches were analyzed on IC-ESI-MS/MS for bleed matrix effects on glyphosate and AMPA quantification as well as in the subsequent blank injections for assessment of carryovers.

Investigation of sample matrix effects on quantification

Ground-, river-, and treated waste waters were used to assess the matrix effects caused by real samples on quantification of glyphosate and AMPA using IC-ESI-MS/MS. After filtration, standards and internal standards were spiked into 100 mL of the sample at 500 ng L^{-1} for ground-, and river water and at 1500 ng L^{-1} for treated waste water. Sample preparation of the spiked samples (**A**) was performed in triplicates where at step **1** the samples were enriched on MISPE at 1.5 mL min^{-1} and the cartridges were eluted at step **2** with 3 mL HCl 0.1 mol L^{-1} to obtain hydrochloric acid extracts (**B**). In step **3**, the extracts were evaporated to dryness to obtain dry extracts (**C**) that were reconstituted in step **4** with 0.5 mL NaOH 25 mmol L^1 to obtain aqueous extracts (**D**). Pure water spiked with the anlytes and internal standard was also prepared following the same procedure and used for comparison. Concentrations of glyphosate and AMPA in the reconstituted extracts were measured on IC-ESI-MS/MS. Matrix effects caused by the samples, ME_{sample}, was calculated by comparing the average area of the internal standard for the environmental sample, A_{sample}, with that for pure water, A_{water}, according to Equation 4.2.

Impact of MISPE bleed on δ^{13}C of glyphosate and AMPA

A leaching bleed from the MISPE cartridge was obtained following the identical procedure described for investigation of MISPE-bleed effects on quantification except the bleed-containing solution (sample **D**) was not diluted but rather used as is. Sample **D** was spiked with standards of glyphosate and AMPA at 55 and 120 mg L^{-1}, respectively, whereas no isotope-labeled standards were used. Carbon isotope-ratio measurements were performed on these samples (denoted **+bleed**) using LC/IRMS and compared to measurements of aqueous solutions of glyphosate and AMPA in pure water that contains the same standards at the same concentrations (denoted **STD**).

Impact of hydrochloric acid on δ^{13}C of glyphosate and AMPA

Standard mixtures of glyphosate and AMPA were prepared in presence and absence of HCl. Concentrations covered 5-90 and 10-180 mg L^{-1} for glyphosate and AMPA, respectively, whereas HCl concentration was 0.1 mol L^{-1} when present. Measurement of these standards was performed on LC-IRMS to compare any potential HCl effect on carbon-isotope ratios. Additional standards were prepared at concentrations above the limits of precise isotope analysis, which were 55 and 120 mg L^{-1} for glyphosate and AMPA, respectively. The additional standards were either prepared (i) with no HCl added (denoted **STD**), or (ii) HCl added to a final concentration of 0.1 mol L^{-1} (denoted **+HCl**), and (iii) HCl 0.1 mol L^{-1} added to standard solutions of glyphosate and AMPA and evaporated at 65 °C under N_2 to dryness, and reconstituted in pure water (denoted **-HCl**). LC-IRMS and/or flow injection analysis was performed for the previous three categories.

4.3 Results and discussion

The term "matrix effect" is used throughout this work to describe any alteration of the analyte response regardless whether the effect occurs in the ion source of the MS (e.g. ion enhancement or suppression) or in the extract-containing vial before measurement (e.g. complex formation). Distinction is, however, made between effects caused by leaching substances from the MISPE materials into the extract, and those caused by the more common co-enrichment of natural matrices of the environmental water. The current work refers to the former as "bleed matrix effects" and to the latter as "sample matrix effects".

4.3.1 Bleed matrix effects on quantification

Organic carbon was found to bleed from the MISPE materials into the aqueous extracts (4-27 mg C L^{-1}) as a result of percolation of pure water through the MISPE cartridges. As a result, response of glyphosate on IC-ESI-MS/MS was found to decrease as the bleed contents increased and led to 80% loss of the glyphosate present in the extract compared to an identical glyphosate concentration (50 µg L^{-1}) in pure water (see Figure 4.2, left panel). Furthermore, substantial carryovers of glyphosate were observed in subsequent blank injections where the carryover magnitude also increased as a function of the bleed contents and amounted up to 25% glyphosate carryover compared to the preceding injected extract (see Figure 4.2, right panel). In contrast, such adverse effects on analyte response or carryovers were not observed for AMPA.

These findings ~~clearly~~ demonstrate that the observed loss of glyphosate response and the associated carryovers are correlated and caused both by the bleed from the MISPE materials. While the known matrix effects of ion suppression in electrospray ion sources (ESI) may explain the bleed matrix effect, it cannot provide an explanation for the associated carryovers of glyphosate in the subsequent blank injections.

Moreover, suppression matrix effects in ESI ion source were shown to influence both glyphosate and AMPA to similar extents in food matrices.[167] In our experiments, however, AMPA did not experience a matrix effect despite its shorter retention time (13 min) compared to glyphosate (21 min). This means, on the one hand, that the bleed effects are analyte-dependent. On the other hand, it may indicate that the bleed-induced effects occur through a mechanism that is not related to the typical suppression effects in ion sources. Such a mechanism could be complexation between the bleed and the

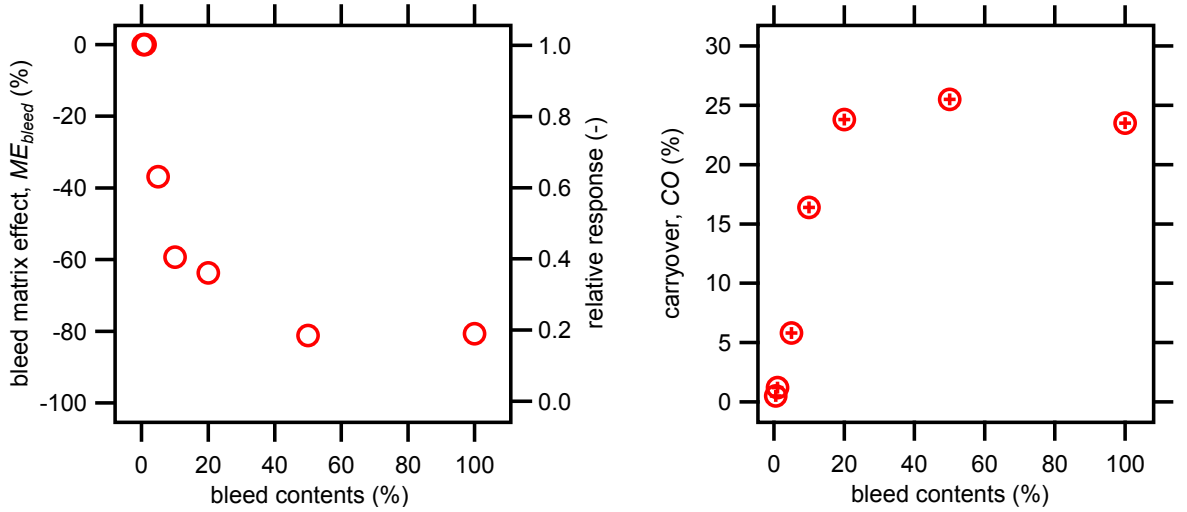

Figure 4.2: Matrix effects originating from the MISPE bleed, ME_{bleed}, on response of glyphosate in IC-ESI-MS/MS as a function of bleed contents in the sample (left), and the associated carryovers (CO) of glyphosate in the first blank after injection of the glyphosate-containing samples (right). Glyphosate concentrations were equal in all samples, $C_{glyph} = 50$ µg L^{-1}.

analyte, which are strong for glyphosate but weak or absent for AMPA.

Postulation on bleed matrix effects and carryovers

Monomers with functional groups capable of interaction with glyphosate are used for the production of the imprinted polymer and it comes as no surprise if they constitute the bleed and consequently complex the extracted glyphosate in the extract. These functional moieties in the bleed are present after elution, sample **B** in Figure 4.3, together with glyphosate but probably can not complex it due to the favorable interactions with HCl in surplus. A complex, however, can form with glyphosate after evaporation of HCl in sample **C**. Once the sample is reconstituted in pure water, sample **D**, the complex dissociates to from free glyphosate existing in equilibrium with the complexed glyphosate.

According to this postulation, only part of the glyphosate in the extract is available and detectable by the IC-ESI-MS/MS which can explain the loss of glyphosate in presence of the bleed. The associated carryovers, on the other hand, would be caused by the temporarily non-available glyphosate in the complexed form. The remaining undissociated complex is hypothesized to retain longer on the IC system and gets progressively dissociated as the hydroxide ion concentration increases in the IC system. Accordingly,

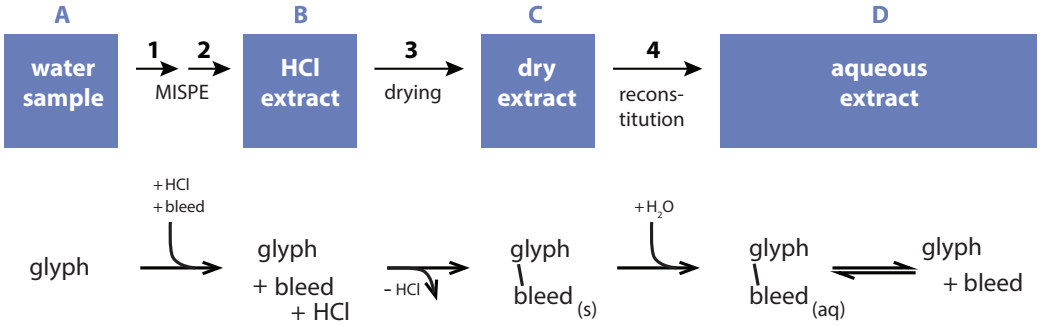

Figure 4.3: Postulation of complex formation between the MISPE bleed and glyphosate throughout the train of sample preparation

part of the newly-formed free-glyphosate in the IC system is detected as a pulse in the subsequent blank leading to the observation of carryovers. Depending on the complexed amount, significant carryovers may appear in only one blank injection or extend further. The carryovers observed in the first blank injection constituted 75% of the total carry-over whereas the remaining 25% appeared in further blanks up to five injections (see Figure S4.6).

Mitigation of MISPE organic-bleed effects

Based on the proposed hypothesis, three approaches were tested on variant steps of the sample preparation procedure in order to mitigate the bleed matrix effects and the carryovers. These approaches included minimization of the leaching bleed by wash procedures of the MISPE cartridges prior to step **1**, removal of the bleed on Oasis HLB at sample **B** & **D**, and breaking the proposed complex between the bleed and glyphosate by using a base at sample **D**. The attempts to minimize the leaching bleed by preconditioning of the cartridges prior to step **1** proved completely ineffective (see S4.5). While removal of the bleed over reversed-phase did not significantly alter the bleed matrix effects (ME_{bleed} from -61% to -54%), the carryovers were attenuated but the remaining carryovers were still substantial (CO from 26% to 12%). The use of NaOH 25 mmol L^{-1} resulted in effective mitigation of the bleed matrix effects (ME_{bleed} from -61% to -3 - 0%) and the associated carryovers (CO from 26% to 1 - 2%) as summarized in Table 4.2.

Table 4.2: Sample preparation modifications for mitigation of matrix effects, ME_{bleed}, and carryovers, CO, originating from the MISPE bleed.

parameter	sample preparation modification				
	none[a]	**B** +Oasis[b]	**D** +Oasis[b]	**D** +NaOH[c]	**B**+Oasis, **D**+NaOH[d]
ME_{bleed} (%)	-61	-58	-54	**0**	**-3**
CO (%)	26	12	16	**1**	**2**

[a] none stands for a bleed-containing sample in pure water;
[b] B+Oasis and D+Oasis used Oasis cartridge to treat the samples where B+Oasis percolated sample B over Oasis cartridge, whereas, D+Oasis percolated sample D over Oasis; [c] D+NaOH used sodium hydroxide 25 mmol L^{-1} to adjust the pH of sample D; [d] B+Oasis, D+NaOH used the combination of b and c.

These findings further support the postulated hypothesis in Figure 4.3 which is a complex formation between glyphosate and the bleed. Although the base used for sample **D** is presumably shifting the equilibrium towards free glyphosate, it does not remove the bleed from the extract. In fact, this is an additional indicator that ion suppression of glyphosate by the bleed in ESI-MS/MS was not the cause of the bleed matrix effect.

4.3.2 Sample matrix effects on quantification

Responses of glyphosate and AMPA on IC-ESI-MS/MS were found to be strongly suppressed by the environmental matrices of river-, ground-, and wastewater after MISPE using the modified sample preparation **D**+NaOH as shown in Table 4.3. Since the implemented sample preparation procedure used sodium hydroxide to eliminate the sample matrix effects ($ME_{bleed} = 0\%$), the observed matrix effects are therefore attributed to the sample. The measured sample matrix effects, ME_{sample}, were -100% for AMPA for all investigated environmental waters, and ranged from -79 to -100% for glyphosate.

Table 4.3: Matrix effects originating from environmental samples, ME_{sample}, for river-, ground-, and wastewater using modified sample preparation **D**+NaOH.

	ME_{sample} (%)		
	river water	ground water	wastewater
glyphosate	-79	-100	-97
AMPA	-100	-100	-100

The co-enriched matrix from the environmental waters obviously induces ion suppression of glyphosate and AMPA signals in ESI-MS/MS which consequently renders the quantitative analysis of the analytes not possible. These results suggest that a cleanup step would be necessary to remove the interfering matrices from the environmental waters in order to attenuate ME_{sample}. Such a step can be implemented on sample **B** in the sample preparation scheme where the eluate of the MISPE passes over reversed-phase. Experiments on sorption of glyphosate and AMPA on Oasis HLB showed no retention and complete breakthrough of the analytes which is consistent with similar findings in literature for cleanup steps for glyphosate and AMPA in milk[168] and soybean extracts[169].

4.3.3 Performance of optimized method MISPE-IC-ESI-MS/MS

Sample preparation using MISPE with the combination of cleanup on Oasis for sample **B** and pH adjustment of aqueous extract **D** (see Figure 4.4) was evaluated for variant water samples in terms of absolute recoveries total matrix effects measured on IC-ESI-MS/MS (see Table 4.4).

Good absolute recoveries over the whole sample preparation procedure (R_{abs}) were obtained for the analytes in variant environmental water matrices which ranged from 26 ± 5 to 97 ± 15% for glyphosate and from 63 ± 7 to 105 ± 26% for AMPA. The total matrix effects (ME_{tot}) originating from both the environmental sample (ME_{sample}) and the MISPE materials (ME_{bleed}) were mostly small enhancing effects for glyphosate (7-15%) and for AMPA (3-6%). Glyphosate in groundwater exhibited an exceptional small recovery of 26 ± 5% associated with an acceptable suppression matrix effect of -12 ± 2%. Estimated method quantification limits (MQL_e) in the investigated environmental samples ranged from 17 ± 5 to 82 ± 27 ng L^{-1} for glyphosate, and from 33 ± 13 to 54

Table 4.4: Absolute recoveries (R_{abs}), total matrix effects (ME_{tot}), and estimated method quantification limit (MQL_e) for glyphosate and AMPA in variant environmental aqueous matrices after sample preparation using reversed-phase at step 2 in addition to reconstitution in sodium hydroxide at step 4 (RP-2+NaOH-4).

	glyphosate			**AMPA**		
	$R_{abs}(\%)$	$ME_{tot}(\%)$	$MQL_e(ngL^{-1})$	$R_{abs}(\%)$	$ME_{tot}(\%)$	$MQL_e(ngL^{-1})$
pure water	87 ± 5[a]	7 ± 1	20 ± 5	51 ± 7	-3 ± 0	73 ± 20
river water	94 ± 7	7 ± 2	20 ± 6	92 ± 8	3 ± 0	37 ± 11
creek water	97 ± 15	15 ± 2	17 ± 5	105 ± 26	5 ± 1	33 ± 13
ground water	26 ± 5	-12 ± 2	82 ± 27	63 ± 7	6 ± 1	54 ± 17
wastewater	78 ± 16	n.a.[b]	n.a.	n.m.[c]	n.a.	n.a.

[a] uncertainties represent propagated errors of triplicate experiments and triplicate measurements with one standard deviation; [b] not available; [c] not measurable due to low level of internal standard.

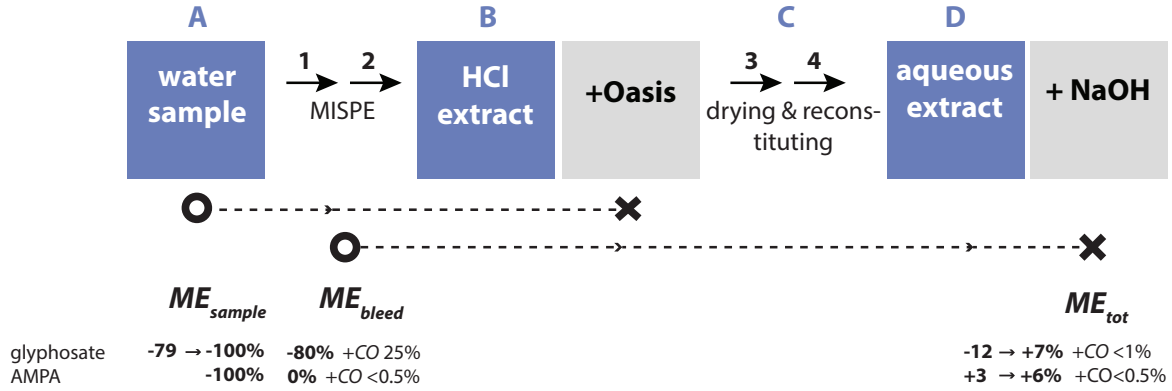

Figure 4.4: Summary of total matrix effects (ME_{tot}) of glyphosate and AMPA on IC-ESI-MS/MS originating from the environmental water sample (ME_{sample}) and the MISPE bleed (ME_{bleed}) and their corresponding mitigation in the developed sample preparation procedure. The letters A, B, C, and D represents the stages of sample preparation; the circles and crosses represent the origin and removal of the matrix effect with respect to the different stages of sample preparation; the mitigation approach is represented in grey boxes.

$\pm$ 17 ng L^{-1} for AMPA. The highest MQL_e was also found for groundwater matrix as a result of the lowest recoveries.

The instrumental setup resulted in chromatograms with sharp peaks for glyphosate with widths equal or less than 1 min, whereas, AMPA exhibited broad and tailed peaks that spanned over 2-3 minutes for most chromatograms (Figure 4.5). These results suggest that the sample preparation over the MISPE is yielding an efficient enrichment of glyphosate and AMPA from environmental waters without significant losses. Oasis HLB after MISPE and a basic pH for the extract can reduce together the variant matrix effects resulting in clean environmental extracts with sufficient enrichment factors, $EF = 100$, for quantification (see Figure 4.4).

4.3.4 Bleed matrix effect and HCl effect on carbon-isotope ratio measurements

The feasibility of MISPE sample preparation to compound-specific isotope analysis (CSIA) was assessed by investigating the impact of hydrochloric acid and the MISPE bleed on integrities of carbon-isotope ratios ($\delta^{13}C$) for glyphosate and AMPA. Deviations ($\Delta\delta^{13}C$) from standards in pure water (STD) are compared in Table 4.5 with the investigated parameters (i.e. +HCl, -HCl, and +bleed). Hydrochloric acid induced substantial biases on carbon-isotope ratios measured on LC/IRMS for glyphosate (-8.2

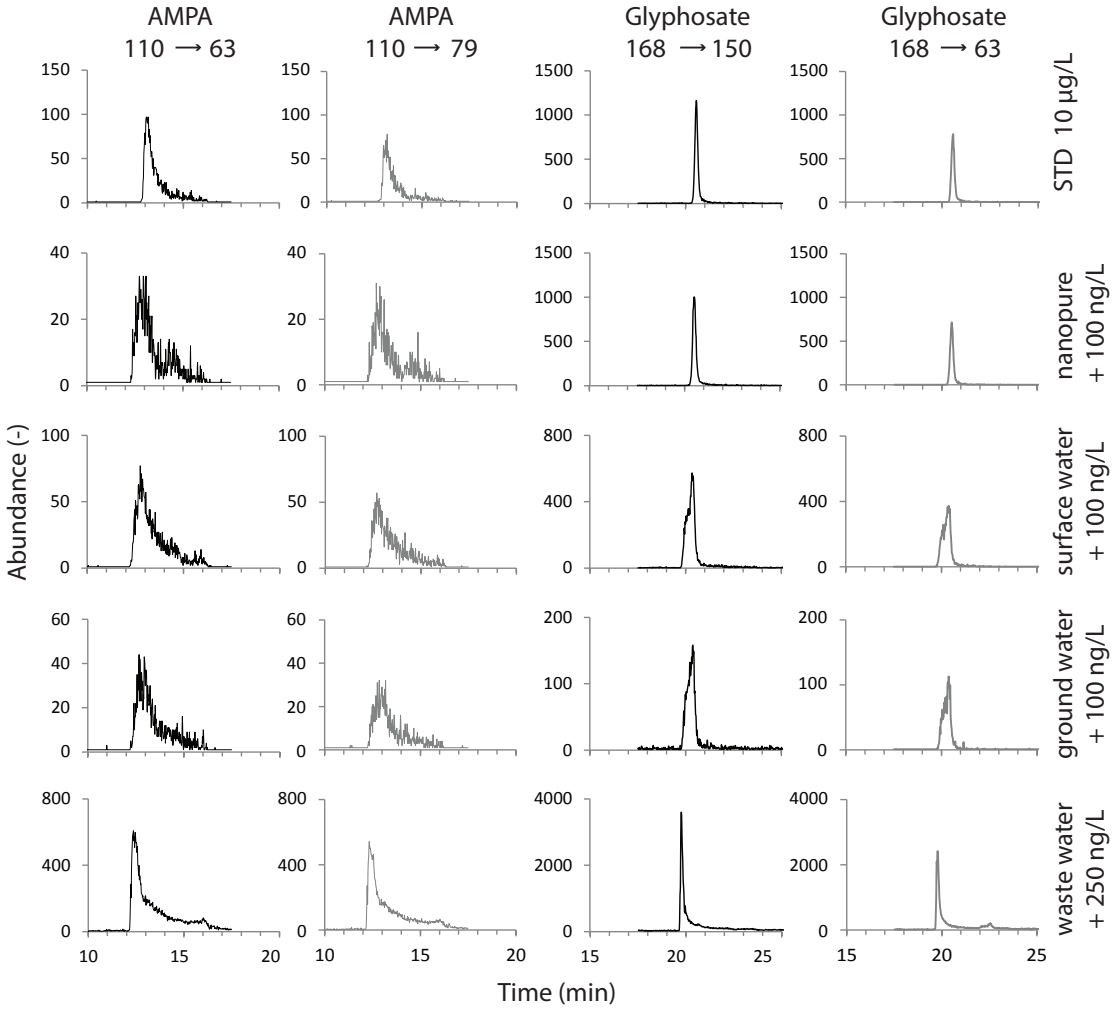

Figure 4.5: Chromatograms of AMPA and glyphosate for the qualifier ion (grey) and quantifier ion (black) in standard solution 10 µg L^{-1} without enrichment (top), and in spiked environmental matrices with enrichment factor of 100 over the validated analytical procedure.

± 0.3‰) and a small bias for AMPA (-1.1± 0.4‰). Comparison of the analytes peak areas acquired on LC/IRMS in presence and absence of HCl shows that presence of HCl yields smaller peak areas for glyphosate which is only 50% of those in absence of HCl (slope of red line in Figure 4.6), whereas, peak areas of AMPA are affected to a lesser extent and they are 69% of those in absence of HCl (slope of blue line in Figure 4.6). This suggests that hydrochloric acid suppresses the efficient conversion of glyphosate and AMPA into the measurement gas CO_2 by 50% (i.e. $100 - 50$) and 31% (i.e. $100 - 69$), respectively. This is further supported by flow injection analysis (FIA/IRMS) of the individual analytes where significant biases were similarly obtained for glyphosate ($\Delta\delta^{13}C$ = -3.8±0.6‰) and AMPA ($\Delta\delta^{13}C$ = -4.0±0.8‰). Since FIA/IRMS bypasses the liquid chromatograph, the observed isotopic fractionation is thus attributed to inhibitory effects on conversion efficiency of the analytes in the interface caused by HCl. In contrast, no significant isotopic biases (<1‰) were detected for the analytes after thermal evaporation of HCl on either LC/IRMS or FIA/IRMS. This means that the removal of HCl and reconstitution in water, steps **3 & 4** in sample preparation, do not have adverse impacts on isotopic integrities of glyphosate and AMPA.

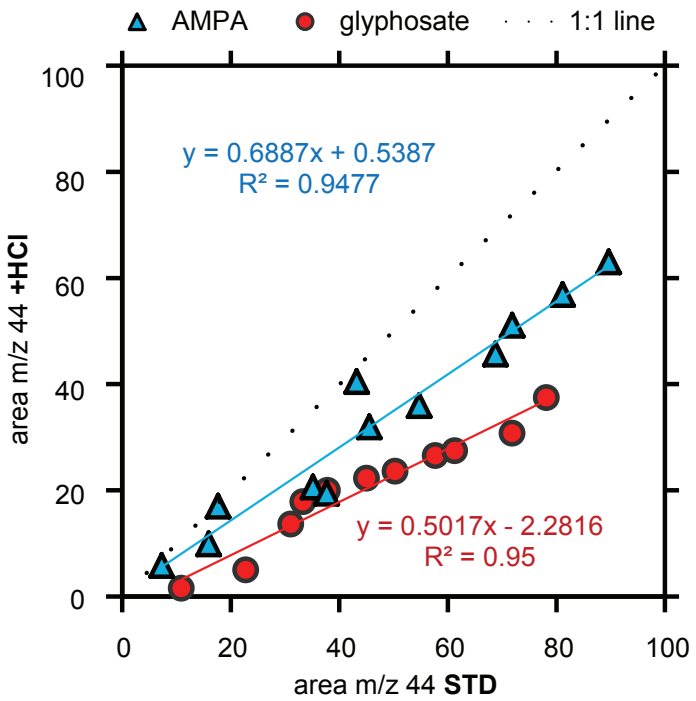

Figure 4.6: Integrated peak areas of glyphosate (red circles) and AMPA (blue triangles) in pure water (STD) and in aqueous solutions of HCl 0.1 mol L^{-1} (+HCl) on LC/IRMS. Linear regressions are shown for glyphosate (red line) and AMPA (blue line) along with the corresponding equations.

δ^{13}C of glyphosate and AMPA in presence of the leaching bleed from the MISPE cartridge (+bleed) slightly shifted by -0.9 ± 0.6‰for glyphosate and 1.2 ± 0.6‰for AMPA. It is worth noting that the bleed presence led to reduction of glyphosate peak area by 52 ± 17% compared to the bleed-free standard (STD), whereas, AMPA peak area was reduced by only 12 ± 1%. Nevertheless, the reduction in peak areas did not cause significant deviations in δ^{13}C ($\Delta\delta^{13}$C ≈ 1‰). These findings provide promising first results for the use of MISPE as an enrichment method for glyphosate and AMPA for carbon isotope measurements. While the current study focused on matrix effects caused by the MISPE and their influence on CSIA of glyphosate and AMPA, further investigations would be necessary for full application of MISPE to CSIA of environmental samples. Such investigations should include the impact of sorption/recovery of the analytes, onto/from MISPE, on isotopic integrity of the analytes in addition to any possible influence of environmental sample matrix on the acquired isotopic signatures.

4.4 Conclusion

The current work demonstrated a systematic identification and quantification of the different matrix effects associated with direct enrichment of underivatized glyphosate and AMPA from environmental waters using water-compatible molecularly-imprinted solid-phase extraction (MISPE). With MISPE, direct enrichment of glyphosate and AMPA from water is effective but it is associated with significant matrix effects that limits an efficient analysis of the obtained extracts due to analyte suppression, complexation, and carryovers. The results suggest that the use of Oasis HLB in combination with the MISPE efficiently eliminates the matrix effects originating from the environmental sample (i.e. analyte suppression). On the other hand, pH adjustment of the obtained extract eliminate the matrix effects originating from the MISPE materials (i.e. complexation and carryovers). The proposed sample preparation approach provides a clean extract that contains sufficient analyte mass for detection and quantification on IC-ESI-MS/MS using only 100 mL environmental sample with method quantification limit, MQL_e, 17-82 ng L^{-1} for glyphosate and 37-54 ng L^{-1} for AMPA. The lowest achieved MQL_es in this study are 3 to 8 times higher than the lowest achieved for derivatization-based protocols[144] of 5 ng L^{-1}. However, the current environmental concentrations determined for glyphosate (i.e. 110 ng L^{-1})[144] and AMPA (i.e. 200 ng L^{-1})[144] are above the MQL_e of this study. Thus, the developed methodology offers a simple and selective alternative to tedious derivatization procedures where the time necessary for the derivatization re-

Table 4.5: Carbon-isotope ratio, $\delta^{13}C$, of standard aqueous solutions of glyphosate and AMPA and associated deviations, $\Delta\delta^{13}C$, due to presence of hydrochloric acid, its removal, and presence of organic bleed.

		LC/IRMS		**FIA[a]/IRMS**	
compound	matrix	δ^{13}C[b] (‰)	$\Delta\delta^{13}$C[c] (‰)	δ^{13}C[b] (‰)	$\Delta\delta^{13}$C[c] (‰)
glyphosate	STD[d]	-18.7 ± 0.3	0.0 ± 0.5	-22.7 ± 0.3	0.0 ± 0.4
	+HCl[e]	-26.9 ± 0.1	**-8.2 ± 0.3**	-26.5 ± 0.5	**-3.8 ± 0.6**
	-HCl[f]	-18.8 ± 0.4	-0.1 ± 0.5	-22.3 ± 0.9	0.4 ± 0.9
	+bleed[g]	-19.6 ± 0.6	-0.9 ± 0.6	n.m.[h]	n.m.
AMPA	STD[d]	-24.9 ± 0.2	0.0 ± 0.3	-30.8 ± 0.7	0.0 ± 1.0
	+HCl[e]	-26.0 ± 0.4	**-1.1 ± 0.4**	-34.8 ± 0.3	**-4.0 ± 0.8**
	-HCl[f]	-25.4 ± 0.3	-0.5 ± 0.4	-31.1 ± 1.4	-0.3 ± 1.6
	+bleed[g]	-23.7 ± 0.5	**1.2 ± 0.6**	n.m.	n.m.

[a] flow injection analysis (FIA) bypasses the liquid chromatography by direct injection of the analytes into the interface followed by the IRMS; [b] carbon-isotope ratio of the compound in the corresponding matrix; [c] deviation of carbon-isotope ratio in the corresponding matrix from the standard (STD); [d,e,f,g] aqueous standards of glyphosate 55 mg L^{-1} and AMPA 120 mg L^{-1} with variant matrices; [d] in pure water; [e] in 0.1 mol L^{-1} HCl aqueous solution; [f] the former solution after evaporation to dryness and reconstitution in pure water; [g] in presence of MISPE bleed; [h] not measured; uncertainties represent propagated errors from triplicate experiments and triplicate measurements with one standard deviation.

action (from 30 min to 24 hours) and minimization of derivation by-products (30 min) can be spared. First results of LC/IRMS and FIA/IRMS along with the good absolute recoveries over the sample preparation (mostly $\geq 80\%$) suggest feasibility of expanding the sample preparation approach to CSIA. Despite the good absolute recoveries over the sample preparation , assessment of analyte fractionation due to sorption-desorption processes on the MISPE is required. Since visibility of matrix effects are not the same on different instruments, the feasibility of using Oasis HLB to remove interferences from the MISPE eluate needs assessment on LC/IRMS. Assessment of analyte fractionation due to sorption/recovery processes on the MISPE would be warranted before performing isotopic analysis of glyphosate and AMPA in environmental samples.

Supporting Information to Chapter 4

S4.1 Gradient program for ion chromatography

Table S4.1: Gradient program of eluent strength used on IC-MS/MS for separation of glyphosate and AMPA.

Time (min)	KOH (mmol L^{-1})	Curve
0.0	7	5
0.5	7	5
9.5	25	5
19.0	60	5
19.1	150	5
26.0	150	5
26.1	7	5
37.0	7	5

S4.2 Conditions for tandem MS analysis

Table S4.2: Parent and product masses, collision energies, and S-lens RF amplitude values for glyphosate, AMPA, and corresponding isotope-labeled internal standards used in this study.

Compound	Parent mass (m/z)	Product mass (m/z)	Collision energy (V)	S-lens RF amplitude (V)
AMPA	110.2	63.1	20	106
	110.2	79.1	30	106
	110.2	81.1	14	106
AMPA IS	114.0	63.0	21	118
	114.0	79.0	31	118
	114.0	81.1	15	118
glyphosate	168.1	63.1	22	81
	168.1	79.1	45	81
	168.1	150.1	12	81
glyphosate IS	171.0	63.0	24	81
	171.0	79.0	43	81
	171.0	153.1	12	81

S4.3 Characteristic parameters of the environmental waters

Table S4.3: Characteristic parameters of environmental waters used in this study for investigation of environmental matrix effects and absolute recoveries of sample preparation.

parameter	unit	river water	creek water	ground water	wwtp effluent
pH	-	8.1	8.2	7.9	8.3
conductivity	µS/cm	341	729	683	1139
alkalinity	mmol/L	3.05	6.12	5.86	6.28
total hardness	mmol/L	1.79	3.55	3.34	3.19
total nitrogen	mg N/L	1.7	6.7	3.5	10.3
DOC	mg C/L	1.6	2.4	1.5	7.1
sodium	mg Na^+/L	7.5	34.0	29.4	139
potassium	mg K^+/L	1.6	4.8	3.8	10.7
ammonium	µg NH_4^+-N/L	10.3	21.7	<5.0	13.4
magnesium	mg Mg^{2+}/L	7.5	18.2	16.5	17.6
calcium	mg Ca^{2+}/L	58.4	109.0	105.2	96.3
chloride	mg Cl^-/L	11.1	48.3	44.9	163
nitrite	µg NO_2^--N/L	<1.0	13.3	<1.0	19.9
nitrate	mg NO_3^-/L	1.6	6.4	3.4	8.1
sulfate	mg SO_4^{2-}/L	24	33	32	34
ortho-phosphate	µg P/L	17.7	94.6	31.5	242
dissolved phosphorus	µg P/L	18.4	102.5	32.2	434
silicate	mg/L	5.4	13.1	12.7	23.5

S4.4 Instrumental detection- and quantification limits of glyphosate and AMPA on IC-ESI-MS/MS

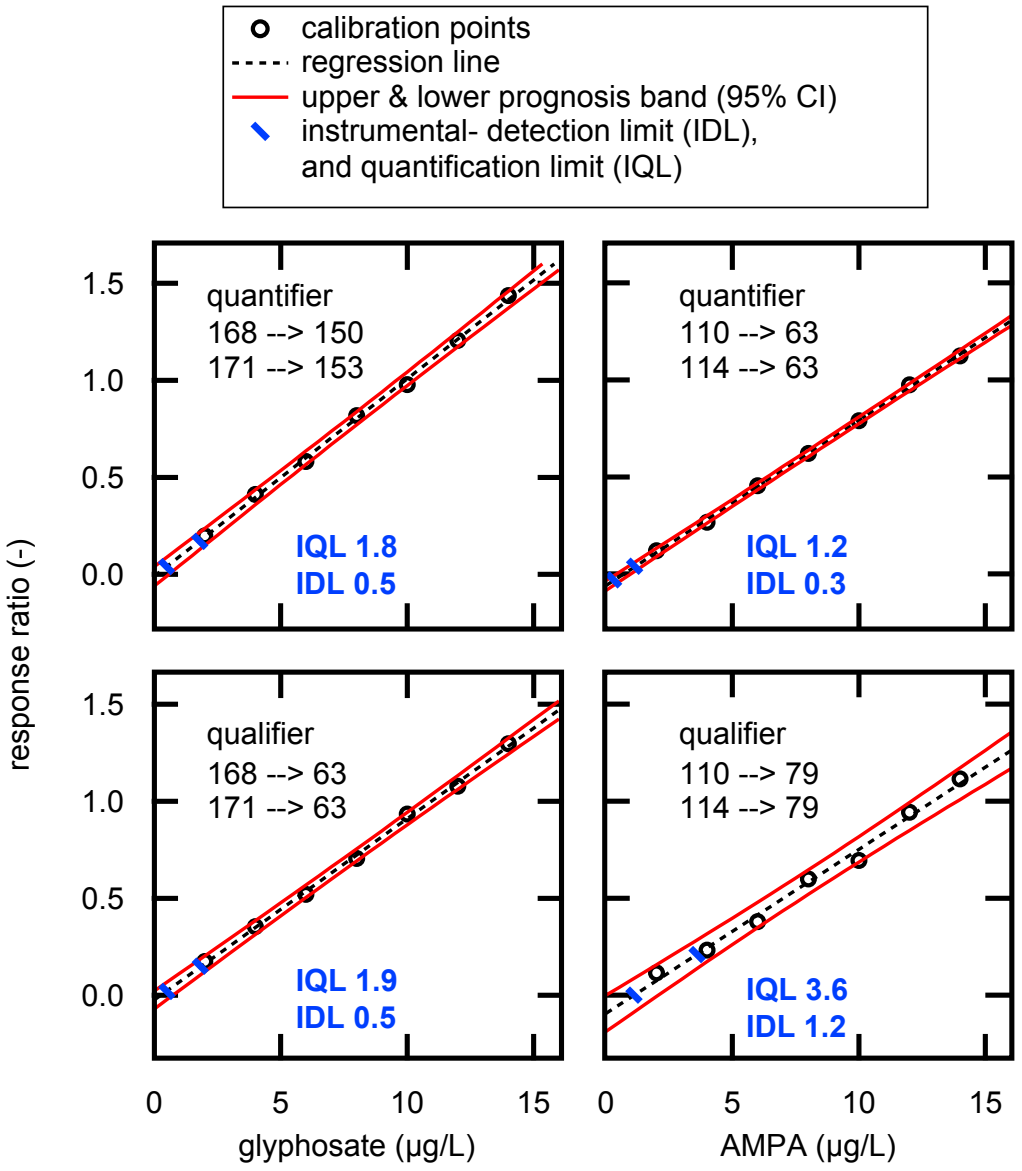

Figure S4.1: Instrumental- detection and quantification limits (IDL&IQL) for glyphosate (left) and AMPA (right) for the quantifier and qualifier transitions. On each plot, the investigated transitions for the standard and the assigned internal standard are given (black) along with the the corresponding IDL and IQL (blue).

S4.5 Procedures of preconditioning the MISPE cartridges

Table S4.4: Levels of dissolved organic carbon bleed in the breakthrough and elution fractions after variant procedures of preconditioning the molecularly-imprinted solid-phase extraction cartridge.

procedure	**i** [b]		**ii** [b]		**iii** [b]		**iv** [b]	
fraction	break [c]	eluate [c]	break	eluate	beak	eluate	break	eluate
pure water [a]	8.3	**3.6**	47.6	22.2	17.0	16.5	8.9	27.2
river water [a]	9.3	**7.3**	48.3	27.5	19.9	20.0	4.7	27.7

all values are in mg C L^{-1} with associated uncertainties of approximately 20%,
[a] the percolated sample was 100 mL of either pure water with no DOC contents (< 0.5 mg C L^{-1}) or river water containing 2.2 mg C L^{-1} which were loaded on the MISPE cartridge after the corresponding wash procedure and before elution, [b] pre-wash procedures were **i** 6 mL pure water, **ii** 100 mL pure water in addition to pressure exertion on the cartridge during washing, **iii** sequential washing with 100 mL pure water, 100 mL hydrochloric acid 0.1 mol L^{-1}, and 100 mL pure water, and **iv** sequential washing with 100 mL pure water, 100 mL hydrochloric acid 0.1 mol L^{-1}, 100 mL methanol 20 vol %, and 100 mL water.
[c] break stands for the breakthrough fraction of the loaded sample, whereas, elute stands for a 3 mL fraction of hydrochloric acid 0.1 mol L^{-1} used to elute the cartridge after loading the sample.

S4.6 Correlation of first- versus total-carryover

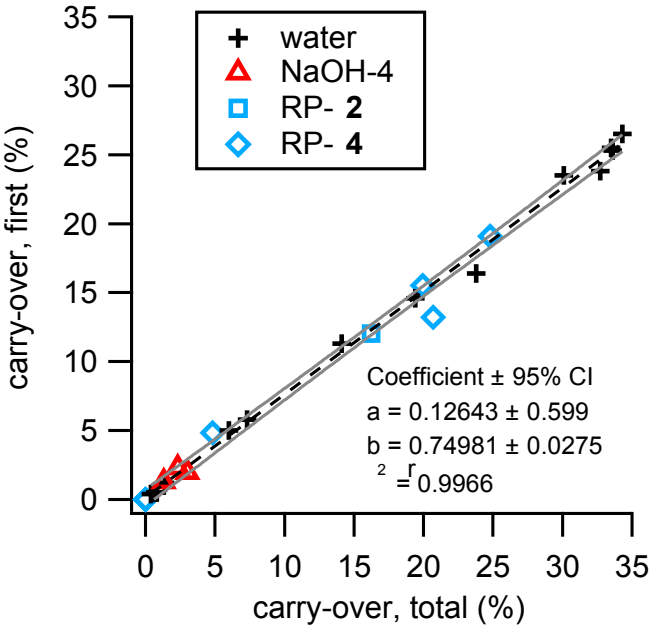

Figure S4.2: Carry-over of glyphosate in the subsequent blank injection (first) versus the carry-over sum in the five subsequent blank injection (total).

S4.7 Measurements of dissolved-organic carbon

Dissolved organic carbon (DOC) was measured using a total organic carbon analyzer (TOC-L, Shimadzu) equipped with a combustion catalytic oxidation unit (680 °C) and a non-dispersive infrared detector. DOC concentrations were carried out after filtration through 0.45 µm filter. The samples were diluted to fall in the linear dynamic range of the instrument which was 0.5-10 mgC L^{-1} with a limit of quantification (LOQ) of 0.5 mgC L^{-1}.

Chapter 5

Conclusions and Outlook

This work aims at expansion of compound-specific isotope analysis (CSIA) applicability to polar organic micopollutants in environmental waters. It was initially hypothesized that the lack of selectivity in sample preparation workflows constitutes a major bottleneck for CSIA of such contaminants. the present work investigated the effectiveness of generic molecular-imprinting techniques for selective sample preparation of a number of polar organic micropollutants in environmental waters. The results suggest that molecularly-imprinted polymers (MIP) significantly enhance the quality of environmental extracts, thereby offering a new perspective for CSIA.

5.1 Effectiveness and limitations of molecular-imprinting approaches for CSIA

The effectiveness of generic molecular-imprinting was assessed for three classes of compounds benzotriazoles, s-triazines, and glyphosate using custom-synthesis and commercially-available MIPs with two approaches: (i) Reversed-phase solid-phase extraction (SPE) followed by MIP and (ii) direct extraction by MIP. The developed methodologies using approach (i) and (ii) were successful at preparing samples amenable to GC/IRMS and LC/IRMS, respectively. The results of this dissertation found that a combinational approach of sequential extraction using sorbents of various selectivities is essential for clean environmental extracts suitable for CSIA. In approach (i), the two examples of $1H$-benzotriazole and triazine demonstrate the necessity for conventional SPE for initial enrichment of large volumes of water required for CSIA (i.e. $\geq$ 10 L), followed by MIP selective cleanup. The results suggest also that the MIP can successfully be implemented in the sample preparation workflow as a first step when ionic interactions are employed or as a second step when hydrogen-bonding are used. Approach (ii) was successfully applied for direct extraction of glyphosate and AMPA from surface-, ground-, and wastewater with good recoveries. Nevertheless, a second step on reversed-phase sorbent for cleaning the extract proved inevitable, which suggests that non-specific binding exhibited by the investigated MIPs towards natural- and effluent organic matter is an important parameter to assess. Investigation of natural organic matter impact from surface water on GC-IRMS measurements revealed that the amount of dissolved organic carbon (DOC) relative to the micropollutant is a useful a priori indicator to assess effectiveness of sample preparation workflows for precise and accurate $\delta^{13}C$ measurements. This study suggests that a ratio of DOC:micropollutant of $\leq$ 10 is required for the en-

vironmental extract to avoid interference with the micropollutant isotopic integrity by DOC. An improvement of approximately 10-fold in the DOC:micropollutant ratio was possible in this work thanks to MIPs (approach (i)), meaning environmental extracts with DOC:micropollutant ratio of ≤ 100 can be analyzed with GC-IRMS. This improvement allows for the measurement of contaminants such as 1*H*-benzotriazole in surface waters (e.g. 2 mg C L^{-1}) occurring at ≥ 3.5 µg L^{-1} which is a relevant environmental condition. At higher DOC:micropollutant ratio (i.e. ≥ 100), the non-specific binding exhibited by MIP towards DOC becomes pronounced and thus exceeds the MIP-GC-IRMS capacity presented in this study.

The generic protocol of synthesis used in this work, non-covalent imprinting using ratios 1 template : 4 functional monomer : 20 crosslinker, offered good selectivity to handle river water extracts. In contrast, the example of wastewater influent and effluent showed that approach (i) with merely two-steps did not offer sufficient selectivity to obtain a clean extract for GC-IRMS. Thus, increasing the total selectivity of the current sample preparation workflow would be necessary to achieve clean extracts for wastewater samples. Implementation of additional sample cleaning techniques, such as liquid-liquid extraction or preparative chromatography[83], is successful at increasing the selectivity of sample preparation to analyze wastewater as shown in Figure 5.2. Another methodology would be to further enhance the MIP selectivity by suppression of the non-specific binding sites present in the polymer skeleton using chemical modification after synthesis[170] as depicted in figure 5.1. For example, an imprinted polymer for the recognition of pyridine, quinoline, and acridine was reacted with acyl chlorides of varying size resulting in an enhanced selectivity by factors of up to 5-folds[171].

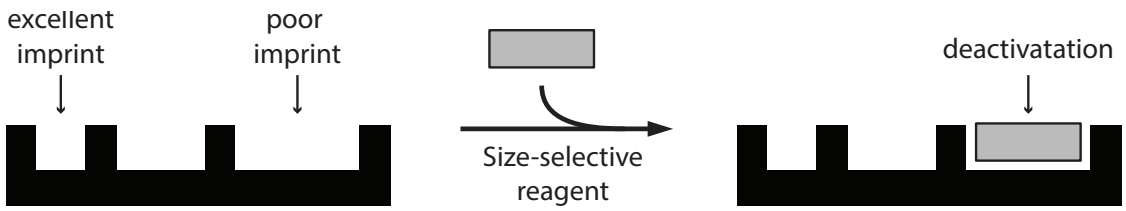

Figure 5.1: Chemical modification of heterogeneous binding sites in a molecularly-imprinted polymer by deactivation of poor imprints using size-selective reagent.[170]

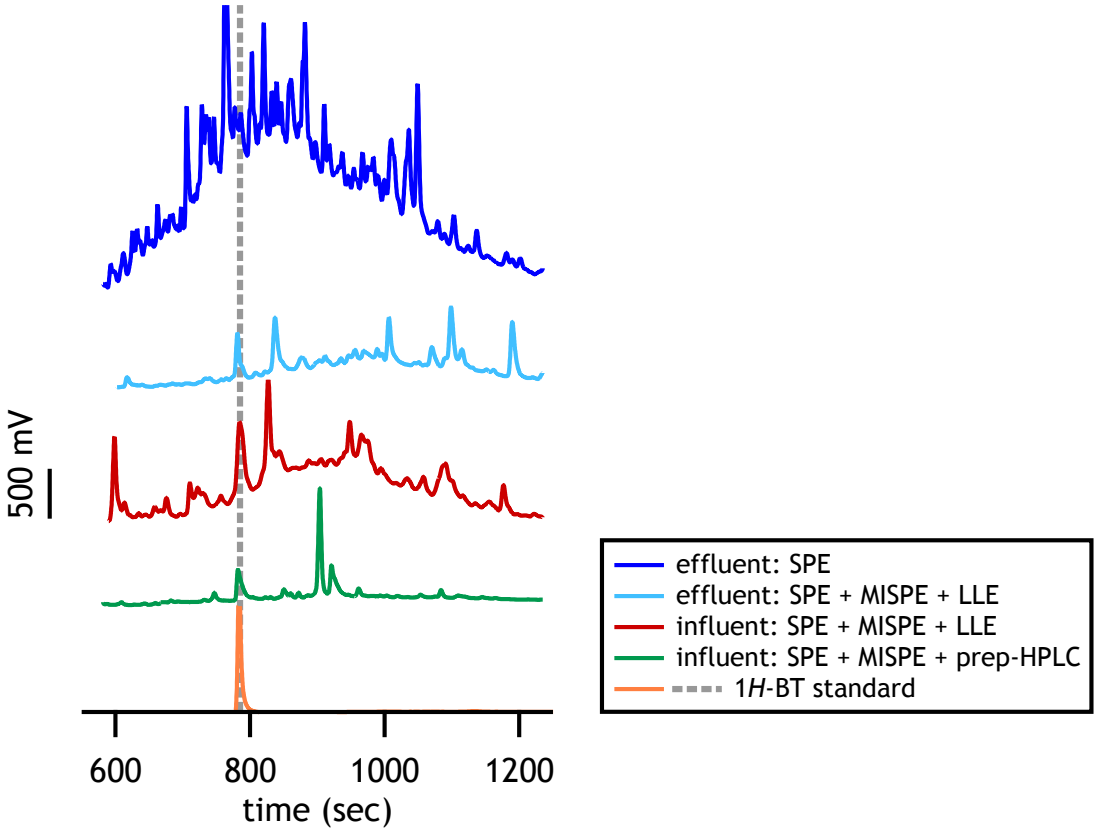

Figure 5.2: GC-IRMS chromatograms for C isotope ratio measurements (signals at m/z 44) of influent and effluent samples from WWTP containing 1*H*-benzotriazole after different sample treatments steps. Sample prepared with only SPE is shown for WW effluent (dark blue); additional MISPE and liquid-liquid extraction shown for WW effluent (light blue) and WW influent (red); additional MISPE and preparative chromatography shown for WW influent (green). The bottom chromatogram and the dashed lines stand for the retention time of 1*H*-benzotriazole in standard solutions in dichloromethane.

5.2 Implications for other contaminants

The successful examples in this study enabled CSIA for various aquatic environments with micropollutant occurrences in the low µg/L range. The applicability of this study to other polar organic micropollutants can in principle be further expanded to many pesticides, pharmaceuticals, and other contaminants. Table 5.1 lists some examples for different polar organic micropollutants in typical environmental matrices and a proposed approach for sample preparation for CSIA. Contaminants with occurrences at the ng/L range still need further development and research. For instance, water volumes necessary for CSIA of micropollutant lower than 100 ng/L is $\geqslant$ 100 L. Thus, automation of the large volume percolation over SPE (i) or MISPE (ii) is vital in order to make

sample preparation less tedious and more robust. The increase in DOC:micropollutant ratio associated with lower occurrences would require more selectivity in the analytical procedure. While further optimization in sample preparation may still gain five-folds reduction of DOC:micropollutant ratios of the sample, it will probably reach its limits due to complex workflows or unrealistic cost of materials. On the instrumental end, increasing the acceptable ratio of DOC:micropollutant would be necessary and can be achieved by the use of longer columns (e.g. 150 m)[172], and multi-dimensional chromatographic systems[173–178].

Table 5.1: Examples of pesticides, pharmaceuticals, and other polar organic micropollutants under real environmental conditions with applicability to one of the two approaches developed in this dissertation.

Category	Compound	Matrix[a,b,c]	Conc. (µg/L)	Approach
pesticides	propanil	SW[a]	1.8[179]	i
	malathion	SW	1.1[180]	i
	MCPA[d]	SW	0.4[180]	i or ii
	diuron	SW	1.7[181]	i
	dimethoate	SW	1.1[181]	i
	diazinon	SW	1.3[181]	i
	metolachlor	SW	up to 1.5[182]	i
pharmaceuticals	diclofenac	WW (EFF)	1.5 (1.0)[183]	i or ii
	gabapentin	WW (EFF)	1.8 (1.3)[183]	ii
	levetiracetam	WW (EFF)	3 (1.3)[183]	ii
	metformin	WW (EFF)	44 (6.1)[183]	ii
	4-Acetamidoantipyrine[e]	WW (EFF)	2.3 (2.1)[183]	i
	4-Aminopyrine[f]	WW (EFF)	1.8 (2)[183]	i
others	DEET[g]	WW (EFF)	3.2 (0.3)[183]	i
	tolyltriazole[h]	WW (EFF)	2.7 (1.6)[183]	i

[a] surface water; [b] wastewater influent; [c] wastewater effluent;
[d] 2-methyl-4-chlorophenoxyacetic acid;
[e] metabolite of aminopyrine/metamizol; [f] metabolite of aminopyrine;
[g] N,N-Diethyl-meta-toluamide, active ingredient in insect repellent; [h] corrosion inhibitor.

Bibliography

[1] Schwarzenbach, R. P., Egli, T., Hofstetter, T. B., von Gunten, U., Wehrli, B., Global water pollution and human health, *Annu. Rev. Environ. Resour.*, **2010**, 35, 109–136.

[2] Schwarzenbach, R. P., Escher, B. I., Fenner, K., Hofstetter, T. B., Johnson, C. A., von Gunten, U., Wehrli, B., The challenge of micropollutants in aquatic systems., *Science*, **2006**, 313, 1072–7.

[3] Hollender, J., Singer, H., McArdell, C. S., *Dangerous Pollutants (Xenobiotics) in Urban Water Cycle*, chap. Polar organic micropollutants in the water cycle, Springer, **2008**, 103–116.

[4] Richardson, S. D., Ternes, T. A., Water analysis: Emerging contaminants and current issues, *Analytical Chemistry*, **2011**, 83, 4614–4648.

[5] Stamm, C., Alder, A. C., Fenner, K., Hollender, J., Krauss, M., McArdell, C. S., Ort, C., Schneider, M. K., Spatial and temporal patterns of pharmaceuticals in the aquatic environment: A review, *Geography Compass*, **2008**, 2, 920–955.

[6] Ternes, T., The occurrence of micopollutants in the aquatic environment: a new challenge for water management, *Water Science and Technology*, **2007**, 55, 327–332.

[7] Stamm, C., Räsänen, K., Burdon, F., J. Altermatt, F., Jokela, J., Joss, A., Ackermann, M., Eggen, R. I. L., *Advances in Ecological Research*, vol. 55, chap. Unravelling the Impacts of Micropollutants in Aquatic Ecosystems: Interdisciplinary Studies at the Interface of Large-Scale Ecology, Academic Press, **2016**, 183–223.

[8] Huntscha, S., Singer, H. P., McArdell, C. S., Frank, C. E., Hollender, J., Multiresidue analysis of 88 polar organic micropollutants in ground, surface and wastewater using online mixed-bed multilayer solid-phase extraction coupled to high performance liquid chromatographytandem mass spectrometry, *Journal of Chromatography A*, **2012**, 1268, 74–83.

[9] Fent, K., Weston, A. A., Caminada, D., Ecotoxicology of human pharmaceuticals, *Aquatic Toxicology*, **2006**, 76, 122–159.

[10] Schipper, P. N. M., Vissers, M. J. M., van der Linden, A. M. A., Pesticides in groundwater and drinking water wells: overview of the situation in the netherlands, *Water Science and Technology*, **2008**, 57, 1277–1286.

[11] Fenner, K., Canonica, S., Wackett, L. P., Elsner, M., Evaluating pesticide degradation in the environment: Blind spots and emerging opportunities, *Science*, **2013**, 341, 752–758.

[12] Hofstetter, T. B., Schwarzenbach, R. P., Bernasconi, S. M., Assessing transformation processes of organic compounds using stable isotope fractionation., *Environ. Sci. Technol.*, **2008**, 42, 7737–7743.

[13] Hofstetter, T. B., Berg, M., Assessing transformation processes of organic contaminants by compound-specific stable isotope analysis, *TrAC-Trends Anal. Chem.*, **2011**, 30, 618 – 627.

[14] Hofstetter, T. B., Bolotin, J., Pati, S. G., Skarpeli-Liati, M., Spahr, S., Wijker, R. S., Isotope effects as new proxies for organic pollutant transformation, *CHIMIA*, **2014**, 68, 788–792.

[15] Elsner, M., Zwank, L., Hunkeler, D., Schwarzenbach, R. P., A new concept linking observable stable isotope fractionation to transformation pathways of organic pollutants., *Environ. Sci. Technol.*, **2005**, 39, 6896–916.

[16] Elsner, M., Imfeld, G., Compound-specific isotope analysis (CSIA) of micropollutants in the environment current developments and future challenges, *Current Opinion in Biotechnology*, **2016**, 41, 60–72.

[17] Schmidt, T. C., Jochmann, M. A., Origin and fate of organic compounds in water: Characterization by compound-specific stable isotope analysis, *Annual Review of Analytical Chemistry, Vol 5*, **2012**, 5, 133–155.

[18] Hunkeler, D., Meckenstock, R., Sherwood Lollar, B., Schmidt, T. C., Wilson, J. C., A guide for assessing biodegradation and source identification of organic ground water contaminants using compound specific isotope analysis (CSIA), Office of research and development, US EPA, **2008**.

[19] Sessions, A. L., Isotope-ratio detection for gas chromatography., *J. Sep. Sci.*, **2006**, 29, 1946–61.

[20] Godin, J.-P., Fay, L.-B., Hopfgartner, G., Liquid chromatography combined with mass spectrometry for ^{13}C isotopic analysis in life science research, *Mass Spectrometry Reviews*, **2007**, 26, 751–774.

[21] Zhang, L., Kujawinski, D. M., Jochmann, M. A., Schmidt, T. C., High-temperature reversed-phase liquid chromatography coupled to isotope ratio mass spectrometry, *Rapid Commun. Mass Spectrom.*, **2011**, 25, 2971–2980.

[22] Jochmann, M. A., Schmidt, T. C., *Compound-Specific Stable Isotope Analysis*, chap. Instrumentation for compound-specific isotope analysis, UK: Royal Society of Chemistry, **2012**, 125–127.

[23] Krummen, M., Hilkert, A. W., Juchelka, D., Duhr, A., Schlüter, H.-J., Pesch, R., A new concept for isotope ratio monitoring liquid chromatography/mass spectrometry, *Rapid Commun. Mass Spectrom.*, **2004**, 18, 2260–2266.

[24] Elsner, M., Stable isotope fractionation to investigate natural transformation mechanisms of organic contaminants: principles, prospects and limitations, *J. Environ. Monit.*, **2010**, 12, 2005–2031.

[25] Ivdra, N., Fischer, A., Herrero-Martín, S., Giunta, T., Bonifacie, M., Richnow, H.-H., Carbon, hydrogen and chlorine stable isotope fingerprinting for forensic investigation on hexachlorocyclohexanes, *Environ. Sci. Technol.*, **2016**, 51, 446–454.

[26] Gilevska, T., Gehre, M., Richnow, H.-H., Multidimensional isotope analysis of carbon, hydrogen and oxygen as tool for identification of the origin of ibuprofen, *Journal of Pharmaceutical and Biomedical Analysis*, **2015**, 115, 410–417.

[27] Kaown, D., Shouakar-Stash, O., Yang, J., Hyun, Y., Lee, K.-K., Identification of multiple sources of groundwater contamination by dual isotopes, *Ground Water*, **2014**, 52, 875–885.

[28] Spahr, S., Bolotin, J., Schleucher, J., Ehlers, I., von Gunten, U., Hofstetter, T. B., Compound-specific carbon, nitrogen, and hydrogen isotope analysis of *N*-nitrosodimethylamine in aqueous solutions, *Anal. Chem.*, **2015**, 87, 2916–2924.

[29] Arnold, W. A., Bolotin, J., von Gunten, U., Hofstetter, T. B., Evaluation of functional groups responsible for chloroform formation during water chlorination using compound specific isotope analysis, *Environ. Sci. Technol.*, **2008**, 42, 7778–7785.

[30] Hunkeler, D., Laier, T., Breider, F., Jacobsen, O. S., Demonstrating a natural origin of chloroform in groundwater using stable carbon isotopes, *Environ. Sci. Technol.*, **2012**, 46, 6096–6101.

[31] Wijker, R. S., Bolotin, J., Nishino, S. F., Spain, J. C., Hofstetter, T. B., Using compound-specific isotope analysis to assess biodegradation of nitroaromatic explosives in the subsurface, *Environ. Sci. Technol.*, **2013**, 47, 6872–6883.

[32] Maier, M. P., Prasse, C., Pati, S. G., Nitsche, S., Li, Z., Radke, M., Meyer, A. H., Hofstetter, T. B., Ternes, T. A., Elsner, M., Exploring trends of C and N isotope fractionation to trace transformation reactions of diclofenac in natural and engineered systems, *Environ. Sci. Technol.*, **2016**, 50, 10933–10942.

[33] Schürner, H. K. V., Maier, M. P., Eckert, D., Brejcha, R., Neumann, C.-C., Stumpp, C., Cirpka, O. A., Elsner, M., Compound-specific stable isotope fractionation of pesticides and pharmaceuticals in a mesoscale aquifer model, *Environ. Sci. Technol.*, **2016**, 50, 5729–5739.

[34] Badin, A., Broholm, M. M., Jacobsen, C. S., Palau, J., Dennis, P., Hunkeler, D., Identification of abiotic and biotic reductive dechlorination in a chlorinated ethene plume after thermal source remediation by means of isotopic and molecular biology tools, *J. Contam. Hydrol.*, **2016**, 192, 1–19.

[35] Rosell, M., Gonzalez-Olmos, R., Rohwerder, T., Rusevova, K., Georgi, A., Kopinke, F.-D., Richnow, H.-H., Critical evaluation of the 2D-CSIA scheme for distinguishing fuel oxygenate degradation reaction mechanisms, *Environ. Sci. Technol.*, **2012**, 46, 4757–4766.

[36] Passeport, E., Landis, R., Lacrampe-Couloume, G., Lutz, E. J., Mack, E. E., West, K., Morgan, S., Sherwood Lollar, B., Sediment monitored natural recovery evidenced by compound specific isotope analysis and high-resolution pore water sampling, *Environ. Sci. Technol.*, **2016**, 50, 12197–12204.

[37] Ratti, M., Canonica, S., McNeill, K., Bolotin, J., Hofstetter, T. B., Isotope fractionation associated with the photochemical dechlorination of chloroanilines, *Environ. Sci. Technol.*, **2015**, 49, 9797–9806.

[38] Skarpeli-Liati, M., Pati, S. G., Bolotin, J., Eustis, S. N., Hofstetter, T. B., Carbon, hydrogen, and nitrogen isotope fractionation associated with oxidative transformation of substituted aromatic n-alkyl amines, *Environ. Sci. Technol.*, **2012**, 46, 7189–7198.

[39] Jochmann, M. A., Schmidt, T. C., *Compound-Specific Stable Isotope Analysis*, chap. Introduction to compound-specific isotope analysis, UK: Royal Society of Chemistry, **2012**, 2.

[40] Elsner, M., Jochmann, M., Hofstetter, T., Hunkeler, D., Bernstein, A., Schmidt, T., Schimmelmann, A., Current challenges in compound-specific stable isotope analysis of environmental organic contaminants, *Anal. Bioanal. Chem.*, **2012**, 403, 2471–2491.

[41] Masqué, N., Marc, R. M., Borrull, F., New polymeric and other types of sorbents for solid-phase extraction of polar organic micropollutants from environmental water, *TrAC Trends in Analytical Chemistry*, **1998**, 17, 384–394.

[42] Núñez, M., Borrull, F., Pocurull, E., Fontanals, N., Sample treatment for the determination of emerging organic contaminants in aquatic organisms, *TrAC Trends in Analytical Chemistry*, **2017**, 97, 136–145.

[43] Meier-Augenstein, W., Applied gas chromatography coupled to isotope ratio mass spectrometry, *J Chromatogr A*, **1999**, 842, 351–371.

[44] Ricci, M. P., Merritt, D. A., Freeman, K. H., Hayes, J. M., Acquisition and processing of data for isotope-ratio-monitoring mass spectrometry, *Organic Geochemistry*, **1994**, 21, 561–571.

[45] Zaidi, S. A., Molecular imprinting polymers and their composites: a promising material for diverse applications, *Biomaterials Science*, **2017**, 5, 388–402.

[46] Cieplak, M., Kutner, W., Artificial biosensors: How can molecular imprinting mimic biorecognition?, *Trends in Biotechnology*, **2016**, 34, 922–941.

[47] Martín-Esteban, A., Recent molecularly imprinted polymer-based sample preparation techniques in environmental analysis, *Trends in Environmental Analytical Chemistry*, **2016**, 9, 8–14.

[48] Komiyama, M., Takeuchi, T., Mukawa, T., Asanuma, H., *Molecular Imprinting: From Fundamentals to Applications*, Wiley-VCH Verlag GmbH & Co. KGaA, **2004**.

[49] Sellergren, B., Lanza, F., *Techniques and Instrumentation in Analytical Chemistry*, vol. Volume 23, book section Molecularly imprinted polymers in solid phase extractions, Elsevier, **2001**, 355–375.

[50] Hall, A. J., Manesiotis, P., Emgenbroich, M., Quaglia, M., De Lorenzi, E., Sellergren, B., Urea host monomers for stoichiometric molecular imprinting of oxyanions, *The Journal of Organic Chemistry*, **2005**, 70, 1732–1736.

[51] Whitcombe, M., Molecularly-imprinted polymers database, **2017**, URL `www.MIPdatabase.com`.

[52] Geng, H. R., Miao, S. S., Jin, S. F., Yang, H., A newly developed molecularly imprinted polymer on the surface of TiO_2 for selective extraction of triazine herbicides residues in maize, water, and soil, *Analytical and Bioanalytical Chemistry*, **2015**, 407, 8803–8812.

[53] Su, L.-Q., Gao, Y., Qin, S.-L., Li, J.-J., Determination of atrazine in vegetables with extraction by a magnetitechitosan molecularly imprinted polymer and gas chromatography, *Analytical Letters*, **2016**, 49, 2177–2192.

[54] Zhou, T., Ding, J., Ni, L., Yu, J., Li, H., Ding, H., Chen, Y., Ding, L., Preparation of magnetic superhydrophilic molecularly imprinted resins for detection of triazines in aqueous samples, *Journal of Chromatography A*, **2017**, 1497, 38–46.

[55] Yaqub, S., Latif, U., Dickert, F. L., Plastic antibodies as chemical sensor material for atrazine detection, *Sensors and Actuators B: Chemical*, **2011**, 160, 227–233.

[56] Gkementzoglou, C., Kotrotsiou, O., Stoukides, M., Kiparissides, C., On the synthesis of molecularly imprinted polymers for analytical and sensor applications, *Macromolecular Symposia*, **2013**, 331-332, 26–33.

[57] Saylan, Y., Akgnll, S., imen, D., Derazshamshir, A., Bereli, N., Ylmaz, F., Denizli, A., Development of surface plasmon resonance sensors based on molecularly imprinted nanofilms for sensitive and selective detection of pesticides, *Sensors and Actuators B: Chemical*, **2017**, 241, 446–454.

[58] Ruggieri, F., D'Archivio, A. A., Di Camillo, D., Lozzi, L., Maggi, M. A., Mercorio, R., Santucci, S., Development of molecularly imprinted polymeric nanofibers by electrospinning and applications to pesticide adsorption, *Journal of Separation Science*, **2015**, 38, 1402–1410.

[59] Liu, G., et al., Preparation of a magnetic molecularly imprinted polymer using g-C_3N_4-Fe_3O_4 for atrazine adsorption, *Materials Letters*, **2015**, 160, 472–475.

[60] Zhang, Y., Liu, R., Hu, Y., Li, G., Microwave heating in preparation of magnetic molecularly imprinted polymer beads for trace triazines analysis in complicated samples, *Analytical Chemistry*, **2009**, 81, 967–976.

[61] Murray, A., Örmeci, B., Lai, E. P. C., Removal of endocrine disrupting compounds from wastewater using polymer particles, *Water Science and Technology*, **2016**, 73, 176–181.

[62] Zhang, C., Yang, Z., Zhang, C., Sun, Y., Kinetics of photocatalytic degradation of atrazine on molecularly imprinted titania film, *Asia-Pacific Journal of Chemical Engineering*, **2013**, 8, 318–322.

[63] Boonjob, W., Yu, Y., Mir, M., Segundo, M. A., Wang, J., Cerdá, V., Online hyphenation of multimodal microsolid phase extraction involving renewable molecularly imprinted and reversed-phase sorbents to liquid chromatography for automatic multiresidue assays, *Analytical Chemistry*, **2010**, 82, 3052–3060.

[64] Turiel, E., Tadeo, J. L., Martin-Esteban, A., Molecularly imprinted polymeric fibers for solid-phase microextraction, *Analytical Chemistry*, **2007**, 79, 3099–3104.

[65] Wen, Y., Chen, L., Li, J., Ma, Y., Xu, S., Zhang, Z., Niu, Z., Choo, J., Molecularly imprinted matrix solid-phase dispersion coupled to micellar electrokinetic chromatography for simultaneous determination of triazines in soil, fruit, and vegetable samples, *Electrophoresis*, **2012**, 33, 2454–2463.

[66] Li, X., Wang, Y., Sun, Q., Xu, B., Yang, Z., Wang, X., Molecularly imprinted dispersive solid-phase extraction for the determination of triazine herbicides in grape seeds by high-performance liquid chromatography, *Journal of Chromatographic Science*, **2016**, 54, 871–877.

[67] Andrade, F. N., Nazario, C. E. D., Santos-Neto, A. J., Lancas, F. M., Development of on-line molecularly imprinted solid phase extraction-liquid chromatography-mass spectrometry for triazine analysis in corn samples, *Analytical Methods*, **2016**, 8, 1181–1186.

[68] Dauwe, C., Sellergren, B., Influence of template basicity and hydrophobicity on the molecular recognition properties of molecularly imprinted polymers, *Journal of Chromatography A*, **1996**, 753, 191–200.

[69] Díaz-Álvarez, M., Turiel, E., Martín-Esteban, A., Molecularly imprinted polymer monolith containing magnetic nanoparticles for the stir-bar sorptive extraction of triazines from environmental soil samples, *Journal of Chromatography A*, **2016**, 1469, 1–7.

[70] Chen, J., Bai, L., Tian, M., Zhou, X., Zhang, Y., Hollow-fiber membrane tube embedded with a molecularly imprinted monolithic bar for the microextraction of triazine pesticides, *Analytical Methods*, **2014**, 6, 602–608.

[71] Sellergren, B., *Techniques and Instrumentation in Analytical Chemistry*, vol. Volume 23, book section The non-covalent approach to molecular imprinting, Elsevier, **2001**, 113–184.

[72] Ronald, H. S., Klaus, M., Ecevit, Y., *The Noncovalent Approach*, book section Molecularly Imprinted Materials, CRC Press, **2004**, 25–57.

[73] Ferrer, I., Lanza, F., Tolokan, A., Horvath, V., Sellergren, B., Horvai, G., Barcel, D., Selective trace enrichment of chlorotriazine pesticides from natural waters and sediment samples using terbuthylazine molecularly imprinted polymers, *Analytical Chemistry*, **2000**, 72, 3934–3941.

[74] Schmidt, T. C., Jochmann, M. A., Origin and fate of organic compounds in water: Characterization by compound-specific stable isotope analysis, *Annu. Rev. Anal. Chem.*, **2012**, 5, 133–155.

[75] Thullner, M., Centler, F., Richnow, H. H., Fischer, A., Quantification of organic pollutant degradation in contaminated aquifers using compound specific stable isotope analysis - review of recent developments, *Org. Geochem.*, **2012**, 42, 1440 – 1460.

[76] Merritt, D. A., Hayes, J. M., Factors controlling precision and accuracy in isotope-ratio-monitoring mass-spectrometry, *Anal. Chem.*, **1994**, 66, 2336–2347.

[77] Aelion, M. C., Höhener, P., Hunkeler, D., Aravena, R., *Environmental Isotopes in Biodegradation and Bioremediation*, Boca Raton: CRC Press, **2010**.

[78] Jochmann, M. A., Schmidt, T. C., *Compound-specific Stable Isotope Analysis*, The Royal Society of Chemistry, **2012**.

[79] Skarpeli-Liati, M., Turgeon, A., Garr, A. N., Arnold, W. A., Cramer, C. J., Hofstetter, T. B., pH-Dependent equilibrium isotope fractionation associated with compound-specific nitrogen and carbon isotope analysis by SPME-GC/IRMS, *Anal. Chem.*, **2011**, 83, 1641–1648.

[80] Zwank, L., Berg, M., Schmidt, T. C., Haderlein, S. B., Compound-specific carbon isotope analysis of volatile organic compounds in the low-microgram per liter range, *Anal. Chem.*, **2003**, 75, 5575–5583.

[81] Berg, M., Bolotin, J., Hofstetter, T. B., Compound-specific nitrogen and carbon isotope analysis of nitroaromatic compounds in aqueous samples using solid-phase microextraction coupled to GC/IRMS., *Anal. Chem.*, **2007**, 79, 2386–93.

[82] Horst, A., Lacrampe-Couloume, G., Sherwood Lollar, B., Compound-specific stable carbon isotope analysis of chlorofluorocarbons in groundwater, *Anal. Chem.*, **2015**, 87, 10498–10504.

[83] Schreglmann, K., Hoeche, M., Steinbeiss, S., Reinnicke, S., Elsner, M., Carbon and nitrogen isotope analysis of atrazine and desethylatrazine at sub-microgram per liter concentrations in groundwater, *Anal. Bioanal. Chem.*, **2013**, 405, 2857–2867.

[84] Martín-Esteban, A., Molecularly-imprinted polymers as a versatile, highly selective tool in sample preparation, *TrAC Trends Anal. Chem.*, **2013**, 45, 169–181.

[85] Sellergren, B., Polymer- and template-related factors influencing the efficiency in molecularly imprinted solid-phase extractions, *TrAC Trends Anal. Chem.*, **1999**, 18, 164–174.

[86] Sellergren, B., Noncovalent molecular imprinting: antibody-like molecular recognition in polymeric network materials, *TrAC Trends Anal. Chem.*, **1997**, 16, 310–320.

[87] Sellergren, B., Imprinted polymers with memory for small molecules, proteins, or crystals, *Angewandte Chemie International Edition*, **2000**, 39, 1031–1037.

[88] Turiel, E., Martín-Esteban, A., Molecularly imprinted polymers for sample preparation: A review, *Analytica Chimica Acta*, **2010**, 668, 87–99.

[89] Sun, Z., Schuessler, W., Sengl, M., Niessner, R., Knopp, D., Selective trace analysis of diclofenac in surface and wastewater samples using solid-phase extraction with a new molecularly imprinted polymer, *Anal. Chim. Acta*, **2008**, 620, 73–81.

[90] Hollender, J., Zimmermann-Steffens, S. G., Koepke, S., Krauss, M., McArdell, C. S., Ort, C., Singer, H. P., von Gunten, U., Siegrist, H., Elimination of organic micropollutants in a municipal wastewater treatment plant upgraded with a full-scale post-ozonation followed by sand filtration, *Environ. Sci. Technol.*, **2009**, 43, 7862–7869.

[91] Schymanski, E. L., Singer, H. P., Longrée, P., Loos, M., Ruff, M., Stravs, M. A., Ripollés Vidal, C., Hollender, J., Strategies to characterize polar organic contamination in wastewater: Exploring the capability of high resolution mass spectrometry, *Environ. Sci. Technol.*, **2014**, 48, 1811–1818.

[92] Huntscha, S., Hofstetter, T. B., Schymanski, E. L., Spahr, S., Hollender, J., Biotransformation of benzotriazoles: insights from transformation product identification and compound-specific isotope analysis., *Environ. Sci. Technol.*, **2014**, 48, 4435–4443.

[93] Chapuis, F., Pichon, V., Lanza, F., Sellergren, B., Hennion, M. C., Retention mechanism of analytes in the solid-phase extraction process using molecularly imprinted polymers: Application to the extraction of triazines from complex matrices, *Journal of Chromatography B*, **2004**, 804, 93–101.

[94] Spahr, S., Huntscha, S., Bolotin, J., Maier, M. P., Elsner, M., Hollender, J., Hofstetter, T. B., Compound-specific isotope analysis of benzotriazole and its derivatives, *Anal. Bioanal. Chem.*, **2013**, 405, 2843–2856.

[95] Schimmelmann, A., Lewan, M. D., Wintsch, R. P., D/H isotope ratios of kerogen, bitumen, oil, and water in hydrous pyrolysis of source rocks containing kerogen types I, II, IIS, and III, *Geochim. Cosmochim. Acta*, **1999**, 63, 3751–3766.

[96] Schimmelmann, A., Albertino, A., Sauer, P. E., Qi, H., Molinie, R., Mesnard, F., Nicotine, acetanilide and urea multi-level ^{2}H-, ^{13}C-and ^{15}N-abundance reference materials for continuous-flow isotope ratio mass spectrometry, *Rapid Commun. Mass Spectrom.*, **2009**, 23, 3513–3521.

[97] Komiyama, M., Takeuchi, T., Mukawa, T., Asanuma, H., *Molecular Imprinting*, book section Experimental Methods (2) Evaluation of Imprinting Efficiency, Wiley-VCH Verlag GmbH & Co. KGaA, **2004**, p48.

[98] Sherwood Lollar, B., Hirschorn, S. K., Chartrand, M. M. G., Lacrampe-Couloume, G., An approach for assessing total instrumental uncertainty in compound-specific carbon isotope analysis: Implications for environmental remediation studies, *Anal. Chem.*, **2007**, 79, 3469–3475.

[99] Matsui, J., Miyoshi, Y., Doblhoff-Dier, O., Takeuchi, T., A molecularly imprinted synthetic polymer receptor selective for atrazine, *Anal. Chem.*, **1995**, 67, 4404–4408.

[100] Manesiotis, P., Hall, A. J., Courtois, J., Irgum, K., Sellergren, B., An artificial riboflavin receptor prepared by a template analogue imprinting strategy, *Angewandte Chemie International Edition*, **2005**, 44, 3902–3906.

[101] Laurence, C., Berthelot, M., Observations on the strength of hydrogen bonding, *Perspectives in Drug Discovery and Design*, **2000**, 18, 39–60.

[102] Wegelin, M., Canonica, S., Mechsner, K., Fleischmann, T., Pesaro, F., Metzler, A., Solar water disinfection: Scope of the process and analysis of radiation experiments, *Aqua: Journal of Water Supply Research and Technology*, **1994**, 43, 154–169.

[103] Claudio, B., *Molecularly Imprinted Materials*, chap. Chromatographic techniques, CRC Press, **2004**, 517–552.

[104] Hamilton, R. J., Sewell, P. A., *Introduction to High Performance Liquid Chromatography*, chap. Chromatographic theory, Dordrecht: Springer Netherlands, **1982**, 13–17.

[105] Suto, N., Kawashima, H., Classification of nine malathion emulsion samples by using carbon isotope ratios and the ratio of organic solvents, *Science & Justice*, **2017**, 57, 1–5.

[106] Kujawinski, D. M., Wolbert, J. B., Zhang, L., Jochmann, M. A., Widory, D., Baran, N., Schmidt, T. C., Carbon isotope ratio measurements of glyphosate and ampa by liquid chromatography coupled to isotope ratio mass spectrometry, *Analytical and Bioanalytical Chemistry*, **2013**, 405, 2869–2878.

[107] Meyer, A. H., Penning, H., Lowag, H., Elsner, M., Precise and accurate compound specific carbon and nitrogen isotope analysis of atrazine: Critical role of combustion oven conditions, *Environmental Science & Technology*, **2008**, 42, 7757–7763.

[108] Wu, L., Yao, J., Trebse, P., Zhang, N., Richnow, H. H., Compound specific isotope analysis of organophosphorus pesticides, *Chemosphere*, **2014**, 111, 458–463.

[109] Kawashima, H., Katayama, Y., Source evaluation of diazinon using stable carbon isotope ratio, *Environmental Forensics*, **2010**, 11, 363–371.

[110] Annable, W. K., Frape, S. K., Shouakar-Stash, O., Shanoff, T., Drimmie, R. J., Harvey, F. E., ^{37}Cl, ^{15}N, ^{13}C isotopic analysis of common agro-chemicals for identifying non-point source agricultural contaminants, *Applied Geochemistry*, **2007**, 22, 1530–1536.

[111] Kawashima, H., The measurement of stable carbon isotope ratios of eight methamidophos samples, *Journal of Forensic Sciences*, **2015**, 60, 1360–1364.

[112] Reinnicke, S., Simonsen, A., Srensen, S. R., Aamand, J., Elsner, M., C and N isotope fractionation during biodegradation of the pesticide metabolite 2,6-dichlorobenzamide (BAM): Potential for environmental assessments, *Environmental Science & Technology*, **2012**, 46, 1447–1454.

[113] Elsayed, O. F., Maillard, E., Vuilleumier, S., Nijenhuis, I., Richnow, H. H., Imfeld, G., Using compound-specific isotope analysis to assess the degradation of chloroacetanilide herbicides in lab-scale wetlands, *Chemosphere*, **2014**, 99, 89–95.

[114] Torrentó, C., Bakkour, R., Ryabenko, E., Ponsin, V., Prasuhn, V., Hofstetter, T. B., Elsner, M., Hunkeler, D., Fate of four herbicides in an irrigated field cropped with corn: lysimeter experiments, *11th Applied Isotope Geochemistery Conference*, **2015**, 13, 158–161.

[115] Torrentó, C., Bakkour, R., Melsbach, A., Ponsin, V., Lihl, C., Prasuhn, V., Hofstetter, T. B., Elsner, M., Hunkeler, D., Compound-specific isotope analysis (CSIA) for assessing pesticide dynamics in soil and vadose zone, in *EGU General Assembly Conference Abstracts*, vol. 19, 14833.

[116] Meyer, A. H., Penning, H., Elsner, M., C and N isotope fractionation suggests similar mechanisms of microbial atrazine transformation despite involvement of different enzymes (AtzA and TrzN), *Environ. Sci. Technol.*, **2009**, 43, 8079–8085.

[117] Penning, H., Srensen, S. R., Meyer, A. H., Aamand, J., Elsner, M., C, n, and h isotope fractionation of the herbicide isoproturon reflects different microbial transformation pathways, *Environmental Science & Technology*, **2010**, 44, 2372–2378.

[118] Saranjampour, P., Vebrosky, E. N., Armbrust, K. L., Salinity impacts on water solubility and n-octanol/water partition coefficients of selected pesticides and oil constituents, *Environmental Toxicology and Chemistry*, **2017**, 36, 2274–2280.

[119] Stevenson, D., Molecular imprinted polymers for solid-phase extraction, *TrAC Trends in Analytical Chemistry*, **1999**, 18, 154–158.

[120] Caro, E., Marce, R. M., Borrull, F., Cormack, P. A. G., Sherrington, D. C., Application of molecularly imprinted polymers to solid-phase extraction of compounds from environmental and biological samples, *Trac-Trends in Analytical Chemistry*, **2006**, 25, 143–154.

[121] He, C. Y., Long, Y. Y., Pan, J. L., Li, K., Liu, F., Application of molecularly imprinted polymers to solid-phase extraction of analytes from real samples, *Journal of Biochemical and Biophysical Methods*, **2007**, 70, 133–150.

[122] Tamayo, F. G., Turiel, E., Martín-Esteban, A., Molecularly imprinted polymers for solid-phase extraction and solid-phase microextraction: Recent developments and future trends, *Journal of Chromatography A*, **2007**, 1152, 32–40.

[123] Vasapollo, G., Sole, R. D., Mergola, L., Lazzoi, M. R., Scardino, A., Scorrano, S., Mele, G., Molecularly imprinted polymers: Present and future prospective, *International Journal of Molecular Sciences*, **2011**, 12, 5908.

[124] Murray, A., Örmeci, B., Application of molecularly imprinted and non-imprinted polymers for removal of emerging contaminants in water and wastewater treatment: a review, *Environmental Science and Pollution Research*, **2012**, 19, 3820–3830.

[125] Hu, Y. L., Pan, J. L., Zhang, K. G., Lian, H. X., Li, G. K., Novel applications of molecularly-imprinted polymers in sample preparation, *Trac-Trends in Analytical Chemistry*, **2013**, 43, 37–52.

[126] Jochmann, M. A., Blessing, M., Haderlein, S. B., Schmidt, T. C., A new approach to determine method detection limits for compound-specific isotope analysis of volatile organic compounds, *Rapid Commun. Mass Spectrom.*, **2006**, 20, 3639–3648.

[127] Ertel, J. R., Hedges, J. I., Devol, A. H., Richey, J. E., Ribeiro, M. D. G., Dissolved humic substances of the amazon river system, *Limnology and Oceanography*, **1986**, 31, 739–754.

[128] Merritt, D. A., Hayes, J. M., Nitrogen isotopic analyses by isotope-ratio-monitoring gas chromatography/mass spectrometry, *Journal of the American Society for Mass Spectrometry*, **1994**, 5, 387–397.

[129] Brand, W. A., High precision isotope ratio monitoring techniques in mass spectrometry, *Journal of Mass Spectrometry*, **1996**, 31, 225–235.

[130] Fry, B., Brand, W., Mersch, F. J., Tholke, K., Garritt, R., Automated analysis system for coupled .delta.13C and .delta.15N measurements, *Analytical Chemistry*, **1992**, 64, 288–291.

[131] Werner, R. A., Brand, W. A., Referencing strategies and techniques in stable isotope ratio analysis, *Rapid Commun. Mass Spectrom.*, **2001**, 15, 501–519.

[132] Zhang, Z., Xiao, H., Zheng, N., Gao, X., Zhu, R., Compound-specific isotope analysis of amino acid labeling with stable isotope nitrogen (^{15}N) in higher plants, *Chromatographia*, **2016**, 79, 1197–1205.

[133] Tuelp, H. C., Goss, K.-U., Schwarzenbach, R. P., Fenner, K., Experimental determination of lser parameters for a set of 76 diverse pesticides and pharmaceuticals, *Environ. Sci. Technol.*, **2008**, 42, 2034–2040.

[134] Adamska, K., Kadlec, K., Voelkel, A., Application of inverse liquid chromatography for surface characterization of biomaterials, *Chromatographia*, **2016**, 79, 473–480.

[135] Bi, E., Schmidt, T. C., Haderlein, S. B., Sorption of heterocyclic organic compounds to reference soils: Column studies for process identification, *Environmental Science & Technology*, **2006**, 40, 5962–5970.

[136] Bi, E., Schmidt, T. C., Haderlein, S. B., Environmental factors influencing sorption of heterocyclic aromatic compounds to soil, *Environmental Science & Technology*, **2007**, 41, 3172–3178.

[137] Bi, E. P., Schmidt, T. C., Haderlein, S. B., Practical issues relating to soil column chromatography for sorption parameter determination, *Chemosphere*, **2010**, 80, 787–793.

[138] Baylis, A. D., Why glyphosate is a global herbicide: strengths, weaknesses and prospects, *Pest Management Science*, **2000**, 56, 299–308.

[139] Woodburn, A. T., Glyphosate: production, pricing and use worldwide, *Pest Management Science*, **2000**, 56, 309–312.

[140] Duke, S. O., Powles, S. B., Glyphosate: a once-in-a-century herbicide, *Pest Management Science*, **2008**, 64, 319–325.

[141] Schütte, G., Eckerstorfer, M., Rastelli, V., Reichenbecher, W., Restrepo-Vassalli, S., Ruohonen-Lehto, M., Saucy, A.-G. W., Mertens, M., Herbicide resistance and biodiversity: agronomic and environmental aspects of genetically modified herbicide-resistant plants, *Environmental Sciences Europe*, **2017**, 29, 5.

[142] Gomes, M. P., Smedbol, E., Chalifour, A., Hnault-Ethier, L., Labrecque, M., Lepage, L., Lucotte, M., Juneau, P., Alteration of plant physiology by glyphosate and its by-product aminomethylphosphonic acid: an overview., *Journal of experimental botany*, **2014**, 65 17, 4691–703.

[143] Grandcoin, A., Piel, S., Baurès, E., Aminomethylphosphonic acid (AMPA) in natural waters: Its sources, behavior and environmental fate, *Water Research*, **2017**, 117, 187–197.

[144] Poiger, T., Buerge, I. J., Bchli, A., Mller, M. D., Balmer, M. E., Occurrence of the herbicide glyphosate and its metabolite AMPA in surface waters in switzerland determined with on-line solid phase extraction LC-MS/MS, *Environmental Science and Pollution Research*, **2017**, 24, 1588–1596.

[145] Battaglin, W. A., Meyer, M. T., Kuivila, K. M., Dietze, J. E., Glyphosate and its degradation product AMPA occur frequently and widely in U.S. soils, surface water, groundwater, and precipitation, *JAWRA Journal of the American Water Resources Association*, **2014**, 50, 275–290.

[146] Lupi, L., Miglioranza, K. S. B., Aparicio, V. C., Marino, D., Bedmar, F., Wunderlin, D. A., Occurrence of glyphosate and ampa in an agricultural watershed from the southeastern region of argentina, *Science of The Total Environment*, **2015**, 536, 687–694.

[147] Guyton, K. Z., Loomis, D., Grosse, Y., El Ghissassi, F., Benbrahim-Tallaa, L., Guha, N., Scoccianti, C., Mattock, H., Straif, K., Carcinogenicity of tetrachlorvinphos, parathion, malathion, diazinon, and glyphosate, *The Lancet Oncology*, **2015**, 16, 490–491.

[148] Stalikas, C. D., Konidari, C. N., Analytical methods to determine phosphonic and amino acid group-containing pesticides, *Journal of Chromatography A*, **2001**, 907, 1–19.

[149] Koskinen, W. C., Marek, L. J., Hall, K. E., Analysis of glyphosate and aminomethylphosphonic acid in water, plant materials and soil, *Pest Management Science*, **2016**, 72, 423–432.

[150] Gill, J. P. K., Sethi, N., Mohan, A., Analysis of the glyphosate herbicide in water, soil and food using derivatising agents, *Environmental Chemistry Letters*, **2017**, 15, 85–100.

[151] Mogusu, E. O., Wolbert, J. B., Kujawinski, D. M., Jochmann, M. A., Elsner, M., Dual element ($^{15}N/^{14}N$, $^{13}C/^{12}C$) isotope analysis of glyphosate and ampa by derivatization-gas chromatography isotope ratio mass spectrometry (GC/IRMS) combined with LC/IRMS, *Analytical and Bioanalytical Chemistry*, **2015**, 407, 5249–5260.

[152] Arkan, T., Molnár-Perl, I., The role of derivatization techniques in the analysis of glyphosate and aminomethyl-phosphonic acid by chromatography, *Microchemical Journal*, **2015**, 121, 99–106.

[153] Hanke, I., Singer, H., Hollender, J., Ultratrace-level determination of glyphosate, aminomethylphosphonic acid and glufosinate in natural waters by solid-phase extraction followed by liquid chromatographytandem mass spectrometry: performance tuning of derivatization, enrichment and detection, *Analytical and Bioanalytical Chemistry*, **2008**, 391, 2265–2276.

[154] Mallat, E., Barcelo, D., Analysis and degradation study of glyphosate and of aminomethylphosphonic acid in natural waters by means of polymeric and ion-exchange solid-phase extraction columns followed by ion chromatography post-column derivatization with fluorescence detection, *Journal of Chromatography A*, **1998**, 823, 129–136.

[155] Patsias, J., Papadopoulou, A., Papadopoulou-Mourkidou, E., Automated trace level determination of glyphosate and aminomethyl phosphonic acid in water by on-line anion-exchange solid-phase extraction followed by cation-exchange liquid chromatography and post-column derivatization, *Journal of Chromatography A*, **2001**, 932, 83–90.

[156] Corbera, M., Hidalgo, A., Salvado, V., Wieczorek, P. P., Determination of glyphosate and aminomethylphosphonic acid in natural water using the capillary electrophoresis combined with enrichment step, *Analytica Chimica Acta*, **2005**, 540, 3–7.

[157] Khrolenko, M. V., Wieczorek, P. P., Determination of glyphosate and its metabolite aminomethylphosphonic acid in fruit juices using supported-liquid membrane preconcentration method with high-performance liquid chromatography and uv detection after derivatization with p-toluenesulphonyl chloride, *Journal of Chromatography A*, **2005**, 1093, 111–117.

[158] Mogusu, E. O., *Compound-specific isotope analysis to investigate sources and degradation of glyphosate*, PhD Thesis, Eberhard Karls Universität Tübingen, **2015**.

[159] Sellergren, B., Imprinted polymers with affinity for phosphorylated peptides and proteins, **2009**.

[160] da Mata, K., Corazza, M. Z., de Oliveira, F. M., de Toffoli, A. L., Teixeira Tarley, C. R., Moreira, A. B., Synthesis and characterization of cross-linked molecularly imprinted polyacrylamide for the extraction/preconcentration of glyphosate and aminomethylphosphonic acid from water samples, *Reactive and Functional Polymers*, **2014**, 83, 76–83.

[161] Puzio, K., Claude, B., Amalric, L., Berho, C., Grellet, E., Bayoudh, S., Nehm, R., Morin, P., Molecularly imprinted polymer dedicated to the extraction of glyphosate in natural waters, *Journal of Chromatography A*, **2014**, 1361, 1–8.

[162] Do, M. H., Florea, A., Farre, C., Bonhomme, A., Bessueille, F., Vocanson, F., Tran-Thi, N.-T., Jaffrezic-Renault, N., Molecularly imprinted polymer-based electrochemical sensor for the sensitive detection of glyphosate herbicide, *International Journal of Environmental Analytical Chemistry*, **2015**, 95, 1489–1501.

[163] Gomez-Caballero, A., Diaz-Diaz, G., Bengoetxea, O., Quintela, A., Unceta, N., Goicolea, M. A., Barrio, R. J., Water compatible stir-bar devices imprinted with underivatised glyphosate for selective sample clean-up, *Journal of Chromatography A*, **2016**, 1451, 23–32.

[164] Claude, B., Berho, C., Bayoudh, S., Amalric, L., Coisy, E., Nehmé, R., Morin, P., Preliminary recovery study of a commercial molecularly imprinted polymer for the extraction of glyphosate and AMPA in different environmental waters using MS, *Environmental Science and Pollution Research*, **2017**, 24, 12293–12300.

[165] Berho, C., Claude, B., Coisy, E., Togola, A., Bayoudh, S., Morin, P., Amalric, L., Laboratory calibration of a POCIS-like sampler based on molecularly imprinted polymers for glyphosate and AMPA sampling in water, *Analytical and Bioanalytical Chemistry*, **2017**, 409, 2029–2035.

[166] Deutsches Institute für Normung (DIN), DIN 32645: Chemische Analytik Nachweis-, Erfassungs- und Bestimmungsgrenze., *Berlin, Beuth Verlag.*, **1994**.

[167] Chen, M.-X., Cao, Z.-Y., Jiang, Y., Zhu, Z.-W., Direct determination of glyphosate and its major metabolite, aminomethylphosphonic acid, in fruits and vegetables by mixed-mode hydrophilic interaction/weak anion-exchange liquid chromatography coupled with electrospray tandem mass spectrometry, *Journal of Chromatography A*, **2013**, 1272, 90–99.

[168] Chamkasem, N., Morris, C., Harmon, T., Direct determination of glyphosate, glufosinate, and AMPA in milk by liquid chromatography/tandem mass spectrometry, *Journal of Regulatory Science*, **2015**, 02, 20–26.

[169] Chamkasem, N., Harmon, T., Direct determination of glyphosate, glufosinate, and AMPA in soybean and corn by liquid chromatography/tandem mass spectrometry, *Analytical and Bioanalytical Chemistry*, **2016**, 408, 4995–5004.

[170] Shimizu, K., *Molecularly Imprinted Materials*, chap. Post Modification of Imprinted Polymers, CRC Press, **2004**, 329–345.

[171] Kirsch, N., Alexander, C., Lbke, M., Whitcombe, M. J., Vulfson, E. N., Enhancement of selectivity of imprinted polymers via post-imprinting modification of recognition sites, *Polymer*, **2000**, 41, 5583–5590.

[172] Kawashima, H., Murakami, M., Measurement of the stable carbon isotope ratio of atmospheric volatile organic compounds using chromatography, combustion, and isotope ratio mass spectrometry coupled with thermal desorption, *Atmospheric Environment*, **2014**, 89, 140–147.

[173] Brailsford, A. D., Gavrilovi, I., Ansell, R. J., Cowan, D. A., Kicman, A. T., Two-dimensional gas chromatography with heart-cutting for isotope ratio mass spectrometry analysis of steroids in doping control, *Drug Testing and Analysis*, **2012**, 4, 962–969.

[174] Dumont, E., Tienpont, B., Higashi, N., Mitsui, K., Ochiai, N., Kanda, H., David, F., Sandra, P., Heart-cutting two-dimensional gas chromatography in combination with isotope ratio mass spectrometry for the characterization of the wax fraction in plant material, *Journal of Chromatography A*, **2013**, 1317, 230–238.

[175] Ponsin, V., Buscheck, T. E., Hunkeler, D., Heart-cutting two-dimensional gas chromatographyisotope ratio mass spectrometry analysis of monoaromatic hydrocarbons in complex groundwater and gas-phase samples, *Journal of Chromatography A*, **2017**, 1492, 117–128.

[176] Tobias, H. J., Sacks, G. L., Zhang, Y., Brenna, J. T., Comprehensive two-dimensional gas chromatography combustion isotope ratio mass spectrometry, *Analytical Chemistry*, **2008**, 80, 8613–8621.

[177] Tobias, H. J., Zhang, Y., Auchus, R. J., Brenna, J. T., Detection of synthetic testosterone use by novel comprehensive two-dimensional gas chromatography combustionisotope ratio mass spectrometry, *Analytical Chemistry*, **2011**, 83, 7158–7165.

[178] Nara, H., Nakagawa, F., Yoshida, N., Development of two-dimensional gas chromatography/isotope ratio mass spectrometry for the stable carbon isotopic analysis of C_2-C_5 non-methane hydrocarbons emitted from biomass burning, *Rapid Communications in Mass Spectrometry*, **2006**, 20, 241–247.

[179] Damsio, J., Navarro-Ortega, A., Tauler, R., Lacorte, S., Barcel, D., Soares, A. M. V. M., Lpez, M. A., Riva, M. C., Barata, C., Identifying major pesticides affecting bivalve species exposed to agricultural pollution using multi-biomarker and multivariate methods, *Ecotoxicology*, **2010**, 19, 1084–1094.

[180] Köck, M., Farré, M., Martínez, E., Gajda-Schrantz, K., Ginebreda, A., Navarro, A., Alda, M. L. d., Barceló, D., Integrated ecotoxicological and chemical approach for the assessment of pesticide pollution in the ebro river delta (Spain), *Journal of Hydrology*, **2010**, 383, 73–82.

[181] Herrero-Hernández, E., Andrades, M. S., Álvarez Martín, A., Pose-Juan, E., Rodríguez-Cruz, M. S., Sánchez-Martín, M. J., Occurrence of pesticides and some of their degradation products in waters in a Spanish wine region, *Journal of Hydrology*, **2013**, 486, 234–245.

[182] Leu, C., Singer, H., Stamm, C., Müller, S. R., Schwarzenbach, R. P., Variability of herbicide losses from 13 fields to surface water within a small catchment after a controlled herbicide application, *Environmental Science & Technology*, **2004**, 38, 3835–3841.

[183] Otto, J., Singer, H., Gtz, C., Substanzen zur Überprüfung des Reinigungseffekts weitergehender Abwas-serbehandlungsverfahren, Fachbericht im Auftrag des Bundesamts für Umwelt BAFU, Report, Eawag, **2014**.